Universidade de Aveiro
Ano 2021

Adriana Catarina da Costa Gomes

Metalofármacos com atividade antibacteriana e incorporação em membranas de nanocelulose para aplicação em cicatrização de feridas

Metallodrugs with antibacterial activity and their incorporation into nanocellulose membranes for wound healing applications

Universidade de Aveiro
Ano 2021

Adriana Catarina da Costa Gomes

Metalofármacos com atividade antibacteriana e incorporação em membranas de nanocelulose para aplicação em cicatrização de feridas

Metallodrugs with antibacterial activity and their incorporation into nanocellulose membranes for wound healing applications

Dissertação apresentada à Universidade de Aveiro para cumprimento dos requisitos necessários à obtenção do grau de Mestre em Biotecnologia, ramo Molecular, realizada sob a orientação científica da Doutora Bárbara Leite Ferreira, Investigadora do CICECO, Departamento de Química, Universidade de Aveiro, e coorientação científica da Doutora Carmen Freire Barros, Investigadora Principal do CICECO, Departamento de Química, Universidade de Aveiro.

“Everything is theoretically impossible, until it is done.”

– Robert A. Heinlein

o júri

presidente

Prof. Doutor Jorge Manuel Alexandre Saraiva
Professor Associado do Departamento de Química da Universidade de Aveiro

Doutora Ana Catarina Costa Gomes Alves
Investigadora Auxiliar do CICECO/Departamento de Química da Universidade de Aveiro

Doutora Bárbara Joana Martins Leite Ferreira
Investigadora do CICECO/Departamento de Química da Universidade de Aveiro

agradecimentos

Em primeiro lugar, gostaria de agradecer à Doutora Bárbara Ferreira e à Doutora Carmen Freire por terem aceite embarcar comigo neste desafio, por toda a orientação, paciência e compreensão. Foi um prazer trabalhar junto de duas pessoas que praticam ciência com tanto entusiasmo e dedicação.

Gostaria ainda de agradecer ao Doutor Ricardo Mendes e à Doutora Carla Vilela por todas as contribuições e, em especial, à Doutora Carla Pereira e à Engenheira Celeste Azevedo por toda a ajuda na aquisição de resultados.

Aos amigos que Aveiro me deu, quero deixar uma palavra de agradecimento por todos os momentos que me proporcionaram, sem vocês estes cinco anos não teriam sido o que foram. Obrigada Raquel, vais para sempre ser a minha companheira. Obrigada Rita, trago-te num lugar especial do meu coração. Obrigada Carlota e Silvina por todas as jantaradas. Obrigada Marina e Bernardo, vão ser sempre um motivo de orgulho. Obrigada Diana e Daniel, sem vocês os jogos de tabuleiro não seriam tão emocionantes. Obrigada Flávia, por me ajudares desde o primeiro dia, pelos abraços, pelos chocolates, pelos risos. Sem ti não teria conseguido.

Aos amigos que já trazia, quero agradecer por continuarem a partilhar a vida comigo, ainda que de século em século. É um orgulho crescer ao vosso lado e aperceber-me que, na essência, continuamos os mesmos (pré)adolescentes. Luís, Rafa, Pedro, Ju, Tiago e Jonas, muito obrigada.

À minha família, agradeço pelo apoio incondicional. Em especial aos meus pais e à minha irmã, por sempre acreditarem em mim e apoiarem as minhas vontades, por todo o amor, por todo o incentivo, por toda a proteção. Não tenho palavras para vos agradecer tanto como deveria.

Por último, um agradecimento muito especial ao Gil, por fazer com que a vida valha a pena. Obrigada pelo amor, pelo companheirismo, pela paciência, pelo amparo, e sobretudo por cuidares da minha alimentação. Mereces o mundo.

A todos vocês, do fundo do meu coração, obrigada! São a minha sorte grande.

palavras-chave

Cicatrização de feridas, Celulose bacteriana, Metalofármacos, Entrega de fármacos, Atividade antibacteriana

resumo

As feridas têm um impacto significativo na sociedade, não só nos pacientes, como também no sistema de saúde. Além disso, nem sempre seguem o processo de cicatrização esperado. A incidência de complicações, como infeções, pode inibir a sua cicatrização e aumentar o custo dos cuidados de saúde. Neste sentido, os curativos surgem como uma possível solução, uma vez que são cruciais para promover a cura e o tratamento de feridas.

Numa sociedade cada vez mais consciente dos problemas ambientais, os curativos à base de biopolímeros estão a tornar-se cada vez mais eminentes devido à sua abundância, carácter renovável, capacidade de absorção de exsudados e não-citotoxicidade. A celulose é um exemplo de um polissacarídeo amplamente estudado, sendo cada vez mais utilizada na cicatrização de feridas. Em particular, a celulose bacteriana possui propriedades físico-químicas, mecânicas e biológicas únicas. Além disso, pode ser modificada e funcionalizada de modo a possuir melhores desempenhos. A estrutura nanofibrilar da celulose bacteriana proporciona condições ideais para a cicatrização de feridas, e pode ser usada como sistemas de libertação de fármacos, uma vez que possui capacidade de incorporar e libertar moléculas bioativas.

Por outro lado, a resistência aos antibióticos é uma das maiores ameaças à saúde global, visto que reduz a capacidade de combater doenças infeciosas comuns. Neste sentido, os metalofármacos com atividade antibacteriana surgem como uma possível alternativa aos antibióticos. Estes complexos metálicos farmacologicamente ativos exibem novas propriedades e podem ter atividade biológica melhorada devido à combinação sinérgica dos ligandos com o centro metálico. Além disso, os metalofármacos possuem geometrias e estruturas tridimensionais únicas que geralmente estão associadas a elevadas taxas de sucesso clínico.

Deste modo, os principais objetivos deste trabalho eram sintetizar e caracterizar metalofármacos com atividade antibacteriana, e incorporá-los em membranas de celulose bacteriana para aplicação em cicatrização de feridas. Assim, este trabalho incluiu a síntese e caracterização de complexos de cobalto(II), cobre(II), níquel(II) e zinco(II), com levofloxacina ou ciprofloxacina, na presença ou ausência de ligandos dadores de N. Os catorze complexos caracterizados exibiram atividade antibacteriana contra *Staphylococcus aureus*. Um dos complexos foi incorporado com sucesso em membranas de celulose bacteriana, aumentando a sua estabilidade térmica. Foi ainda obtido um perfil de libertação adequado para administração tópica. Portanto, este trabalho não só é um bom ponto de partida para a comunidade científica, como também se pode tornar numa solução para um problema que afeta milhões de pessoas.

keywords

Wound healing, Bacterial cellulose, Metallodrugs, Drug delivery, Antibacterial activity

abstract

Wounds have a significant impact on society, not only on those who suffer from them but also on the health care system. Moreover, wounds do not always follow the expected healing process. The incidence of complications, such as infections, can inhibit wound healing and increase the cost of health care. Therefore, wound dressings emerge as a possible solution since they are crucial in promoting wound healing.

In an increasingly environmentally conscious society, biopolymers-based wound dressings are becoming more eminent because of their abundance, renewable character, exudates' absorption capacity, and non-citotoxicity. Cellulose is an example of a widely studied polysaccharide, being increasingly used in wound healing applications. In particular, bacterial cellulose (BC) has a unique morphology and unique physicochemical, mechanical, and biological properties. In addition, BC can be modified and functionalized in order to have better performances. Moreover, bacterial cellulose has a nanofibrillar structure that provides ideal conditions for wound healing, and BC-based materials can act as drug delivery systems due to their ability to incorporate and release bioactive molecules.

On the other hand, antibiotic resistance is one of the biggest threats to global health since it is reducing the ability to treat common infectious diseases. Metallodrugs with antibacterial activity emerge as a possible alternative to antibiotics. These pharmacologically active metal complexes display new properties and might have enhanced biological activity due to the synergistic combination between the ligands and the metal. Besides, metallodrugs possess different geometries and three-dimensional structures that are generally associated with higher clinical success rates.

Thus, the main goals of this work were to synthesize and characterize metallodrugs with antibacterial activity, and to incorporate them into BC membranes for wound healing applications. Hence, this work included the synthesis and characterization of cobalt(II), copper(II), nickel(II), and zinc(II) complexes of levofloxacin and ciprofloxacin, in the presence and absence of N-donor ligands. All fourteen complexes characterized exhibited antibacterial activity against *Staphylococcus aureus*. One of them was successfully incorporated into BC membranes, increasing their thermal stability. A rapid release profile, suitable for topical administration, was obtained. Therefore, this work serves as a good starting point for the scientific community, but it also might be a future solution for a problem that affects millions of people.

List of Figures

List of Tables

Abbreviations

BC – Bacterial Cellulose

Bipy – 2,2'-Bipyridine

CNCs – Cellulose nanocrystals

Cip – Ciprofloxacin

Dipy – 2,2'-Dipyridylamine

EA – Elemental Analysis

FDA – Food and Drug Administration

FTIR – Fourier Transform Infrared Spectroscopy

FTIR-ATR – Fourier Transform Infrared Spectroscopy - Attenuated Total Reflection

FT-Raman – Fourier Transform Raman Spectroscopy

GRAS – Generally Recognized as Safe

Lev – Levofloxacin

MHA – Mueller-Hinton Agar

MHB – Mueller-Hinton Broth

NFC – Nanofibrillated cellulose

Phen – 1,10-Phenanthroline

PHMB – Polyhexamethylene biguanide

PXRD - Powder X-Ray Diffraction

SC XRD – Single-Crystal X-Ray Diffraction

TGA – Thermogravimetric Analysis

UV-Vis – Ultraviolet-visible Spectroscopy

WHO – World Health Organization

Table of Contents

CHAPTER 1 – INTRODUCTION

Framework

Wounds have a significant impact on society, not only on those who suffer from them but also on the health care system. However, this impact is usually not recognized, hence being called the "Silent Epidemic". In order to understand this phenomenon, it is important to consider some numbers: it is estimated that for every 1 million people, approximately 3500 live with a wound, of which, around 525 have them for at least one year. This scenario corresponds to around 1.5 to 2 million people with a chronic wound across Europe.[1]

Additionally, wounds do not always follow the expected healing process. The incidence of complications, such as infections, can inhibit wound healing and increase the cost of health care. As an example, a hospital that performs 10 thousand operations per year can expect between 300 and 400 infections, which results in 3300 to 4000 additional bed-days, approximately extra 1.74 to 2.32 million euros, and 15 to 20 more infection-related deaths.[1]

Therefore, in order to solve this "Silent Epidemic", there has been a growing investment in the Global Advanced Wound Care Market, which is estimated to reach 10.93 billion euros by 2025. This is due to the increasing demands for wound care treatments combined with the development of science and technology, which is reflected in the launch of increasingly more effective new drugs and products that enable faster healing and, therefore, a better quality of life for patients.[2]

In this context, the synthesis of metallodrugs with antibacterial activity and their incorporation into bacterial cellulose membranes resembled an excellent option that, as far as we know, has not been yet described in the literature. Thereby, this dissertation is structured into four different chapters. The Introduction gives the fundamental knowledge about bacterial cellulose and metallodrugs, as well as a review of the state of the art on this topic. In Chapter 2, Experimental Procedures, the reagents and materials used are described, along with the methods and procedures performed, which includes the synthesis of metallodrugs and their incorporation into bacterial cellulose membranes. In Chapter 3, Results and Discussion, all the results obtained are presented and discussed, particularly the characterization of the metallodrugs and the characterization of the bacterial cellulose membranes loaded with the metallodrugs. Lastly, Chapter 4, Conclusions and Future Work, indicates the main conclusions of all the performed work, as well as some proposals for future work.

Introduction

As mentioned above, wound healing represents a major health burden that needs to be urgently solved. Wound dressings emerge as a solution since they are crucial in promoting wound healing. Besides, they provide a physical barrier between the injury and the external environment, preventing additional damage and infection. In this sense, different wound dressings materials, including foams, hydrogels, and films, have been developed and commercialized.[3,4] Moreover, in an increasingly environmentally conscious society, the demand for naturally derived materials for medical treatment is growing. Therefore, biopolymers-based wound dressings are becoming more eminent.[3]

Biopolymers are generally proteoglycans and proteins, such as collagen, gelatin, or keratin, and polysaccharides, for example, alginates or cellulose. These natural polymers are biocompatible, biodegradable, and similar to macromolecules recognized by the human body. Therefore, they have been studied for many years, and nowadays, biopolymers are widely employed in several biomedical applications.[3]

In particular, polysaccharides have a huge potential for the development of wound dressings because of their abundance, absorption capacity, and non-citotoxicity. Additionally, polysaccharides can be functionalized to enhance or add specific properties in order to aid the healing process. Cellulose, for example, is being widely studied and increasingly used in wound healing applications.[3]

For a better understanding of the potential of cellulose as a wound dressing, the fundamental knowledge about this polysaccharide will be given, focusing on bacterial cellulose and its biomedical applications that have already been reported on the literature, in particular wound healing and drug delivery. Afterwards, a basic understanding on metallodrugs will be provided, as well as the state of the art, in order to recognize their potential as antibacterial agents that could be incorporated into bacterial cellulose membranes to prevent infections and contribute to wound healing.

Cellulose

Cellulose is the most abundant natural polymer on Earth since it is the main component of plant cell walls. Moreover, cellulose is also produced by other living organisms, such as marine animals, algae, fungi, and bacteria.[5,6]

Cellulose is a homopolysaccharide, composed of repetitive units of β-D-glucose, linked through β-(1→4)-glycosidic bonds (Figure 1).[6,7] The number of repetition units per chain is named degree of polymerization.[8] Each repetitive unit has three free hydroxyl groups that allow the establishment of intramolecular hydrogen bonds, making the monomeric units rotation around the glycosidic bonds difficult, which increases the chains' rigidity.[9] Moreover, when several cellulose chains are side by side, intramolecular and intermolecular hydrogen bonds are established, producing a stabilized network, which origins straight supramolecular fibers of great tensile strength.[10]

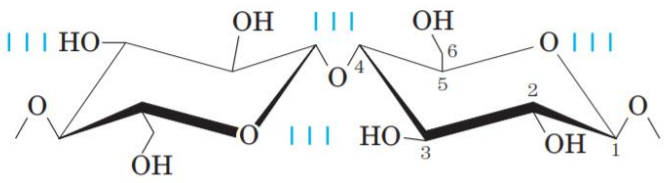

Figure 1. *Molecular structure of a cellulose chain containing two repetitive units of β-D-glucose connected by β-(1 → 4)-glycosidic bonds. Each set of three blue lines represents a hydrogen bond.* (Adapted from [10])

As mentioned, the established hydrogen bonds influence the cellulose structure, conditioning other important properties, such as its rigidity.[11] Moreover, the hydrogen bonding is related to the semi-crystalline nature of cellulose, which is constituted by fibers with both crystalline and amorphous regions.[8,12] Crystalline regions have a high number of interactions and are well-organized regions, which offer great resistance and insolubility in common solvents.[11] On the other hand, the interactions are weaker in amorphous regions, drifting the chains apart and, therefore, making them more likely to establish hydrogen bonds with other molecules, such as water.[9,11] This way, cellulose is able to absorb large amounts of water without dissolving itself.[11]

Crystalline cellulose can occur in four polymorphic forms: I, II, III, and IV (Figure 2). In cellulose I, the native form of cellulose, the chains are arranged in a parallel conformation, leading to two distinct crystalline structures: Iα (triclinic, in other words, the

crystals do not have a symmetrical axis) and Iβ (monoclinic, that is, the crystallographic system is characterized by three unequal and oblique axes).[13]

The remaining crystalline allomorphs, namely II, III, and IV, are synthetic forms of cellulose since they result from modifications of native cellulose, for instance, cellulose II can be obtained through alkaline treatment of cellulose I. In cellulose II, the chains are distributed in an antiparallel arrangement once the hydrogen bonds conformations have changed. On the other hand, in cellulose III and IV, the chains can be organized both in a parallel and antiparallel configuration, depending on the treatment and the form of the modified cellulose.[9,13]

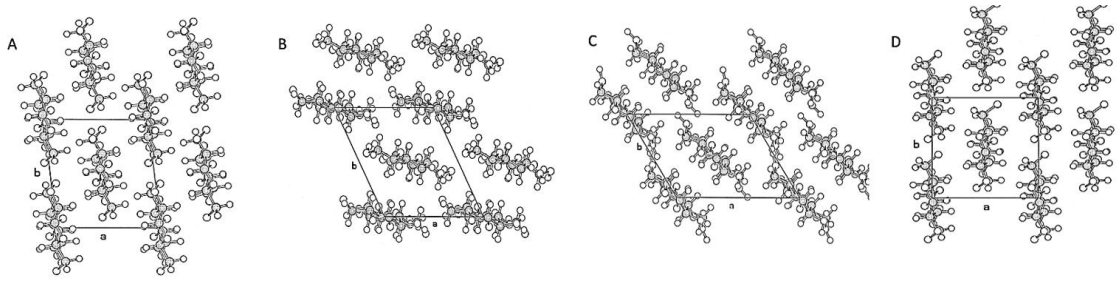

Figure 2. *Polymorphic forms of crystalline cellulose:* ***A.*** *Cellulose Iβ;* ***B.*** *Cellulose II;* ***C.*** *Cellulose III;* ***D.*** *Cellulose IV.* (Adapted from [14])

Materials derived from cellulose have gained greater interest due to their unique physicochemical properties and the fact that cellulose is biodegradable, obtained from renewable resources, and, therefore, presents low environmental and health risks. In fact, cellulose-based materials are already used in several areas, from textile to pharmaceutical industries, being mainly used to produce paperboard and paper. Nevertheless, novel applications are being continuously explored.[15]

In particular, nanocelluloses, which refers to cellulose substrates with at least one dimension in the nanometric range, have opened the possibility of using cellulose in a wider range of applications. These cellulose-based nanomaterials display exceptional characteristics, such as high surface area and excellent mechanical properties. Nanocelluloses can be roughly divided into three groups, namely cellulose nanocrystals (CNCs), nanofibrillated cellulose (NFC), and bacterial cellulose (BC).[16] This review focuses only on bacterial cellulose.

Bacterial Cellulose

Bacterial cellulose (BC) is a nanomaterial produced by several species of aerobic nonpathogenic bacteria, being *Gluconacetobacter xylinus* the main producer specie.[15] BC has unique mechanical properties and morphology combined with the outstanding features inherent to cellulose, such as its biological and physicochemical properties, which give BC increased interest and improved potential for several applications.[17,18]

BC production occurs at temperatures between 25 and 30 ºC, under static or agitated culture conditions.[12] Static culture conditions result in the growth of a dense white BC membrane at the air–liquid interface, while agitated culture conditions produce dispersed BC in the culture medium, forming irregular pellets or suspended nanofibers.[12,19] Hestrin-Schramm medium is the most used culture medium, which contains glucose (20.0 g/L), yeast extract (5.0 g/L), peptone (5.0 g/L), disodium hydrogen phosphate (2.7 g/L), and citric acid monohydrate (1.15 g/L).[12,20] Once produced, BC must be washed with water and immersed in sodium hydroxide to remove residues, such as cells and nutrients. Posteriorly, it is important to establish a neutral pH value.[12]

At an early stage of a static culture, the dissolved oxygen allows the bacterial population to grow and produce cellulose in the liquid phase, causing turbidity. Once the dissolved oxygen is consumed, only the bacteria on the surface are able to maintain activity and produce cellulose in the form of a membrane.[12] From a biochemical point of view, BC synthesis consists of three main steps: glucose residues are polymerized into β-(1→4)-glucan, which is released as linear chains to the extracellular medium, where due to interactions, such as hydrogen bonds, the organization and crystallization of the glucan chains occurs.[15,21]

Regarding microstructure, BC is characterized by a porous three-dimensional network, consisting of cellulose nanofibrils with diameters between 20 to 100 nm and about 100 μm in length. Furthermore, elementary fibrils, which constitute microfibrils, have a diameter of about 2 to 4 nm (Figure 3).[22,23]

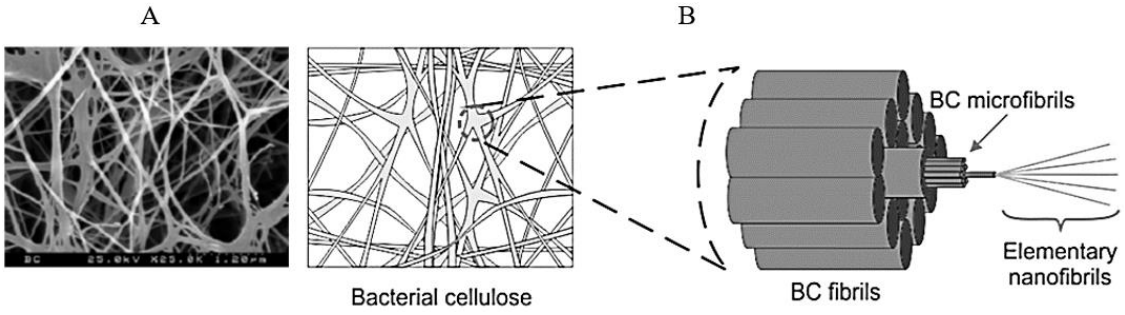

Figure 3. A. *Three-dimensional nanofibrillar structure of a BC membrane displayed by SEM analysis by Silva et al. (2014).* **B.** *Hierarchical structure of bacterial cellulose: a three-dimensional network composed of fibrils, microfibrils, and nanofibrils. (Adapted from [24],[25])*

Bacterial cellulose has high thermal stability, crystallinity (60–90 %), degree of polymerization (up to 8000) and water content (up to 99 %), low density (approximately 1.6 g/cm^3), high surface area (150 to 600 m^2/g), and high mechanical strength, with a Young's modulus of about 118 GPa and a tensile strength up to 300 MPa for a single filament.[13,15,22-26] The combination between high surface area and high porosity contributes not only to the increase of water absorption capacity, which is between 60 to 700 times the dry weight of BC, but also to the increase of the capacity to retain it, which exceeds 1:50.[27]

Although bacterial cellulose has a molecular structure similar to the cellulose extracted from plants, some differences are important to highlight, such as the fact that plant cellulose predominantly presents the crystalline form Iβ, while bacterial cellulose mainly exhibits the form Iα.[13,28] Another important difference is that bacterial cellulose has higher purity since lignocellulosic components, in particular, lignin, hemicelluloses, and pectin, are not produced along with BC.[15] Besides, bacterial cellulose has a higher water retention capacity, a higher degree of polymerization, and a higher surface area, mechanical strength, and crystallinity than plant cellulose.[8,29,30] Most of these differences result mainly from the unique morphological characteristics and nanometric dimensions of BC.[12]

Modification and functionalization

Although BC presents many favorable properties for different uses, sometimes it is necessary to modify some of them, such as the surface properties and microstructure, since not all are ideal for every application and, consequently, they must be personalized for a specific use.[26,31] These modifications could, for example, increase the biological

compatibility, mechanical and thermal stability, and the overall performance of BC-based materials.[31]

The innumerous modifications strategies that can be applied to BC are distinguished into two classes, in particular, *in situ* and *ex situ* modifications, involving both physical or chemical methods. In the *in situ* modifications, the changes are induced during BC biosynthesis, for example, through alterations in the culture conditions. On the other hand, in the *ex situ* modifications, the changes are incorporated after BC production and purification.[26]

As mentioned above, the desired properties could be obtained through *in situ* modifications, by changing culture conditions or carbon sources, or by adding different materials or molecules to the culture medium.[27] As an example, Singhsa *et al*. (2018) produced bacterial cellulose with six different carbon sources and five strains of *Komagataeibacter xylinus* in static and agitated culture conditions. As expected, the two culture methods produced distinct BC-based products. In static conditions, a BC membrane was formed at the air-liquid interface, while in agitated conditions BC particles were obtained (Figure 4). Moreover, it was observed that the BC crystallinity, the crystallite size, and the polymorphic distribution were not affected by the carbon sources used. However, different bacterial strains and incubation conditions promote changes in the crystallinity and mass fraction of the Iα allomorph.[32] Therefore, culture parameters play a crucial role in the overall characteristics of BC, so they must be chosen wisely and according to the intended application.[27]

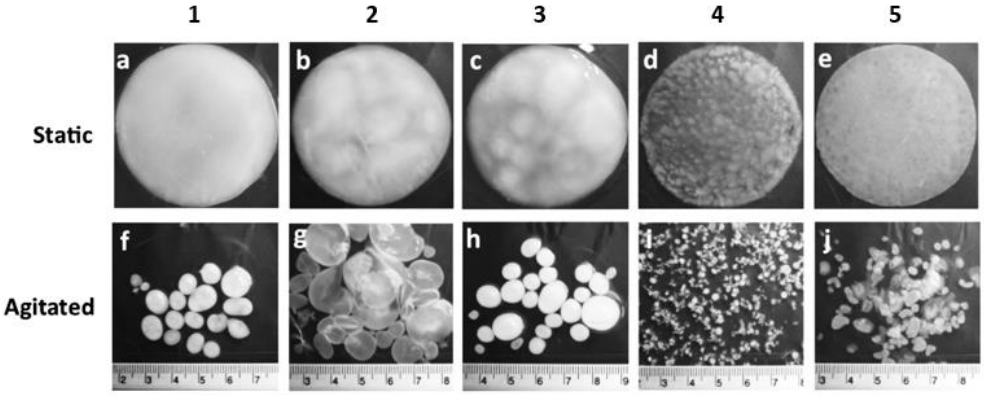

Figure 4. *Optical images of BC produced by five strains of K. xylinus (**1**-**5**) in static (**a**–**e**) and agitated (**f**–**j**) conditions, obtained by Singhsa et al. (2018). (Adapted from [32])*

Furthermore, several chemical techniques can be applied to modify BC, including acid hydrolysis, esterification, polymer grafting, cross-linking, sulfonation, and fluorescent labeling.[31] For instance, Orlando *et al*. (2020) functionalized BC by introducing antibacterial functional groups. Two active agents were used for the covalent derivatization of the hydroxyl groups of glucose, namely glycidyl trimethylammonium chloride and glycidyl hexadecyl ether. The modified hydrogel showed promising features as a wound dressing.[33]

Additionally, Keskin *et al*. (2017) produced keratin/BC nanocomposites via both *in* and *ex situ* modification approaches.[34] Both methods have yielded successful results, demonstrating enhanced skin keratinocytes and fibroblast cells' attachment, showing potential for skin tissue engineering.[34] However, even though in some cases *in situ* approaches are capable of changing the morphology and the properties of BC as intended, some materials, when added to the medium, can cause adverse effects, producing BC with undesired properties. Therefore, *ex situ* modifications are more suitable in these cases.[27]

On the other hand, different physical methods can be employed to modify BC in order to improve its performance, such as surface fibrillation, electric discharge, irradiation, electric currents, and physical cross-linking.[31,35] For instance, Fijałkowski *et al*. (2017) exposed bacterial cellulose to a rotating magnetic field during its cultivation. Changes in the microstructure, degree of porosity, and in water-related parameters were observed, namely increased water capacity, swelling ability, and rehydration capacity.[36]

Another example is the work developed by Paximada *et al*. (2016), which subjected bacterial cellulose suspensions to ultrasonic treatments for different time intervals. The authors observed that shorter treatments led to less bundled fibrils with decreased width, while longer treatments increased the width of fibrils due to an entanglement of their structure. The water holding capacity was proportional to the sonication time, while viscosity and stability increased for shorter treatments. It was concluded that shorter treatments may improve bacterial cellulose properties.[37]

Biomedical applications

The development and selection of a material always depend on its application since it must ensure the desired properties in order to serve its purpose without causing adverse and

undesirable reactions.[38] For example, a biomaterial for a biomedical application must be biocompatible, as it must not cause cytotoxicity or any other side effect, such as irritation, allergic reaction, inflammation, or rejection.[6,38]

As mentioned above, bacterial cellulose has several characteristics that may be advantageous for application in the biomedical field, for instance, its biocompatibility, high crystallinity, flexibility, porosity, stability, and purity. In addition, these characteristics and other properties can be adjusted or introduced, for example, by varying culture conditions or by chemical modifications, as previously referred, so that the biomaterial has a better performance.[6,29,39]

These unique properties of BC, which are the result of its structural and morphological characteristics, combined with the fact that it is a biomaterial generally recognized as safe (GRAS) by the FDA (Food and Drug Administration), stimulate its use in biomedical applications, for instance, in wound healing and drug delivery. Thus, bacterial cellulose is highly attractive since it can become a competitive product when applied successfully in medicine, offering several advantages over conventional materials.[13,40]

Wound healing

Skin plays an important role not only because it is the body's protective barrier but also because it performs many important functions. These functions may be disturbed or even lost when an injury, such as a burn or ulcer, occurs. Therefore, when the skin is injured, it must be immediately covered in order to promote healing, prevent contamination, and repair and restore its functions.[29]

However, wound healing is a complex and long-lasting process, so science has moved towards finding ways to accelerate it. The development of new wound dressings can allow the overcoming of the disadvantages associated with conventional ones, which can adhere to the wound, damaging it and slowing down the wound healing process.[18] On the other hand, the usage of new materials as wound dressings, such as biopolymers, is quite promising due to their excellent properties, including biocompatibility, biodegradability, and the ability to support cell growth.[7]

An ideal wound dressing must keep the wound moisturized, allow gas exchanging, absorb wound's exudate, accelerate re-epithelialization and healing time, reduce pain, and prevent infections.[41] A biomaterial capable of responding to these needs is bacterial cellulose. BC has a nanofibrillar structure that provides ideal conditions for wound healing, being able to display better performances than the most used wound dressings.[6,42]

Nowadays, there are several bacterial cellulose-based wound dressings available commercially, namely Biofill®, Bioprocess®, and Xcell®. These products arose in the 1990s when was carried out extensive research on bacterial cellulose application as a wound dressing.[40,42] For instance, Fontana *et al*. (1990) reported the first application of Biofill®, bacterial cellulose pellicles of varying thickness, as temporary skin substitutes.[43] The authors found many advantages, such as the immediate pain relief, a good barrier against infection, and faster healing. Biofill® has been used for several skin injury treatments such as severe body burns, chronic ulcers, and both donor and receptor sites in skin grafts.[43]

Some years later, in 2006, the first results of BC membranes' application to treat second- and third-degree burns were published by Czaja *et al*.[44] According to this study, cellulose membranes have important features that facilitate the wound healing process, such as a high degree of adherence to the body, maintenance of a proper environment around the wound, absorbance of the wound's exudates, the ability to observe the healing process, and oxygen permeability (Figure 5).[44]

Figure 5. *Bacterial cellulose dressing applied on a wound. (Adapted from [44])*

Moreover, BC can be conjugated with several molecules in order to develop dressings with improved properties, for instance, with enhanced cellular adhesion and tissue regeneration ability.[39] Also, BC does not show antibacterial properties, so it can be combined with other compounds, such as metal-based agents, antibiotics, or nature-derived antibacterial molecules to avoid infections.[18,39] These BC-based materials represent the next

generation of wound dressings and display great importance to future regenerative medicine.[39]

For instance, Lin *et al*. (2017) developed a dextran/BC hydrogel. Bacterial cellulose was combined with dextran, which plays a key role in wound healing, promoting cell growth and skin maturation. The *in vivo* test showed that the wound healing process was accelerated, and the skin maturation was facilitated, suggesting that dextran/BC hydrogel is a promising wound dressing for clinical applications, considering that its performance was better than commercial wound dressings. Although, additional studies are needed to investigate its application as a therapy for different types of wounds.[45]

On the other hand, Pal *et al*. (2017) functionalized bacterial cellulose with silver nanoparticles. The nanoparticles were photochemically deposited onto the BC network and chemically bonded to the cellulose fiber surfaces. The developed materials showed high antibacterial activity against Gram-negative bacteria. Besides, no significant amount of silver was released even after a long soaking time, indicating reduced risk of toxicity, and the materials were stable in moist environments, which may contribute to wound healing. Thus, considering all the properties of the materials, the authors conclude that they could be beneficial in general wound healing and surgical cases.[46]

Burn wounds that initially seem superficial can become full-thickness. In order to reduce burn wound progression, a cooling agent below room temperature is normally used, causing the patient a risk of hypothermia when the burned area is large. To overcome this problem, Holzer *et al*. (2020) used wound dressings based on non-pre-cooled BC with high-water content. The results showed that the burn was cooled, and that the intradermal temperature, as well as the damage of the tissue, were reduced, accelerating the wound healing.[47]

Additionally, Mohamad *et al*. (2019) assembled an acrylic acid/BC hydrogel loaded with keratinocytes and fibroblasts in order to treat burn wounds. *In vivo* studies showed that acrylic acid/BC hydrogel loaded with cells provoked faster healing than the hydrogel alone, which revealed better results when compared with the untreated group. Therefore, the acrylic acid/BC hydrogel has promising applications not only as a wound dressing but also as a cell carrier.[48]

More recently, Wahid *et al*. (2021) produced BC-based dressings with ε-polylysine, a polypeptide that exhibits antimicrobial activity, crosslinked by polydopamine. The resulting membranes showed sturdy antibacterial activity in both *in vitro* and *in vivo* assays. Besides, they also promoted a complete healing of infected wounds in the animal models, and the histological studies indicated the growth of smoother and greater newborn skin in comparison to the untreated group. Therefore, these membranes display an excellent potential as wound dressings.[49]

Drug delivery

As previously mentioned, besides wound healing, the application of bacterial cellulose on drug delivery has been drawing attention since BC-based materials can act as drug delivery systems due to their ability to incorporate and release bioactive molecules.[31,50]

The selection of the drug loading method should take into account its physicochemical characteristics, such as solubility, stability, and intended concentration and release rate. The loading procedure is also influenced by the type of BC (native wet, semi-dried, or freeze-dried), the modifications made, and the used bacteria strain.[51]

The loading techniques can be differentiated as *in situ*, if they occur during the assembly of the BC network, and *post*-synthesis, in case of occurring after its biosynthesis and purification. Usually, *in situ* loading techniques are less frequent due to, for example, the possibility of impairment of the producing bacteria by the bioactive molecule, and also because the added molecules can be removed during the washing process. On the other hand, *post*-synthesis procedures are the most used, including sorption techniques under submerse conditions and softly agitation. Although this procedure is easy to perform, it is also time-consuming. Therefore, faster alternatives, such as vortexing, can be used.[51]

One of the main advantages of BC-based materials as drug delivery systems is the ability to achieve the right drug concentration and to control its release rate, for example, by altering the average pore size.[6] Moreover, the material type of these drug delivery systems can be adjusted into microparticles, hydrogels, and membranes, according to the application and the type of administration, which could be internal, that is, oral administration, or external, namely transdermal and topical administration.[31]

There are several studies reporting BC-based materials as drug delivery systems for oral administration. For instance, Badshah *et al*. (2017) developed BC-based matrices loaded with famotidine, a histamine-2 blocker, and tizanidine, a skeletal muscle relaxant. The *in vitro* dissolution studies were in agreement with immediate release criteria since 80 % of drug release occurred in the first 15 minutes. The results also indicated that BC-based matrices have exceptional drug delivery characteristics. The authors conclude that the developed matrices in hydrated, semi-hydrated, and freeze-dried form have the potential for applications in single polymer-based oral drug delivery, overcoming the problems associated with conventional tablet dosage form.[52]

On the other hand, transdermal administration enables drug delivery into the systemic circulation through the skin. This type of administration offers a therapeutic effect with lower drug doses and reduces gastrointestinal side effects since it escapes the gastrointestinal tract. Nevertheless, large molecules cannot be delivered through transdermal administration given that they are not small enough to penetrate the skin.[31] BC has been widely explored as a transdermal drug delivery system. As an example, Silva *et al*. (2014) loaded BC membranes with diclofenac sodium salt, which is a typical non-steroidal anti-inflammatory drug. The *in vitro* release studies showed that the BC membranes provided similar permeation rates to those observed with commercial patches and lower than those obtained with a commercial gel. These results allowed the authors to conclude that the developed membranes have enormous potential for transdermal administration due to the simplicity of preparation and the ease of application.[24]

Additionally, topical administration is considered local once the drug is released at or near the target site. Thus, the required drug dosage is lower, and the efficiency is higher.[31] This type of administration is particularly used in wound healing since it enables certain features, such as antibacterial activity in order to prevent infections. For instance, Trovatti *et al*. (2011) prepared lidocaine/BC membranes. The *in vitro* permeation studies showed that the permeation rate of lidocaine in BC membranes was lower than those obtained with conventional delivery systems, indicating that the used methodology can be applied for the dermal administration of lidocaine concerning the ease of application.[53]

On the other hand, Liyaskina *et al*. (2017) saturated BC with fusidic acid, which is an antibiotic produced by the *Fusidium coccineum* fungus. The membranes presented high

antibacterial activity against *Staphylococcus aureus*, showing potential as wound dressings (Figure 6).[54] In a different study, de Mattos *et al*. (2018) loaded BC with polyhexamethylene biguanide, an antiseptic also known as polyhexanide or PHMB. The results showed that the developed wound dressing had an *in vitro* antiseptic efficacy against *Staphylococcus aureus* comparable to the clinically used wound dressings. The authors conclude that the method is suitable for use in clinical emergencies, which demand quick treatments with infection-reducing methods and biocompatible materials.[55]

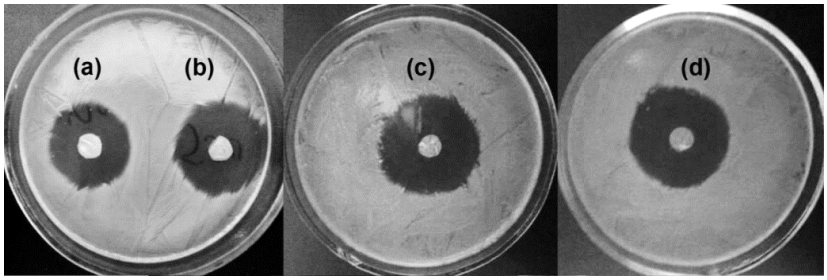

Figure 6. *Antibacterial activity of fusidic acid/BC membranes against S. aureus after 24 h of exposure, obtained by Liyaskina et al. (2017). The concentrations of fusidic acid increase from **a)** to **d)**. (Adapted from [53])*

Ye *et al*. (2018) grafted amoxicillin onto regenerated bacterial cellulose, which showed enhanced antibacterial activity against fungus, Gram-negative, and Gram-positive bacteria. Moreover, the healing of the wound infection in the *in vivo* model was accelerated, indicating that the developed material has a huge potential in wound dressing applications for clinical purposes.[56] Recently, Lemnaru *et al*. (2020) developed BC dressings loaded with amoxicillin and bacitracin. The studies showed a lower bacterial growth rate in the presence of the new dressings, demonstrating their potential in preventing infections and in promoting wound healing.[57]

In this sense, considering the ability of BC-based materials to incorporate and release bioactive molecules, the idea of incorporating metallodrugs with antibacterial activity into bacterial cellulose membranes in order to prevent infections and promote wound healing seemed a promising option that, as far as we know, has not been described in the literature yet. Therefore, for a better understanding, metallodrugs will be the focus from now on.

Metallodrugs

According to WHO, World Health Organization, antibiotic resistance is one of the biggest threats to global health since it is rising to dangerously high levels worldwide, and new resistance mechanisms are emerging and spreading around the globe, threatening the ability to treat common infectious diseases.[58] Nowadays, 700 thousand people die every year due to drug-resistant diseases, a number that can go up to 10 million in 2050.[59] The urgent need to combat the increasing resistance against antibiotics is reflected in the increased investment in the Global Antibiotic Resistance Market, which is expected to reach 10.81 billion euros by 2025.[60]

Metallodrugs with antibacterial activity emerge as a possible alternative to antibiotics. Several reports on antibacterial metallodrugs have been published as a possible answer to the "era of resistance".[61] However, even though the data suggest that metallodrugs are less likely to provoke resistance in bacteria, further work is required to answer with certainty to this question.[62] Metallodrugs can be defined as pharmacologically active metal complexes constituted by ligands, generally organic molecules, coordinated to a metallic center. Therefore, they display new properties and have enhanced biological activity due to the synergistic combination between the ligands and the metal.[63,64]

Comparatively to therapeutic organic molecules, metallodrugs possess several advantages since they have access to modes of action that cannot be achieved with organic molecules by themselves. For instance, the different geometries and the three-dimensionality of metallodrugs are generally associated with higher clinical success rates since their shape strongly influences their biological activity.[62]

The discovery of metallodrugs with potential for therapeutical applications started at the beginning of the 20th century when an arsenic compound, Salvarsan, became the first effective treatment of syphilis.[62] Years later, the discovery and clinical development of cisplatin, a platinum complex, was a milestone in the history of metallodrugs since it was highly effective against several types of cancer. However, cisplatin induced several side effects, such as toxicity and nausea, and some types of cancer acquired resistance to this metallodrug.[65]

These findings motivated the research for different approaches in order to develop metallodrugs more suitable for specific therapeutical applications.[66] For example, the simple combination of different metal ions and specific ligands allows the production of metallodrugs with novel structures and with new or improved biological activities, such as anti-inflammatory, anticancer, and antibacterial.[61] As mentioned above, several reports emphasizing the antibacterial activity of metallodrugs were published, mostly using antibiotics, or other molecules with similar biological activity, as ligands.[62] Nevertheless, interdisciplinary research is needed in order to advance the knowledge about metallodrugs and, consequently, to facilitate their design as effective antimicrobials, offering a realistic alternative to antibiotics.[61]

Metal complexes

Metal complexes are constituted by a central metallic ion or atom, which is coordinated to a certain number of molecules, atoms, or ions, named ligands. The central metal is a Lewis acid, since it can accept a pair of electrons, and the ligands are Lewis bases, once they can donate a pair of electrons. Metal complexes can be positively or negatively charged or neutral. A coordination compound is a neutral compound that comprises metal complexes.[67,68] The structure of metal complexes is defined by their coordination number and geometry. The coordination number is the number of ligands bonded to the central metal, and the coordination geometry is the geometrical arrangement of the ligands, as well as the symmetry of the whole complex, supposing that the metal is in a central position. The coordination number can predict the geometry of the metal complex (Figure 7). The most common coordination numbers are 4, 5, and 6, even though there are metal complexes with lower and higher coordination numbers.[67,68]

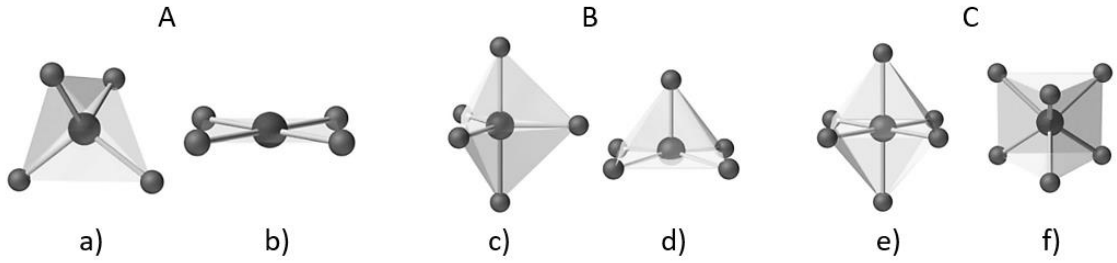

Figure 7. *Most frequent geometries in metal complexes.* ***A.*** *Coordination number: 4. a) Tetrahedral; b) Square Planar.* ***B.*** *Coordination number: 5. c) Trigonal bipyramidal; d) Square pyramidal.* ***C.*** *Coordination number: 6. e) Octahedral; f) Trigonal prismatic. (Adapted from [68])*

As previously mentioned, a ligand is an atom, ion, or molecule that has one or more donor atoms. Donor atoms have pairs of electrons available to coordinate with the central metal, and generally, they are non-metallic, for example, carbon, nitrogen, and oxygen. Ligands are classified electronically, according to the number of electrons donated to the central metal, and structurally, according to the number of connections established with the central metal, also known as denticity. For instance, a ligand bonded by one atom is defined as monodentate, by two atoms as bidentate, and so on. A polydentate ligand has several donor atoms and can coordinate simultaneously through them to one or more central metal. Moreover, a bridging ligand coordinates simultaneously to more than one metal through one or more donor atoms, forming a polynuclear specie.[67,68]

When a bidentate ligand coordinates its two donor atoms to the same central metal, a chelate ring is formed. A chelate is a metal complex once a polydentate ligand, the chelating agent, bonds to the central metal by one or more atoms, establishing several chelate rings. The chelate effect announces that monodentate ligands form, with a certain metal, less stable complexes than polydentate ligands with the same donor atoms. In other words, the stability of the complexes increases with the number of possible chelate rings.[67]

Metal complexes have unique electronic, magnetic, and spectroscopic properties since the oxidation state of the metal can vary, as well as the numbers and types of coordinated ligands, allowing various coordination numbers and geometries. The metal is a structural center that organizes the ligands, which can not only control the reactivity of the metal itself but also play a critical role in determining the nature of the secondary coordination sphere, which is biologically relevant. Moreover, ligands can suffer modifications mediated by the metal. All these variables provide metal complexes an

enormous diversity in their design and, consequently, great potential for therapeutic purposes.[70,71]

Metal ions

As previously mentioned, metal ions offer unique properties and play a critical role in metal complexes, offering several advantages that are lacking in organic molecules. To a better understanding, some of these properties and advantages are mentioned and discussed below.[64]

- Charge variation: In aqueous solution, metal ions can bind to molecules and/or other ions and, depending on the ligand and the coordination number of the resulting complex, its charge can be positive, neutral, or negative, forming cationic, neutral, or anionic species, respectively.[64] While metal ions are electron deficient, biological molecules are electron-rich. These opposing charges are attracted, which leads to a tendency for metal ions to bind and interact with biological molecules.[70]
- Structure: As mentioned before, metal complexes can exhibit a great variety of structures with different coordination numbers and geometries. The overall shape of the complex varies depending on the metal and its oxidation state.[68]
- Lewis acid properties: Metal ions can accept electrons and polarize the chemical bonds of the coordinated ligands, facilitating their hydrolysis.[64]
- Partially filled *d* shell: The electronic and magnetic properties of metal complexes are influenced by the variable number of electrons in the *d* shell.[72]
- Redox activity: Metals tend to undergo oxidation and reduction reactions due to the multiplicity of oxidation states that they can display.[68]

Metal ions play important roles in living beings since they are involved in crucial biochemical reactions, being able to act as cofactors, catalysts, or stabilizers of several proteins and enzymes. Moreover, numerous biological processes require metal ions to function properly, for example, the role of iron in carrying oxygen throughout the body and shuttling electrons.[70,73] Besides, deficiency of some metal ions can lead to diseases like anemia in case of iron insufficiency, growth retardation resulting from a diet deprived of zinc, and heart disease in infants due to low copper intake.[70] However, high concentrations

of metal ions may result in toxicity. Therefore, it is extremely important to maintain the optimum levels of these trace elements.[74]

Cobalt

Cobalt is an essential trace element for the human body since it plays a significant role in several biological processes. Cobalt is a key constituent of vitamin B12 (cobalamin), where it adopts an octahedral geometry and exists in the +1-oxidation state, but it is also able to vary its oxidation state between +2 and +3. Vitamin B12 is important in different processes, such as DNA synthesis and regulation, cell growth, the formation of red blood cells, and maintenance of normal brain and nerve function.[75,76] Moreover, cobalt has a considerable role in the synthesis of amino acids and neurotransmitters.[77]

Cobalt ions can get into the human body through food, the skin, the respiratory system, and as a component of biomaterials. After entering the body, cobalt ions bind with proteins and are transported to the tissues and cells through the bloodstream. Food, namely green vegetables and fresh cereals, is the most responsible pathway for the intake of cobalt, most of which is inorganic. Inorganic forms of cobalt are toxic since they can cause harmful effects in the cells the longer they stay in the human body.[77] Nevertheless, cobalt is less toxic than non-essential metals, and the human body possesses mechanisms to overcome its overload.[75] However, when the excess level of cobalt is not controlled by these mechanisms, it can cause hypothyroidism, fibrosis in the lungs, asthma, and overproduction of erythrocytes. On the other hand, cobalt deficiency can cause disturbances in vitamin B12 synthesis. It is also associated with hypothyroidism, anemia, and an increased risk of developmental abnormalities in infants.[77]

Dwyer *et al*. (1952) evaluated the biological properties of cobalt complexes for the first time.[75,78] Since then, several cobalt complexes, usually with an octahedral geometry, have been reported due to their biological potential. These complexes present many advantages, such as availability, ease of synthesis, and aqueous stability. Besides, the coordination between cobalt ions and ligands directly enhances their biological activity. Until now, literature reports demonstrated that cobalt complexes have a huge potential for

wide-ranging therapeutical applications with diverse modes of action, but there is much more to explore and many questions to answer.[75]

Copper

Copper is the most studied metal, and it is essential for all living beings. This metal plays a crucial role in numerous biological processes like wound healing, the formation of the immune cells, maintenance of healthy skin as well as a healthy and effective immune response, and in the growth, structural integrity, and function of blood vessels.[79] Moreover, copper is involved in many metabolic reactions since it is an indispensable constituent of several enzymes such as cytochrome oxidase, peroxidase, lactase, and catalase.[77,80]

Copper is not formed in the body, so it must be obtained from water and food, mainly cereals and dried fruits.[77,79] Copper is absorbed in the gut, then it bounds to albumin and is transported to the liver where it is processed. After, this metal is distributed to other tissues through the bloodstream by the protein ceruloplasmin.[77] This way, the digestive system assimilates the amount of copper necessary for good health, and the excess is excreted.[79] On the other hand, despite copper deficiency is rare among healthy people, it frequently occurs in infants. Copper deficiency can decrease the number of white blood cells, cause fatigue, and develop osteoporosis and anemia.[77] Besides, there are some inherited disorders, like Wilson's and Menke's diseases, which incite disturbances in the management of the levels of copper.[79]

Copper complexes have been intensively studied over the last decade, existing several reports on their design, synthesis, and development. Nowadays, these complexes are considered the best alternative to cisplatin. Copper offers unique properties and advantages to metal complexes, such as the capacity to vary its oxidation states between +1, +2, and +3, being the +2 oxidation state the most common. Cu(II) complexes usually display square pyramidal or octahedral geometries, although complexes with other geometries are known. Besides, copper can also enhance the biological affinity of certain molecules, producing a synergistic effect. Therefore, copper complexes have the potential to display several biological activities. However, their mechanisms of action are not clear yet, so studies must

continue to be carried out so that their therapeutic applications can be well established without pending doubts.[79,80,81]

Nickel

Although the biological activity of nickel is slightly uncertain in humans, its importance is widely recognized. Nickel is found in nucleic acids, particularly RNA, and it might influence proteins' structure or function.[77] Nickel is also present in some enzymes involved in the use and/or production of gases, which play central roles in the cycles of carbon, oxygen, and nitrogen.[76] Moreover, it is thought that nickel is a cofactor involved in the activation of some of the enzymes related to the metabolism of glucose. Therefore, additional research is needed in order to better understand the real biological role of nickel in the human body.[77]

One pathway for nickel intake is food, for instance, vegetables, fruits, and cereals, but it can also occur through breathing and smoking. Nickel is essential for humans in small quantities. The excess of this metal can cause several health problems such as cancer and tissue damage. On the other hand, nickel deficiency is not able to cause severe diseases, only biological and biochemical changes like disturb the incorporation of calcium into the skeleton, reduce iron resorption, and affect carbohydrate metabolism.[77]

Over the last years, there has been an increased interest in nickel complexes, which commonly display tetrahedral, square planar, or octahedral geometries. However, in comparison with other transition metals, reports on nickel complexes are less frequent in literature, maybe due to the lack of knowledge concerning the biological role of nickel in the human body. Moreover, nickel complexes display disadvantages when it comes to their synthesis and understanding their mode of action. Nevertheless, some studies report nickel complexes with different biological activities, which demonstrates their potential as therapeutical agents.[68,71]

Zinc

Zinc is the second trace element most abundant in the human body and is very important in biological systems due to certain chemical properties. For instance, zinc is associated with more than 300 enzymes, which play vital roles, for example, in the synthesis of proteins and nucleic acids. Moreover, this metal is crucial in cellular growth and differentiation, in the regulation of the transcription and translation of the genetic message, and in the metabolism of lipids, carbohydrates, and energy. Besides, zinc is essential for healthy skin and immune system, playing a critical role against infections.[77,82,83]

The principal intake of zinc is through food, mainly meat, seafood, legumes, and dried fruits. However, there are many people with zinc deficiency, which is an important public health problem that happens mostly in developing countries. Zinc deficiency can cause severe effects, especially in young children, like reduced immune function, weight loss, skin lesions, and delayed wound healing. These problems can be overcome by zinc supplementation and food fortification.[77,82]

Furthermore, zinc complexes with organic molecules are strong but flexible, which facilitates the modification of cellular membranes and biological molecules, such as nucleic acids and proteins.[82] In particular, the divalent zinc ion is redox inactive, since because of its d^{10} configuration, it does not show variable valence, so it does not have ligand field constraints on its coordination. Thus, in this case, only ligand size and charge determine the coordination number and geometry of the complexes, being the tetrahedral geometry the most commonly found.[83,84] Therefore, zinc offers metal complexes interesting properties, for instance, flexible coordination and fast ligand exchange. Nonetheless, there is still a lot to discover about zinc complexes, for example, by exploring new designs, evaluating their biological potential, and understanding their mechanisms of action.[82]

N-donor ligands

N-donor ligands are generally heterocyclic organic molecules that are able to act as chelating agents since they can coordinate to metal ions through nitrogen atoms. Several molecules belonging to different families can be used as N-donor ligands. These ligands play interesting roles in metal complexes once their incorporation can lead to better biological

affinity because it facilitates the binding of the complexes with biological molecules such as DNA.[85] Moreover, numerous N-donor ligands exhibit biological activity, for example, antibacterial and anticancer, which can be enhanced by the coordination with the metal ion. Therefore, these metal complexes have a high potential to act as therapeutical agents since the use of N-donor ligands is a tremendous asset once they can not only give stability to the complexes but also add significant biological properties.[61]

1,10-phenanthroline

1,10-phenanthroline plays an important role in the development of novel metal complexes by acting as a chelating agent since it has available atoms to coordinate with metal ions. This coordination ability is determined by the structural features of the molecule, which is a hydrophobic, rigid planar, and electron-poor heteroaromatic system with nitrogen atoms perfectly placed in juxtaposition, which favors metal binding (Figure 8).[86] These properties also contribute to its capacity of stabilizing metal ions in lower oxidation states, presenting a charge-transfer character, and acting as an intercalating or groove binding specie with DNA and RNA.[86,87] Besides, 1,10-phenanthroline is also capable of cleaving DNA.[86]

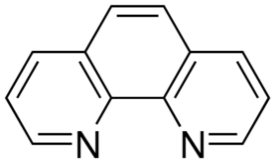

Figure 8. Molecular structure of 1,10-phenanthroline. (Adapted from [85])

Moreover, 1,10-phenanthroline exhibits significant *in vitro* antimicrobial activity against several bacterial and fungal pathogens because of its ability to act as a chelator and to sequester metal ions in biological systems. In particular, 1,10 phenanthroline is able to inhibit metalloproteins, disturb microbial cell homeostasis, and interfere with metals acquisition, bioavailability, and metabolism for vital reactions. All of these mechanisms can lead to the obstruction of microbial growth, nutrition, development, cellular differentiation, and adhesion, being also crucial in preventing the *in vivo* infection progression.[61]

The combination of all these remarkable chemical, structural, and biological features aroused curiosity in metal complexes with 1,10-phenanthroline, which have been intensively studied for their properties. Among other advantages, these complexes demonstrate improved activity in relation to the free molecule.[61,86] Nevertheless, their mechanisms of action and their difference from the resistance-prone antibiotics are not completely understood yet, whereby studies must continue to strive.[61]

2,2'-bipyridine

2,2'-bipyridine plays an important role in coordination chemistry since it is one of the most used ligands.[89] This chelating agent exhibits two nitrogen atoms almost in an idyllic configuration to coordinate with a metal center, which leads to the formation of extremely stable complexes, even when the metal ions used are more labile (Figure 9).[90] In the solid-state, molecules of 2,2'-bipyridine are strictly planar with two pyridine rings in a *trans* configuration. Due to structural features, these molecules are involved in hydrogen bonding, host-guest or aromatic-aromatic interactions, and charge-transfer.[89]

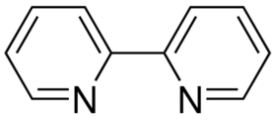

Figure 9. *Molecular structure of 2,2'-bipyridine. (Adapted from [88])*

In the last thirty years, several metal complexes with 2,2'-bipyridine have been described and they are extremely important given their contribution to the understanding of the complexation process of metal ions, in particular the thermodynamics, kinetics, and bonding.[89,90] Generally, 2,2'-bipyridine coordinates as a bidentate ligand by both nitrogen atoms to the same metal center, but it can also act as a monodentate or bridging ligand in relation to multiple metal ions.[89] 2,2'-bipyridine complexes with nearly every metal in the periodic table were reported on the literature, as well as with numerous biologically active molecules, demonstrating the wide range of possibilities in the development of novel metal complexes with 2,2'-bipyridine.[90]

2,2'-dipyridylamine

2,2'-dipyridylamine is a distinguished chelate agent given that it is able to form hydrogen-bonded networks through the active amine (Figure 10). Besides, the amine group confers advantages to 2,2'-dipyridylamine over other N-donor ligands, such as 2,2'-bipyridine and 1,10-phenanthroline, being one of them the ability to form superstructures.[92] Although only recently 2,2'-dipyridylamine has attracted increasing interest, their first metal complexes were reported sixty years ago, and since then, they have been demonstrating high structural flexibility.[93,94]

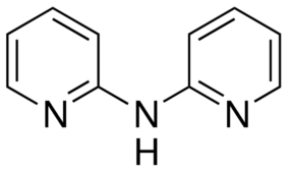

Figure 10. Molecular structure of 2,2'-dipyridylamine. (Adapted from [92])

In mononuclear complexes, 2,2'-dipyridylamine can act as a monodentate ligand, through only one nitrogen atom of the pyridine ring, and as a bidentate ligand, via both nitrogen atoms of the pyridine rings or through one nitrogen atom of the pyridine ring and the deprotonated nitrogen atom of the amide group. Nonetheless, this molecule is also able to chelate with several metal ions via diverse coordination modes.[94] Although 2,2'-dipyridylamine is not as used as other N-donor ligands, it has been drawing attention mainly due to its coordination versatility and to its capacity of stabilizing the metal complexes.[93,94]

4,4'-bipyridine

4,4'-bipyridine is a good chelating agent due to its exobidentate nature since it has two binding sites arranged in a divergent fashion; its linear and rigid structure, which helps to predict the resultant geometries; and its appropriate length (Figure 11).[96,97] These features are particularly suited for constructing a variety of networks with several transition metals.[96] In these networks, the proper length of 4,4'-bipyridine allows the creation of cavities of molecular dimension, which give the networks the potential to act as microporous solid materials.[96,98]

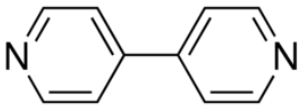

Figure 11. *Molecular structure of 4,4'-bipyridine. (Adapted from [96])*

The geometry of the networks depends on several factors, namely the coordination geometry of the metal, the ratio ligand:metal, and the presence of additional molecules and anions. Differently from metal complexes, networks formed by the coordination between metals and 4,4'-bipyridine can occur in distinct geometries, for instance, linear or zigzag chain, ladder, and square or hexagonal grid.[96,98] Due to the structural and geometric features, these networks present useful inclusion properties such as size and shape specificity, ion exchange, adsorption/desorption, and catalysis.[97] Therefore, the coordination of metals and 4,4'-bipyridine forms interesting structures with high potential. Although there are many reports on several networks with numerous functional properties, there are still many challenges to overcome, being the prediction of their geometry of coordination one of them.[96]

Antibiotics: Quinolones

In 1947, Waksman defined an antibiotic as a "chemical substance produced by microorganisms, which has the capacity to inhibit the growth of and even to destroy bacteria and other microorganisms".[100] Nowadays, despite several definitions coexist in literature, the most accepted one is that antibiotics are antibacterial agents, in other words, molecules that are selectively against bacterial life. Therefore, antibiotics are used to treat bacterial infections.[101,102]

The first antibiotic was described in 1893, when Bartolomeo Gosio obtained a product from the cultivation of *Penicillium brevi-compactum* that showed antibiotic activity against *Bacillus anthracis*. This discovery remained forgotten until 1912, when Carl Alsberg and Otis Black resynthesized the substance and named it mycophenolic acid. However, the discovery of penicillin in 1929 by Alexander Fleming is considered the "birth of the antibiotic era", even though Fleming was not able to produce considerable amounts of penicillin neither to elucidate its structure.[101]

Considering the wide array of known antibiotics, a need to classify them surged. Although they can be classified in various ways, the most common classification is based on their molecular structure, spectrum of activity, and mode of action. Antibiotics of the same class generally have identical side effects, toxicity, and effectiveness. Some of the most common classes are, for example, β-lactams, tetracyclines, and quinolones.[103]

Quinolones are one of the most successful classes of synthetic antibiotics.[104] The first reported quinolone was nalidixic acid, in 1962, resulting from an impurity isolated during the synthesis of the antimalarial drug chloroquine.[101] This way, nalidixic acid, which is considered a first-generation quinolone, triggered the development of other generations with improved activity.[104] Quinolones have many advantages such as high potency, convenient formulations, excellent bioavailability, broad spectrum of activity (including Gram-positive, Gram-negative, and atypical organisms), and low incidence of side effects.[105,106]

The core structure of quinolones is a bicyclic structure related to the compound 4-quinolone (Figure 12).[105] Quinolones exert their antibacterial activity by interfering with DNA synthesis and replication by changing the action of DNA gyrase and DNA topoisomerase IV, which are the responsible enzymes for the unwinding process of the double-stranded DNA into two single-stranded structures that allow the transcription. Quinolones bind to the enzyme-DNA complexes, causing a conformational change in the enzyme, which leads to DNA cleavage and, consequently, to cell death.[105,106]

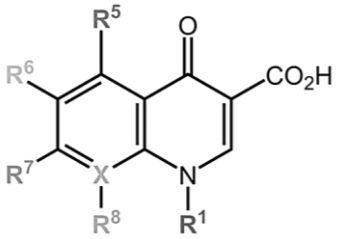

Figure 12. *Core structure of quinolones. The radicals R1, R5, R6, R7, and R8 indicate possible positions for structural modification; X generally corresponds to a C or N atom; In fluoroquinolones, R6 is a F atom. (Adapted from [102])*

The overuse of quinolones led certain bacteria to produce resistance against these antibiotics through different mechanisms, which represents a severe global threat. Therefore, there is an urgent need to discover different routes to develop novel quinolones that are less susceptible to provoke side effects, more cost-effective, with better properties, and with slightly different modes of action in order to prevent bacterial resistance, so that the clinical

utilization of these new antibiotics is not narrowed. Nevertheless, while the search for the next generation quinolones is ongoing, some quinolones, such as levofloxacin and ciprofloxacin, are still used in clinical practice due to their increased antibacterial range and advantageous properties.[107]

The development of bacterial resistance served as a motivation for the breakthrough of metal complexes with quinolones, taking into account their excellent coordination capacity mainly due to their chemical structure.[108] In metal complexes, quinolones can act as a monodentate, bidentate, or bridging ligand. Generally, quinolones coordinate in a bidentate mode, through two oxygen atoms, one of the deprotonated carboxylic group and the other of the ring carbonyl.[109] The coordination of quinolones to a metal ion cause a synergistic effect that can not only enhance the pharmacological activity of the antibiotics but also create new biological properties, such as antifungal, antiparasitic, antiviral, and anticancer.[110]

Levofloxacin

Levofloxacin (Figure 13) is a third-generation quinolone and the *L*-isomer of ofloxacin, and it has a broad spectrum of activity against Gram-positive, Gram-negative, and anaerobic organisms.[105,111,112] Thus, levofloxacin is used in the treatment of several infections, such as skin, respiratory, and genitourinary.[113] Besides, this antibiotic shows a good tolerability profile, without provoking phototoxicity and other several side effects generally associated with quinolones. Therefore, levofloxacin is an important option for the treatment of bacterial infections due to the capacity of combining efficacy and tolerability.[112]

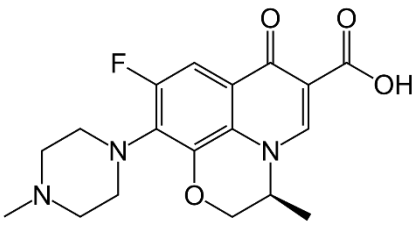

Figure 13. *Molecular structure of levofloxacin. (Adapted from [108])*

In Europe, a levofloxacin treatment must last between 7 to 14 days, with a dosage between 250 mg and 500 mg once daily. This treatment can cause several adverse events, being the most common nausea, constipation, and insomnia. Levofloxacin is usually contraindicated in people with less than 18 years, with a history of tendon disorders related to quinolones administration, and in pregnant or breastfeeding women. Generally, levofloxacin administration is oral or intravenous, and it rapidly spreads into the different tissues and cells, where it undergoes limited metabolism, being posteriorly excreted in the urine.[112]

In literature, many reports study the coordination of levofloxacin with metal ions in order to synthesize novel metal complexes with enhanced antibacterial activity and new biological effects. Therefore, studies must continue not only to evaluate the real therapeutical potential of levofloxacin complexes but also to elucidate their mode of action, understand if they are susceptible to bacterial resistance, discover side effects, and to contribute to the urgent search of new drugs.[63,108]

Ciprofloxacin

Ciprofloxacin (Figure 14) is a broad-spectrum antibacterial agent since it is highly effective against Gram-negative and Gram-positive bacteria, although its activity against anaerobic organisms is limited.[114] Therefore, this second-generation quinolone can be used to treat numerous infections, such as skin, gastrointestinal, and respiratory, and it is particularly powerful in diseases caused by Gram-negative pathogens. Besides potent antibacterial activity, ciprofloxacin presents a good tolerability profile, well-established safety aspects, and good tissue penetration.[114,115] This way, the combination of all these characteristics makes ciprofloxacin a forceful agent to treat bacterial infections.[114]

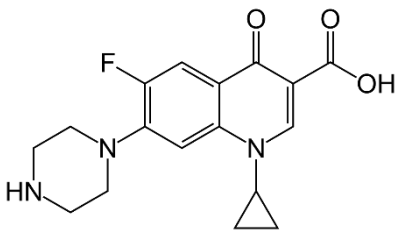

Figure 14. *Molecular structure of ciprofloxacin. (Adapted from [113])*

In the United States, the usual treatment duration is 7 to 14 days, even though some diseases can be treated in less than 7 days. The administration can be oral or intravenous, and the dosage is between 200 and 1500 mg twice a day, depending on the type of disease and administration. Although ciprofloxacin is rarely associated with phototoxicity, it frequently causes side effects such as vomiting, nausea, and severe headache. Ciprofloxacin is usually contraindicated in patients with less than 18 years, in pregnant and breastfeeding women, and persons with hypersensitivity to quinolones. Generally, ciprofloxacin is not metabolized in the organism, so most of it is excreted in the urine and feces.[114]

The number of publications on ciprofloxacin complexes is relatively low when compared to other antibiotic complexes and, consequently, their properties and mechanisms of action are not clear yet. As mentioned before, the coordination between metal ions and biologically active molecules can decrease their toxicity, enhance their activity, and maybe overcome the resistance to their action. Therefore, ciprofloxacin complexes are very promising once they are able to combine the advantages brought by the synergistic effect caused by the coordination with the intrinsic properties of ciprofloxacin.[63,117]

State of the art

As previously mentioned, many reports on metal complexes have been published in the literature for many years. Generally, these reports describe the synthesis, structural characterization, and biological evaluation of the metal complexes. Regarding their synthesis, the most used methodology is one-pot synthesis. It is a sustainable and efficient method since it is able to minimize chemical waste, simplify practical issues, and save time while several formation and transformation steps are carried out in a single pot.[118] The general process for synthesizing metal complexes is to add a solution of the metal salt to a solution of the ligands. Usually, the solutions are aqueous, ethanolic, or methanolic. This process can involve additional procedures, such as stirring, reflux, or temperature, which increment the solubility of the different species as well as promote their mixture and interaction. Examples are given by Chohan *et al.* (2005), Galani *et al.* (2014), and Akram *et al.* (2015).[117,119,120]

Once the final solution is prepared, it can be filtered in order to obtain a limpid solution that typically is left for slow evaporation until a precipitate is formed, as described

in Al-Saif *et al*. (2018).[121] Nevertheless, ways to accelerate the evaporation process can also be used. For instance, Sousa *et al*. (2012) concentrated the final solution on a rotovapor and posteriorly obtained a solid product just after a few hours left at room temperature.[122] Another approach is the solvothermal method, which is performed in sealed recipients containing the final solution, where the solvent reaches temperatures above its boiling point due to the increase of autogenous pressures.[123] For example, Dojer *et al*. (2016) synthesized nickel(II) complexes through solvothermal synthesis.[124]

Another interesting method that has emerged as a promising alternative to slow evaporation is microwave-assisted synthesis. In this approach, microwave energy interacts with solvent molecules, leading to their rotation and, consequently, increasing their kinetic energy and temperature. Thus, the heating of the final solution is more uniform since the energy is generated across it, instead of being provided from an external source. Microwave-assisted synthesis is considered a sustainable chemistry method since it has several advantages, such as short reaction times, low energy consumption, and high efficiency. Besides, in microwave-assisted synthesis, the energy interacts only with the solvent without affecting the remaining reagents.[125] To the best of our knowledge, levofloxacin and ciprofloxacin complexes produced by microwave-assisted synthesis have not been reported in the literature yet. However, Ikotun *et al*. (2019) synthesized a cobalt(II) complex through this method.[126]

On another note, several reports on levofloxacin complexes have been published, and it is extremely important to characterize them and evaluate their biological activity in order to understand their potential as therapeutical agents. For example, Al-Saif *et al*. (2018) synthesized six cobalt(II) complexes with different quinolones, being levofloxacin one of them. In this complex, designated as $[Co(Lev)_2(Cl)_2(H_2O)_2]\cdot 4H_2O$, the Co(II) central metal is coordinated to six ligands: two levofloxacin molecules, two chloride ions, and two water molecules. The quinolones drugs act as unidentate through the nitrogen atom of the pyridone moiety, and the complex exhibits an octahedral geometry. Besides, it has four uncoordinated water molecules. The authors also studied the biological activity of the synthesized complexes, which demonstrated higher antibacterial activity than the free ligands.[121]

Moreover, Sousa *et al*. (2012) synthesized $[Cu(Lev)(Phen)(H_2O)](NO_3)\cdot 2H_2O$, a metal complex where the Cu(II) centre is coordinated to one water molecule, one 1,10-phenanthroline molecule through two nitrogen atoms, and one levofloxacin molecule via

two oxygen atoms, from the carbonyl and carboxyl groups. Therefore, the Cu(II) central metal is penta-coordinated, 1,10-phenanthroline and levofloxacin molecules act as bidentate, and the complex exhibits a distorted square pyramidal geometrical structure. Outside the coordination sphere, the complex has one nitrate counter-ion and two uncoordinated water molecules. The biological studies showed that the complex is as efficient as an antimicrobial as the free antibiotic.[122]

Akram *et al*. (2015) synthesized Co(II), Cu(II), and Ni(II) complexes with levofloxacin and 2,2'-bipyridine. The general designation of the complexes is [M(Lev)(Bipy)Cl], where M is the central metal, which is coordinated to one levofloxacin molecule, one 2,2'-bipyridine molecule, both in a bidentate mode, and one chloride ion. Thus, the metal is penta-coordinated, and the complexes exhibit a distorted square pyramidal geometry. The biological studies showed that all of the metal complexes interact with DNA and that the Ni(II) complex demonstrated significant inhibition of pathogenic bacteria.[120] More recently, Mubarak *et al*. (2021) synthesized two Cu(II) complexes with levofloxacin and two distinct N-donor ligands, being 2,2'-bipyridine one of them. In this complex, $[Cu(Lev)(H_2O)(Bipy)](NO_3)\cdot 2.5H_2O$, the Cu(II) centre is coordinated to one levofloxacin molecule, one 2,2'-bipyridine molecule, both in a bidentate mode, and one water molecule, displaying a distorted square pyramidal geometry. The biological studies showed that the complex exhibited higher antibacterial activity against *P. mirabilis* and *B. subtilis* than levofloxacin.[127]

Additionally, Galani *et al*. (2014) synthesized two novel zinc complexes with 1,10-phenanthroline and 2,2'-bipyridine. The first complex is [Zn(Lev)(Phen)Cl]·MeOH, and the second one is [Zn(Lev)(Bipy)Cl]·2MeOH. In both complexes, the Zn(II) centre is coordinated to one levofloxacin molecule, one N-donor ligand molecule, both acting as bidentate agents, and one chloride ion. Outside the coordination sphere, the complexes have one and two methanol molecules, respectively. The biological studies showed that the two complexes exhibit improved antibacterial activity in comparison with the free drug.[119]

Recently, Kumar *et al*. (2019) synthesized copper complexes with levofloxacin and two other N-donor ligands, being 2,2'-dipyridylamine one of them. In this complex, $[Cu(Lev)(Dipy)Cl]^+$, the Cu(II) central metal is coordinated to one levofloxacin molecule, one 2,2'-dipyridylamine molecule, both in a bidentate mode, and one chloride ion. Thus, the complex exhibits a square pyramidal geometrical structure. The authors also realized a

biological evaluation, which allowed them to verify that the complex displayed higher antibacterial activity than the free levofloxacin.[128]

On the other hand, metal complexes with ciprofloxacin also have been reported. For instance, some years ago, Chohan *et al*. (2005) synthesized Co(II), Cu(II), Ni(II), and Zn(II) complexes with ciprofloxacin. The authors proposed two types of complexes: $[M(Cip)_2(H_2O)_2]$, where M is Co(II), Ni(II), or Zn(II), and $[M(Cip)_2]$, where M is Cu(II). In the first three complexes, the central metal is coordinated to two ciprofloxacin molecules in a bidentate mode, and two water molecules. Thus, the complexes exhibit an octahedral geometry. In the last complex, the Cu(II) centre is coordinated to two ciprofloxacin molecules, which also act as bidentate ligands. Therefore, it has a square planar geometrical structure. The biological studies showed that the synthesized metal complexes exhibited enhanced antibacterial activity in comparison with the parent antibiotic.[117] Similar Co(II) and Ni(II) complexes with ciprofloxacin were obtained years later by Horozić *et al*. (2018).[129]

It is important to mention that a large part of the levofloxacin and ciprofloxacin complexes reported in the literature are not in the form of single crystals with adequate size and quality to be analyzed by single-crystal X-ray diffraction, so their characterization is based on other experimental techniques that allow to infer and propose structures. Nevertheless, these complexes also exhibit a promising biological activity, as described by Chohan *et al*. (2005), Galani *et al*. (2014), and Akram *et al*. (2015).[117,119,120]

Objectives

In this context, the main goals of this dissertation are the synthesis and characterization of metal complexes with antibacterial activity, and their incorporation into bacterial cellulose membranes for wound healing applications. In order to achieve the main goals, several specific objectives have to be accomplished: (1) synthesis and characterization of the metallodrugs; (2) *in vitro* evaluation of the antibacterial activity of the synthesized complexes; (3) incorporation of the selected coordination compounds into bacterial cellulose membranes; (4) characterization of BC-metallodrugs membranes and *in vitro* release assays.

CHAPTER 2 – EXPERIMENTAL PROCEDURES

Reagents and Materials

Synthesis of the complexes

Nickel(II) chloride hexahydrate ($NiCl_2 \cdot 6H_2O$), zinc(II) chloride ($ZnCl_2$), and levofloxacin ($C_{18}H_{20}FN_3O_4$) were purchased from Sigma-Aldrich Co. Cobalt(II) chloride hexahydrate ($CoCl_2 \cdot 6H_2O$) was obtained from Panreac. Copper(II) chloride dihydrate ($CuCl_2 \cdot 2H_2O$) and acetone (CH_3COCH_3) were obtained from CARLO ERBA Reagents. Potassium hydroxide (KOH) was purchased from Pronalab and 1,10-phenanthroline ($C_{12}H_8N_2$) from Alfa Aesar. 2,2'-Bipyridine ($C_{10}H_8N_2$), 2,2'-dipyridylamine ($C_{10}H_9N_3$), and 4,4'-bipyridine ($C_{10}H_8N_2$) were obtained from Fluka. Ciprofloxacin ($C_{17}H_{18}FN_3O_3$) was purchased from TCI. The solvents, methanol (CH_3OH) and ethanol (C_2H_5OH), were of analytical grade and purchased from VWR Chemicals. All reagents and solvents were used as received.

Characterization of the complexes

Potassium bromide (KBr) FTIR grade was obtained from Sigma-Aldrich Co.

Antibacterial studies

The bacterial strain used, *Staphylococcus aureus* (ATCC 6538), was purchased from American Type Culture Collection (ATCC). Mueller-Hinton Agar (MHA), Mueller-Hinton Broth (MHB), and ciprofloxacin were obtained from Liofilchem. Imipenem and ampicillin were purchased from Oxoid.

BC production and purification

Glucose was purchased from Scharlau and disodium phosphate (Na_2HPO_4) from Merck. Yeast extract and peptone were obtained from Oxoid. Citric acid was purchased from Panreac.

Dissolution assays

Phosphate-buffered saline (PBS) pH 7.4 (0.01 M; with NaCl 138 mM and KCl 2.7 mM) was purchased from Sigma-Aldrich Co.

Methods and Procedures

Synthesis of the complexes

Complexes of cobalt(II), copper(II), nickel(II), and zinc(II) with two different antibiotics, levofloxacin or ciprofloxacin, and four different N-donor ligands, 1,10-phenanthroline, 2,2'-bipyridine, 2,2'-dipyridylamine, or 4,4'-bipyridine, were synthesized. Several experimental procedures were performed in order to obtain different metal complexes through distinct techniques.

Figure 15 represents one of the carried out experimental procedures, in which levofloxacin complexes were synthesized. Levofloxacin (289.2 mg; 0.8 mmol) was dissolved in methanol (20 mL) after stirring. Then, the metal salt, $CoCl_2 \cdot 6H_2O$ (95.2 mg; 0.4 mmol), $NiCl_2 \cdot 6H_2O$ (95.0 mg; 0.4 mmol), or $ZnCl_2$ (54.6 mg; 0.4 mmol), was added. In some cases, 1,10-phenanthroline (72.0 mg; 0.4 mmol) or 2,2'-bipyridine (62.4 mg; 0.4 mmol) was added. The reaction mixture was stirred and left for slow evaporation at 25 ºC in the stove in order to ensure constant temperature. After a few days, orange, blue, and yellow powders were deposited.

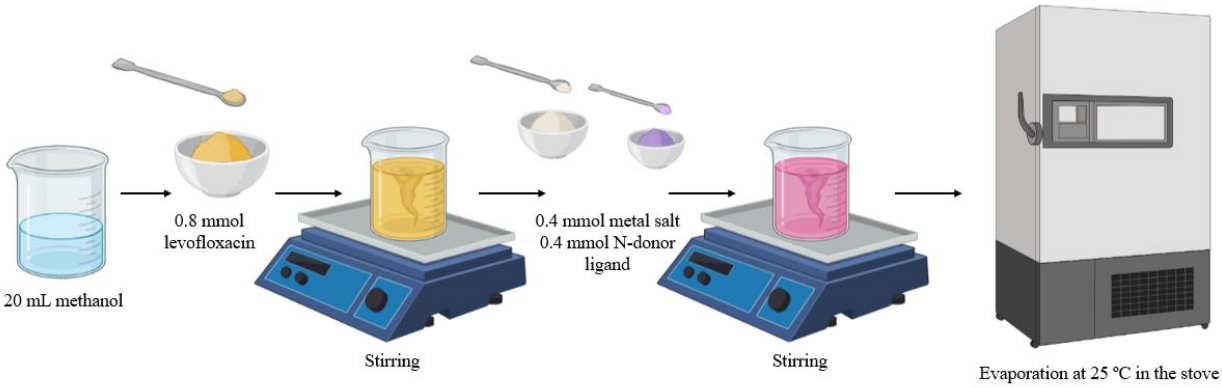

Figure 15. *Schematic representation of the synthesis of Co(II), Ni(II), and Zn(II) complexes with levofloxacin in the presence and absence of the N-donor ligands, 1,10-phenanthroline or 2,2'-bipyridine.*

Table 1 shows the complexes synthesized by the experimental procedure depicted in Figure 15. The table presents the metal ion and the ligands used in each synthesis, a short description of the product obtained, and the identification given to the respective synthesized complex.

Table 1. *Complexes synthesized by the experimental procedure shown in Figure 15.*

Complex	Metal ion	Antibiotic	N-donor ligand	Product
1	Co(II)	Levofloxacin	-	Brownish orange powder
2			1,10-phenanthroline	Dark orange powder
3			2,2'-bipyridine	Brownish orange powder
4	Ni(II)		-	Light green powder
5			1,10-phenanthroline	Bluish green powder
6			2,2'-bipyridine	Bluish green powder
7	Zn(II)		-	Yellow powder
8			1,10-phenanthroline	Yellow powder
9			2,2'-bipyridine	Yellow powder

Figure 16 shows another experimental procedure carried out, specifically microwave-assisted synthesis of copper(II) complexes with levofloxacin in the presence and absence of N-donor ligands. Levofloxacin (144.6 mg; 0.4 mmol) was dissolved in methanol (20 mL), deprotonated with KOH (16.8 mg; 0.3 mmol), and the resultant solution was stirred. Subsequently, the metal salt, $CuCl_2 \cdot 2H_2O$ (68.2 mg; 0.4 mmol), was added. In certain cases, 1,10-phenanthroline (72.0 mg; 0.4 mmol) or 2,2'-bipyridine (62.4 mg; 0.4 mmol) was added. The reaction mixture was stirred and irradiated by microwaves for 15 minutes at 100 ºC using an Anton Paar monowave 300 equipment. The resulting solution was left for slow evaporation at 25 ºC in the stove to maintain constant temperature. After a few days, green powders were deposited.

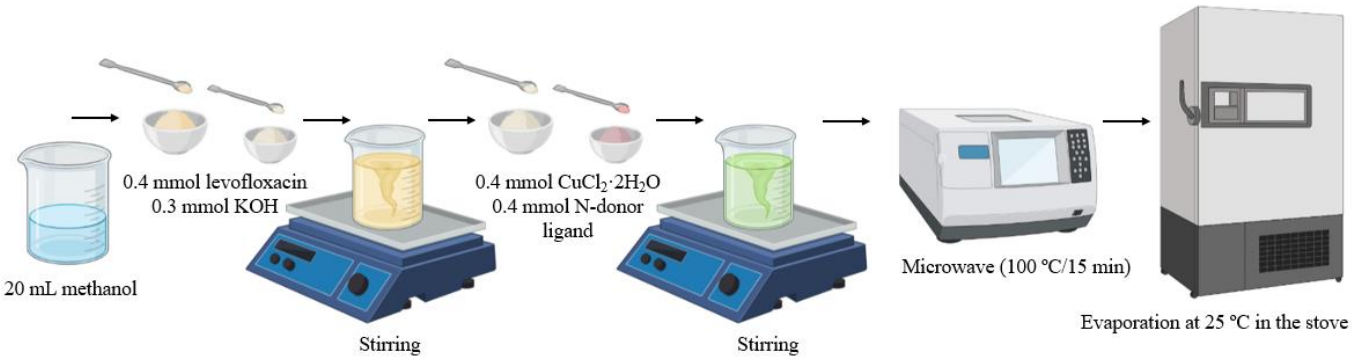

Figure 16. *Schematic representation of the microwave-assisted synthesis of Cu(II) complexes with levofloxacin in the presence and absence of the N-donor ligands, 1,10-phenanthroline or 2,2'-bipyridine.*

Similarly to the previous table, Table 2 reports the complexes synthesized by the experimental procedure represented in Figure 16.

Table 2. *Complexes synthesized by the experimental procedure shown in Figure 16.*

Complex	Metal ion	Antibiotic	N-donor ligand	Product
10	Cu(II)	Levofloxacin	-	Green powder
11			1,10-phenanthroline	Light green powder
12			2,2'-bipyridine	Green powder

Another experimental procedure performed is exhibited in Figure 17, namely the synthesis of a zinc(II) complex with ciprofloxacin. Ciprofloxacin (33.1 mg; 0.1 mmol) was dissolved in ethanol (20 mL) and the resultant solution was stirred. Next, the metal salt, $ZnCl_2$ (13.5 mg; 0.1 mmol), was added, and the reaction mixture was once again stirred. The resulting solution was left for slow evaporation at 25 ºC in the stove in order to assure constant temperature. After a few days, a white powder was deposited.

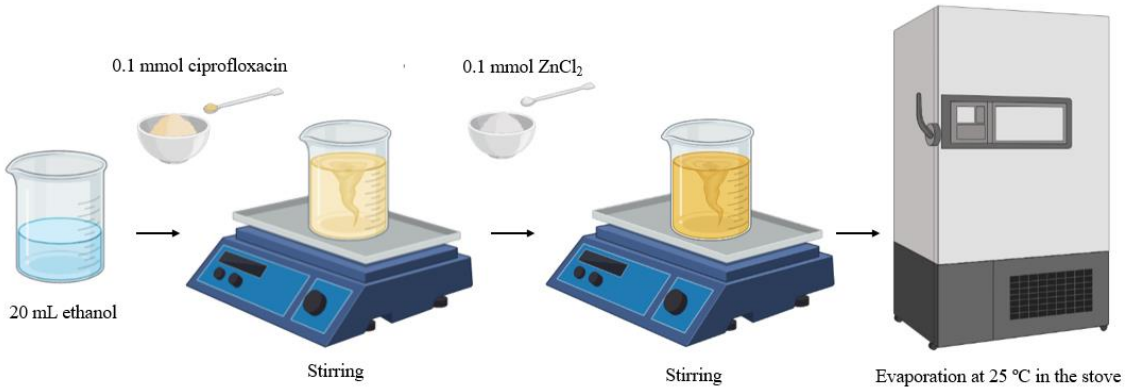

Figure 17. *Schematic representation of the synthesis of a Zn(II) complex with ciprofloxacin.*

On the other hand, Figure 18 displays the synthesis of a nickel(II) complex with ciprofloxacin and 1,10-phenanthroline. Initially, the metal salt, $NiCl_2 \cdot 6H_2O$ (94.9 mg; 0.4 mmol), was dissolved in ethanol (20 mL). Then, this solution and the N-donor ligand, 1,10-phenanthroline (72.1 mg; 0.4 mmol), were added to a previously prepared ethanolic solution (20 mL) of ciprofloxacin (256.2 mg; 0.8 mmol). Subsequently, acetone (30 mL) was added and the reaction mixture was refluxed for 30 minutes at 80 ºC. Afterwards, the solution was filtered and left for slow evaporation at room temperature. After a few days, a blue powder was deposited.

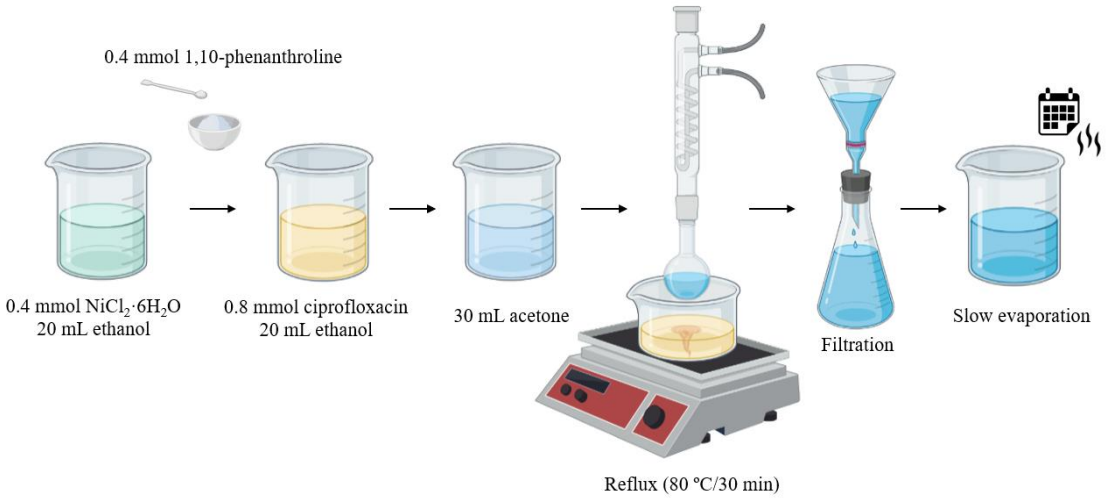

Figure 18. *Schematic representation of the synthesis of a Ni(II) complex with ciprofloxacin and 1,10-phenanthroline.*

Finally, Figure 19 represents the synthesis of a cobalt(II) complex with ciprofloxacin and 2,2'-bipyridine. Initially, ciprofloxacin (132.7 mg; 0.4 mmol) was dissolved in a solvent mixture of ethanol (10 mL) and acetone (20 mL). Afterwards, this solution and the N-donor

ligand, 2,2'-bipyridine (31.1 mg; 0.2 mmol), were added to a previously prepared ethanolic solution (10 mL) of the metal salt, $CoCl_2 \cdot 6H_2O$ (47.7 mg; 0.2 mmol). Then, the reaction mixture was refluxed for 1 hour at 80 ºC, filtered, and left for slow evaporation at room temperature. After a few days, an orange powder was deposited.

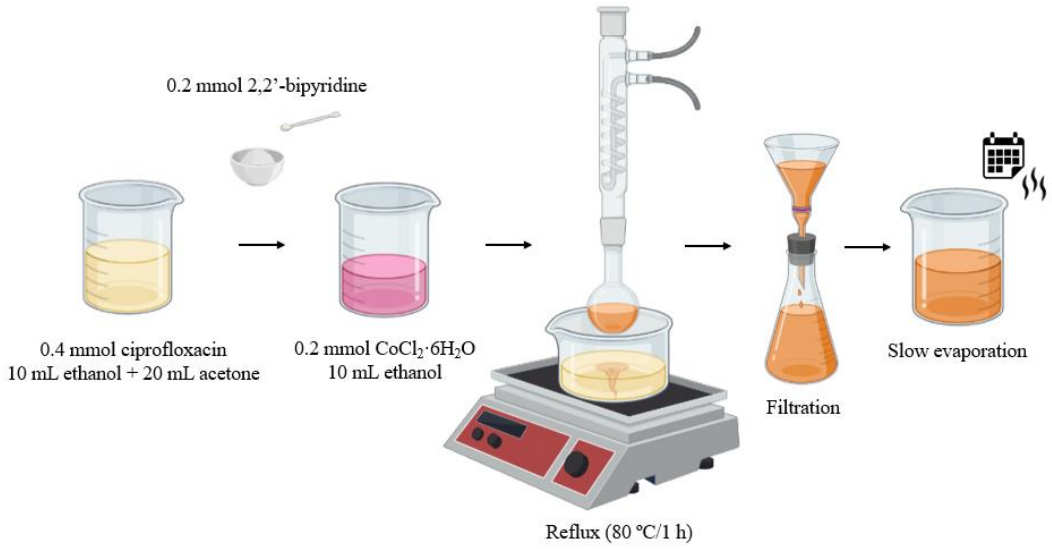

Figure 19. *Schematic representation of the synthesis of a Co(II) complex with ciprofloxacin and 2,2'-bipyridine.*

Table 3 exhibits the ciprofloxacin complexes synthesized by the experimental procedures represented in Figure 17, Figure 18, and Figure 19. As the previous tables, it presents the metal ion and the ligands used in each synthesis, a short description of the product obtained, and the identification given to the respective synthesized complex.

Table 3. *Complexes synthesized by the experimental procedures shown in Figure 17, Figure 18, and Figure 19.*

Complex	Metal ion	Antibiotic	N-donor ligand	Product
13	Zn(II)	Ciprofloxacin	-	White powder
14	Ni(II)		1,10-phenanthroline	Blue powder
15	Co(II)		2,2'-bipyridine	Orange powder

It is important to mention that, at the end of the synthesis, all the final products were filtered off and washed with the solvent used in the respective synthesis procedure. All obtained products are homogeneous, as can be seen in Appendix A.

Characterization of the complexes

Fourier Transform Infrared Spectroscopy (FTIR)

Infrared spectra were recorded on a Mattson–7000 FTIR spectrophotometer, using KBr disks, with 128 scans between 4000 and 280 cm^{-1} and a resolution of 2 cm^{-1}. These spectra allow the identification of specific bands of certain functional groups.

Fourier Transform Raman Spectroscopy (FT–Raman)

Raman spectra were recorded on a Bruker MultiRAM spectrometer, with a Nd-YAG (1064 nm) laser power of 35 mW, a resolution of 4 cm^{-1}, and 1000 scans.

Powder X-Ray Diffraction (PXRD)

Powder XRD data were obtained on a PANalytical Empyrean diffractometer, using Kα(Cu) radiation with a curved graphite monochromator. Intensity data were collected by the step counting method (step 0.05°) in the range $3.5° < 2\Theta < 50$ °.

Elemental Analysis (EA)

In order to acquire information about the percentage of certain elements, namely C, H, and N, the samples were analysed in a Leco CHNS-932 equipment. The values shown are an average of two replicates from each analysis.

Thermogravimetric Analysis (TGA)

The thermal stability and the decomposition profile under heat of the complexes were studied by thermogravimetric analysis, which was carried out under air, with a heating rate of 10 $^{o}C.min^{-1}$, between 20 and 800 ^{o}C, using a Shimadzu TGA-50 equipment. The percentage of weight has been calculated assuming that the final decomposition of the complexes is a mixture of oxides.

Ultraviolet-Visible Spectroscopy (UV–Vis)

UV-Visible spectra were recorded on a GBC UV/VIS 918 spectrophotometer, with a scan speed of 200 nm/min between 250 and 500 nm. All solutions, levofloxacin (30 µg/mL

and 45 µg/mL), Complex **1** (33 µg/mL), Complex **2** (33 µg/mL), Complex **3** (26 µg/mL), Complex **11** (30 µg/mL), and Complex **2** (40 µg/mL) were prepared in ethanol.

Antibacterial studies

Bacterial strains and growth conditions

The bacterial strain used in this study was *Staphylococcus aureus* (ATCC 6538). Fresh bacterial cultures were maintained in Mueller-Hinton Agar (MHA) at 4 ºC. Before each assay, one isolated colony was aseptically transferred to 10 mL of Mueller–Hinton Broth (MHB) and grown overnight at 37 °C. An aliquot of this culture (100 µL) was aseptically transferred to 10 mL of fresh MHB and grown overnight at 37 °C.

Antimicrobial susceptibility test

The antimicrobial activity of metal complexes was tested against *S. aureus*. The bacterial pre-inoculum cultures were grown in MHB growth medium at 37 ºC under shaking at 120 rpm for 18 hours. Beforehand, the density of the bacterial culture was adjusted to 0.5 McFarland in MHB to attain a bacterial concentration of $5x10^7$ colony-forming units (CFU)/mL. Antibiogram was done by disc diffusion method using complexes, starting reagents, and standard antimicrobial sensitivity testing antibiotics. Mueller-Hinton Agar plates were prepared and the test microorganisms were swabbed over the surface of the solidified agar plates using sterile swab spreader. Then, discs with levofloxacin, ciprofloxacin, and their complexes (500, 50, and 5 µg/mL), starting reagents (1000, 100, and 10 µg/mL), and standard antibiotic discs, imipenem (10 µg), ampicillin (10 µg), and ciprofloxacin (5 µg), were impregnated on the inoculated agar plates and incubated for 24 hours at 37 °C. This was followed by measurement of zone of inhibition formed by the test bacteria around the standard antibiotic discs.

Bacterial cellulose production and purification

BC membranes were produced in static conditions using the *Gluconacetobacter sacchari* strain and Hestrin and Shramm (HS) liquid medium (20 g/L glucose, 5 g/L peptone, 5 g/L yeast extract, 2.7 g/L Na_2HPO_4, 1.15 g/L citric acid, pH 5) at 30 ºC. After 3 to 5 days of incubation, BC membranes were removed and treated with 0.5 M NaOH at 90 ºC during

30 minutes. This procedure was repeated three times to eliminate cell content. Next, in order to remove components of the culture medium and other residues, the BC membranes were washed with distilled water. Once washed, the membranes were subjected to a whitening process using a solution of distilled water with 1 % hypochlorite. Then, the BC membranes were thoroughly washed with distilled water until pH 7.0 was reached.[130]

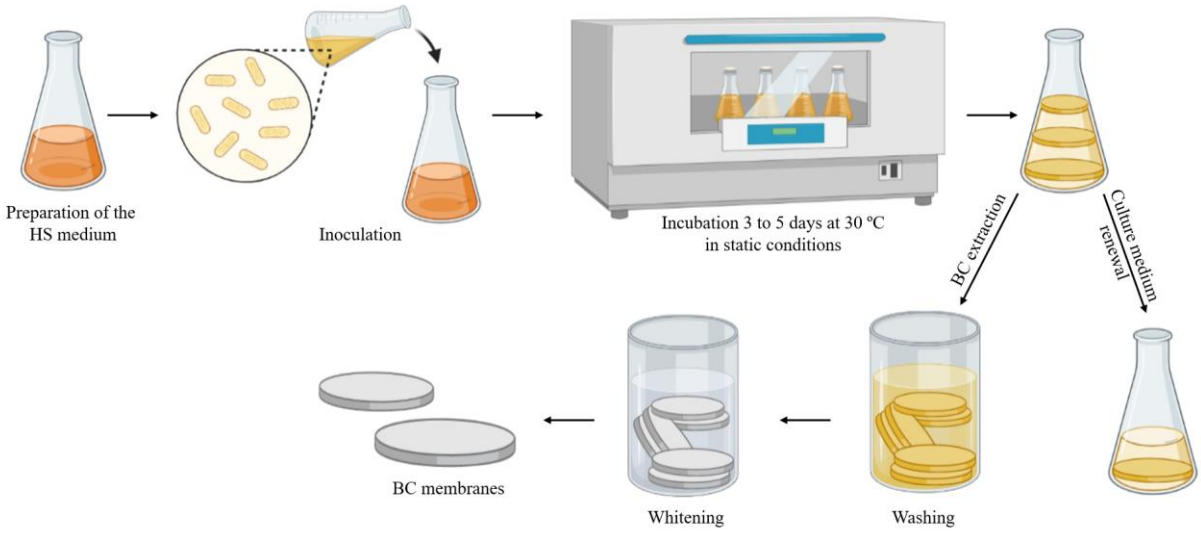

Figure 20. *Schematic representation of BC production.*

Preparation of BC-metallodrug membranes

BC membranes (7 cm of diameter) were weighted and ~70 % of their water content was removed. Afterwards, the membranes were soaked in 4 mL of an aqueous solution of Complex **1** with 500 µg/mL. This process occurred during 48 hours at room temperature in order to guarantee the complete absorption of the solution, resulting in 0.002 g of Complex **1** per membrane. In addition, a pure BC membrane was also reserved. After, the membranes were dried at 40 ºC in a ventilated oven for 12 hours.

Characterization of BC-metallodrug membranes

Pure BC and BC-metallodrug membranes were characterized by several techniques in order to find evidence that confirm the presence of Complex **1** in the BC membranes, as well as possible changes caused by the incorporation.

Fourier Transform Infrared Spectroscopy – Attenuated Total Reflection (FTIR–ATR)

Infrared spectra were recorded on a FTIR Bruker Tensor 27 spectrophotometer, equipped with a Golden Gate ATR, with 256 scans between 4000 and 350 cm^{-1} and a resolution of 4 cm^{-1}.

Fourier Transform Raman Spectroscopy (FT–Raman)

Raman spectra were recorded on a Bruker MultiRAM spectrometer, with a Nd-YAG (1064 nm) laser power of 35 mW, a resolution of 4 cm^{-1}, and 1000 scans.

Thermogravimetric Analysis (TGA)

Thermogravimetric analysis was carried out under N_2, with a heating rate of 10 $^{o}C.min^{-1}$, between 20 and 800 ^{o}C, using a Shimadzu TGA-50 equipment.

Dissolution assays

Linear calibration curve

In order to construct the linear calibration curve of Complex **1**, solutions with several concentrations (40 µg/mL, 36 µg/mL, 32 µg/mL, 24 µg/mL, 16 µg/mL, 8 µg/mL, 4 µg/mL, 2 µg/mL, and 1 µg/mL) were prepared in PBS. UV-Visible spectra were recorded on a Cintra 303 spectrophotometer, with a scan speed of 200 nm/min between 250 and 500 nm. The absorbance values at 287 nm were selected to construct the linear calibration curve.

In vitro metallodrug release

BC-metallodrug membranes were immersed in a container with 150 mL of a 0.01 M phosphate-buffered saline solution (pH 7.4). The release was then carried out during 24 hours at room temperature. At established time intervals, 2 mL of the solution were removed for analysis, and 2 mL of PBS were added in order to maintain a constant volume. The concentration of Complex **1** in each aliquot was determined by UV–Vis through the linear calibration curve previously constructed. The cumulative release percentage of Complex **1** was calculated using Equation 1.

$$Ccumulative = Cn + \frac{2 \times Cn - 1}{150}$$ **Equation 1.**

Cn is the concentration of Complex **1** at time n and Cn–1 corresponds to the concentration of Complex **1** at time n–1.[24]

CHAPTER 3 – RESULTS AND DISCUSSION

Synthesis of the complexes

As previously mentioned, in order to obtain metal complexes of levofloxacin and ciprofloxacin, several methods were performed, namely one-pot synthesis, microwave-assisted synthesis, and solvothermal synthesis. In addition to the two antibiotics, four distinct metal ions were used, specifically cobalt(II), copper(II), nickel(II), and zinc(II), and also four N-donor ligands, namely 1,10-phenanthroline, 2,2'-bipyridine, 2,2'-dipyridylamine, and 4,4'-bipyridine.

Of all the samples synthesized by the several methods performed, fourteen were selected for further studies. For instance, Figure 15 exhibits the synthesis of levofloxacin complexes with cobalt(II), nickel(II), and zinc(II), Figure 16 represents a microwave-assisted synthesis of copper(II) complexes with levofloxacin, Figure 17 displays the synthesis of a zinc(II) complex with ciprofloxacin, Figure 18 shows the synthesis of a nickel(II) complex with ciprofloxacin and 1,10-phenanthroline, and Figure 19 represents the synthesis of a cobalt(II) complex with ciprofloxacin and 2,2'-bipyridine. The obtained complexes are described in Table 1, Table 2, and Table 3.

Characterization of the complexes

The synthesized metal complexes were characterized by several experimental analysis techniques, namely Fourier transform infrared spectroscopy (FTIR), Fourier transform Raman spectroscopy (FT-Raman), powder X-ray diffraction (PXRD), elemental analysis (EA), thermogravimetric analysis (TGA), and ultraviolet-visible spectroscopy (UV–Vis).

The results of the different analysis of Complex **10** were not in agreement and did not indicate enough evidence to conclude that it is a coordination compound, so they will not be displayed.

Fourier Transform Infrared Spectroscopy (FTIR)

Infrared spectroscopy furnishes spectral bands, which provide important information regarding the type of functional groups, crucial to indicate, for example, the coordination between the metal and the ligands.

Figure 21 displays the infrared spectra of the cobalt(II) complexes with levofloxacin, namely Complex **1**, Complex **2**, and Complex **3**.

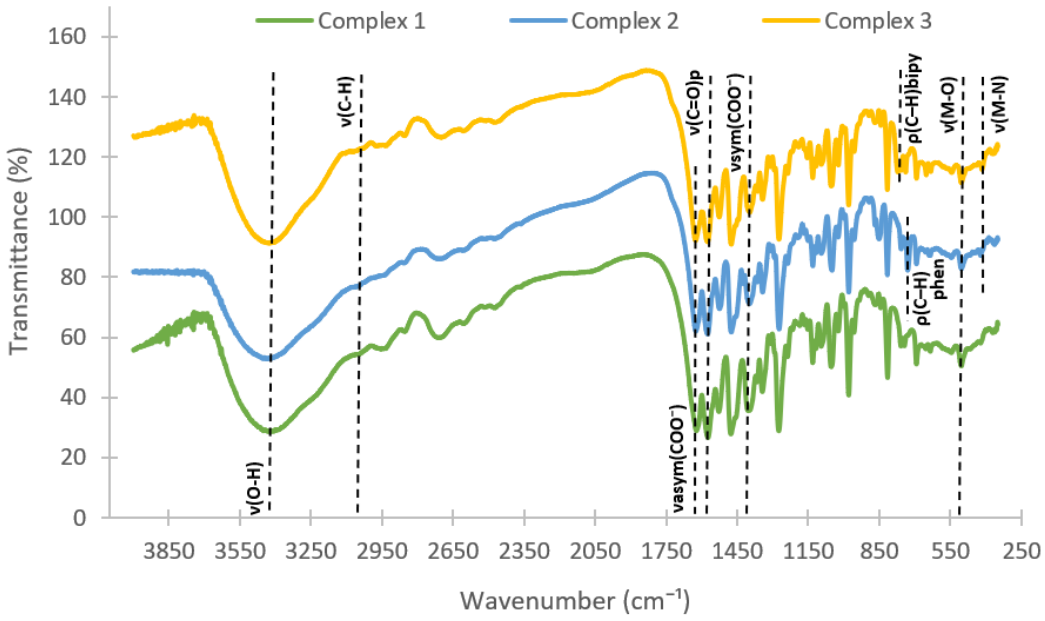

Figure 21. *Infrared spectra of Complex **1**, Complex **2**, and Complex **3**.*

By observing Figure 21, it is possible to verify the presence of absorption bands in the region of 3400 cm^{-1}, which are attributed to the stretching vibrations of coordinated and uncoordinated water molecules. On the other hand, the presence of aromatic molecules is indicated by the bands near 3040 cm^{-1}, corresponding to the ν(C–H) stretching vibration of aromatic rings, and also by the absorption bands around 1520 and 1470 cm^{-1}, which are assigned to the ν(C=C) of aromatic rings.[131]

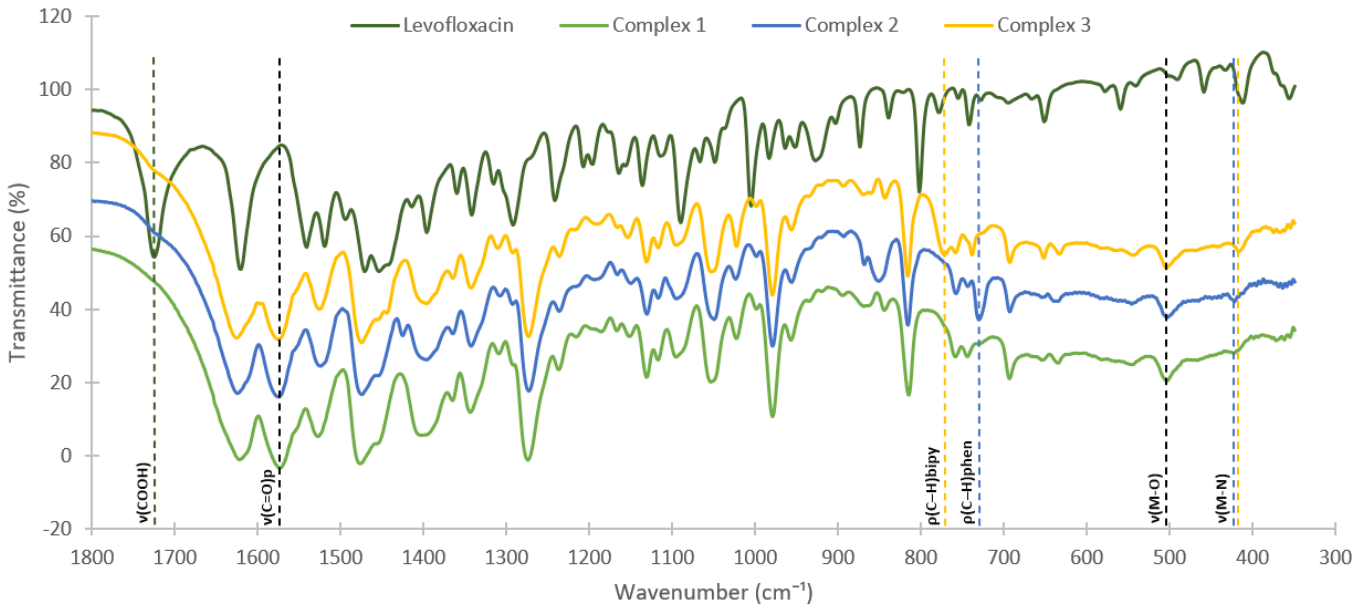

Figure 22. *Zoom of the infrared spectra of levofloxacin, Complex **1**, Complex **2**, and Complex **3**.*

In the infrared spectrum of levofloxacin it is possible to visualize a characteristic band at 1722 cm^{-1}, which is attributed to the stretching vibration of the carbonyl moiety ν(C=O) in the carboxylic group, COOH.[131] In contrast, this peak is absent from the infrared spectra of the complexes, which indicates that the C=O double bond has become a C–O single bond, suggesting a possible coordination with the metal ion. Instead, two bands are present around 1624 and 1395 cm^{-1}, being assigned as $\nu(COO^-)$ asymmetric and symmetric stretching vibrations, respectively. According to literature, the difference between these bands, $\Delta\nu = \nu_{asym}(COO^-) - \nu_{sym}(COO^-)$, is a useful feature to indicate the most probable coordination mode of the ligands. The values of this difference are greater than 200 cm^{-1} ($\Delta\nu > 200$ cm^{-1}), which indicates a monodentate coordination mode of the carboxylate group of levofloxacin. Moreover, there is one more characteristic band in the infrared spectrum of free levofloxacin, at 1618 cm^{-1}, which is attributed to the stretching vibration of the carbonyl moiety in the pyridone, $\nu(C=O)_{pyridone}$. Once again, in the infrared spectra of the complexes, this peak is shifted to lower values, near 1570 cm^{-1}, indicating a possible coordination with the metal ion through the pyridone.[122,132] Taking this into account, it seems that levofloxacin acts as a bidentate ligand by coordinating to the metal ion through two atoms of oxygen, from the pyridone and the carboxylic group.

Additionally, it is possible to verify that the infrared spectra of Complex **2** and Complex **3** exhibit the characteristic band attributed to the out-of-plane ρ(C–H) vibrations

of the corresponding N-donor ligand. In particular, the band at 730 cm^{-1} is assigned to $\rho(C–H)_{phen}$, and the band at 770 cm^{-1} is attributed to $\rho(C–H)_{bipy}$, in the infrared spectra of Complex **2** and Complex **3**, respectively. These bands indicate the presence of the corresponding N-donor ligand in each complex and its coordination to the metal ion.[133]

Finally, lower intensity bands, near 500 cm^{-1} and 420 cm^{-1}, are assigned to ν(M–O) and ν(M–N), suggesting the coordination of the metal ion to levofloxacin *via* oxygen atoms and to N-donor ligands through nitrogen atoms.[132] It is important to note that, in the infrared spectrum of levofloxacin, there is a strong band around 410 cm^{-1}, which does not allow to attribute with certainty the bands near 420 cm^{-1} to the ν(M–N) stretching vibration. Nevertheless, the presence of N-donor ligands is firmly suggested by the bands mentioned above.

Therefore, considering the data obtained by infrared spectroscopy with what is described in the literature, it is safe to assume that levofloxacin acts as a bidentate ligand, since it seems to be coordinated to the metal ion *via* two atoms of oxygen, one from the pyridone and the other from the carboxylic group.[122,132] Moreover, N-donor ligands might also coordinate to the metal ion in a bidentate mode through the two nitrogen atoms.[132,133]

A visual explanation of what has been discussed above can be found in Table 4, where the most important spectral bands of levofloxacin and its complexes are listed.

Table 4. *FTIR assignments (cm^{-1}) of Levofloxacin, Complex **1**, Complex **2**, and Complex **3**.*

Assignments (cm^{-1})	Levofloxacin	Complex 1	Complex 2	Complex 3
ν(COOH)	1722	–	–	–
$\nu_{asym}(COO^-)$	–	1621	1624	1624
$\nu_{sym}(COO^-)$	–	1395	1396	1398
$\nu(C=O)_{pyridone}$	1618	1572	1572	1571
$\rho(C–H)_{phen}$	–	–	731	–
$\rho(C–H)_{bipy}$	–	–	–	774
ν(M–O)	–	502	503	503
ν(M–N)	–	–	421	416

The infrared spectra from Complex **4** to Complex **12** are displayed in Appendix B, since the results and their discussions are very similar to the ones presented above.

Figure 23 shows the infrared spectra of the ciprofloxacin complexes, namely Complex **13**, Complex **14**, and Complex **15**.

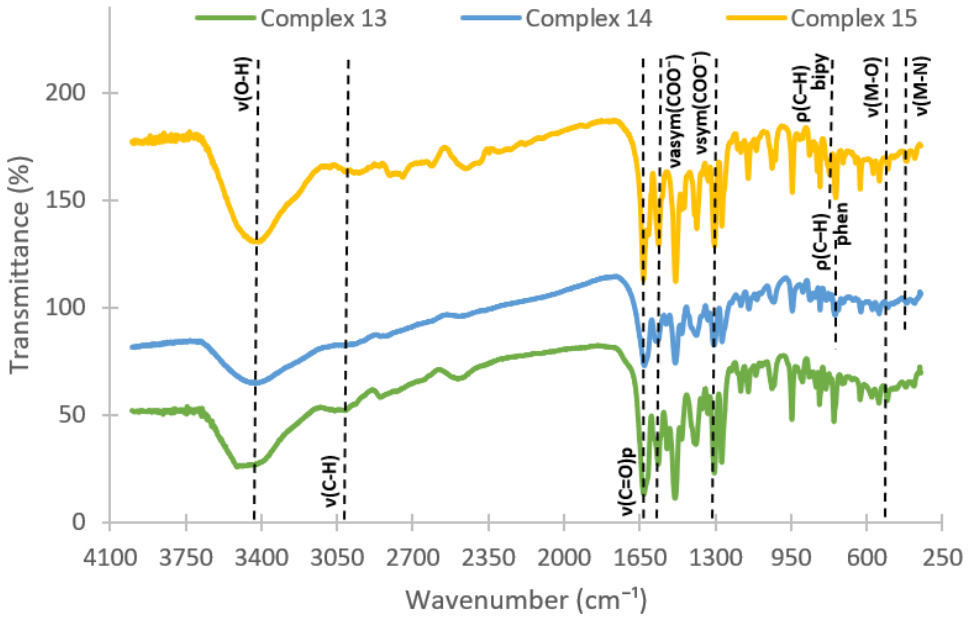

Figure 23. *Infrared spectra of Complex **13**, Complex **14**, and Complex **15**.*

Such as in the infrared spectra of the levofloxacin complexes, in Figure 23 is also possible to notice the bands attributed to the stretching vibrations of coordinated and uncoordinated water molecules, in the region of 3400 cm^{-1}. Similarly, the presence of aromatic molecules is also pointed out by the bands assigned to the ν(C–H) stretching vibration of aromatic rings (near 3040 cm^{-1}) and by the absorption bands corresponding to the ν(C=C) of aromatic rings (around 1520 and 1480 cm^{-1}).[131]

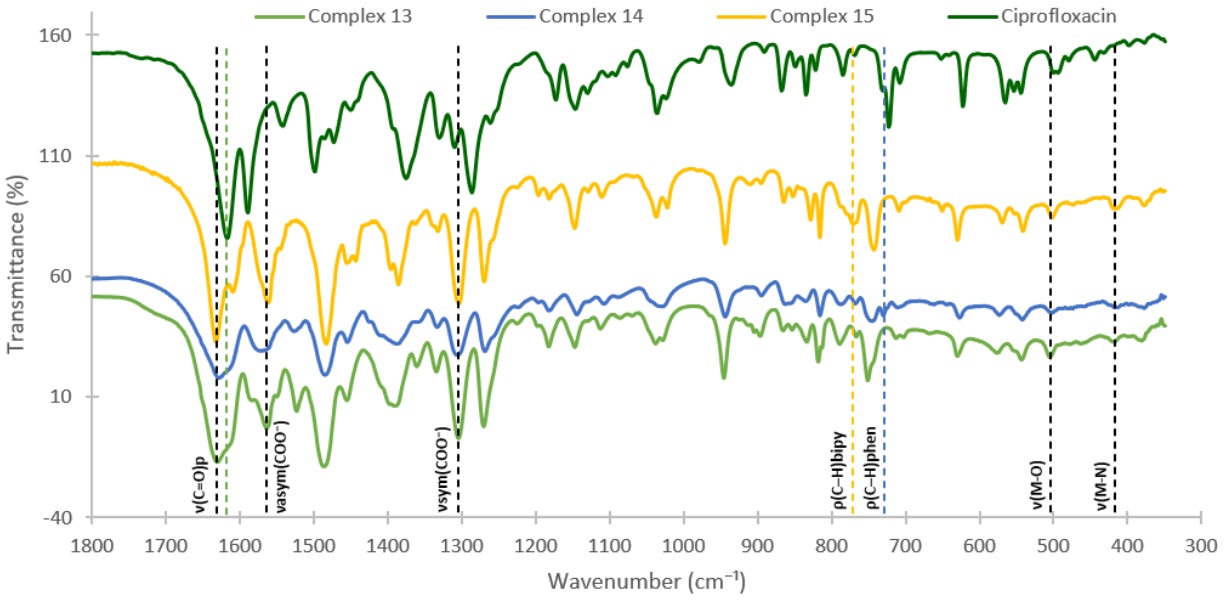

Figure 24. *Zoom of the infrared spectra of ciprofloxacin, Complex **13**, Complex **14**, and Complex **15**.*

According to the literature, the infrared spectrum of ciprofloxacin exhibits two characteristic bands. One of them, near 1707 cm^{-1}, is attributed to the stretching vibration of the carbonyl moiety ν(C=O) in the carboxylic group.[134] However, this band is missing in the infrared spectrum of ciprofloxacin displayed in Figure 24, which, according to Turel *et al.* (1997), is due to the deprotonation of the COOH group.[135] Nevertheless, this peak is also absent from the infrared spectra of the complexes, suggesting a possible coordination with the metal ion. Alternatively, two strong bands are exhibited around 1565 and 1305 cm^{-1}, being assigned as ν(COO^-) asymmetric and symmetric stretching vibrations, respectively. Once again, the values of the difference between these bands, Δν = νasym(COO^-) – νsym(COO^-), are greater than 200 cm^{-1}, indicating a monodentate coordination mode of the carboxylate group of ciprofloxacin. Furthermore, the band attributed to the stretching vibration of the carbonyl moiety in the pyridone, ν(C=O)pyridone, is present in the infrared spectrum of ciprofloxacin at 1618 cm^{-1}. In the infrared spectra of the complexes, this peak is shifted to higher values, around 1630 cm^{-1}, which indicates a possible coordination with the metal ion through the pyridone.[134] Thus, these results suggest that ciprofloxacin might act as a bidentate ligand by coordinating to the metal ion *via* two atoms of oxygen, one from the pyridone and the other from the carboxylic group.[132,134]

Moreover, the infrared spectra of Complex **14** and Complex **15** exhibit the characteristic band attributed to the out–of–plane ρ(C–H) vibrations of the corresponding N-

donor ligand. As demonstrated in Figure 24, the band assigned to $\rho(C–H)_{phen}$, near 730 cm^{-1}, is present in the infrared spectrum of Complex **14**, and the band around 770 cm^{-1}, which is attributed to $\rho(C–H)_{bipy}$, is noticeable in the infrared spectrum of Complex **15**. These bands indicate the presence of the corresponding N-donor ligand in each complex and its coordination to the metal ion.[133] However, these bands are not immediately recognizable since the infrared spectrum of ciprofloxacin displays strong bands in this region, which also influence the spectra of the complexes.

Besides, the presence of lower intensity bands, around 500 cm^{-1} and 415 cm^{-1}, which are assigned to ν(M–O) and ν(M–N), indicates the coordination of the metal ion to ciprofloxacin *via* oxygen atoms and to N-donor ligands through nitrogen atoms.[132]

Therefore, it seems that ciprofloxacin acts as a bidentate ligand by coordinating to the metal ion *via* two atoms of oxygen, one from the pyridone and the other from the carboxylic group.[132,134] Furthermore, N-donor ligands might also coordinate to the metal ion in a bidentate mode through the two nitrogen atoms.[132,133]

In Table 5 are listed the most important spectral bands of ciprofloxacin and its complexes, providing a visual explanation of what has been formerly discussed.

Table 5. *FTIR assignments (cm^{-1}) of Ciprofloxacin, Complex **13**, Complex **14**, and Complex **15**.*

Assignments (cm^{-1})	Ciprofloxacin	Complex 13	Complex 14	Complex 15
ν(COOH)	1707*	–	–	–
$\nu_{asym}(COO^-)$	–	1564	1565	1561
$\nu_{sym}(COO^-)$	–	1303	1305	1302
$\nu(C=O)_{pyridone}$	1618	1630	1628	1633
$\rho(C–H)_{phen}$	–	–	729	–
$\rho(C–H)_{bipy}$	–	–	–	775
ν(M–O)	–	503	501	501
ν(M–N)	–	–	414	416

*This band is absent from the infrared spectrum obtained due to the deprotonation of ciprofloxacin.

Fourier Transform Raman Spectroscopy (FT–Raman)

Raman spectroscopy provides information on chemical structures and physical forms through characteristic spectral patterns and fundamental vibrations.[136]

Figure 25 shows the Raman spectra of Complex **1**, Complex **2**, and Complex **3**.

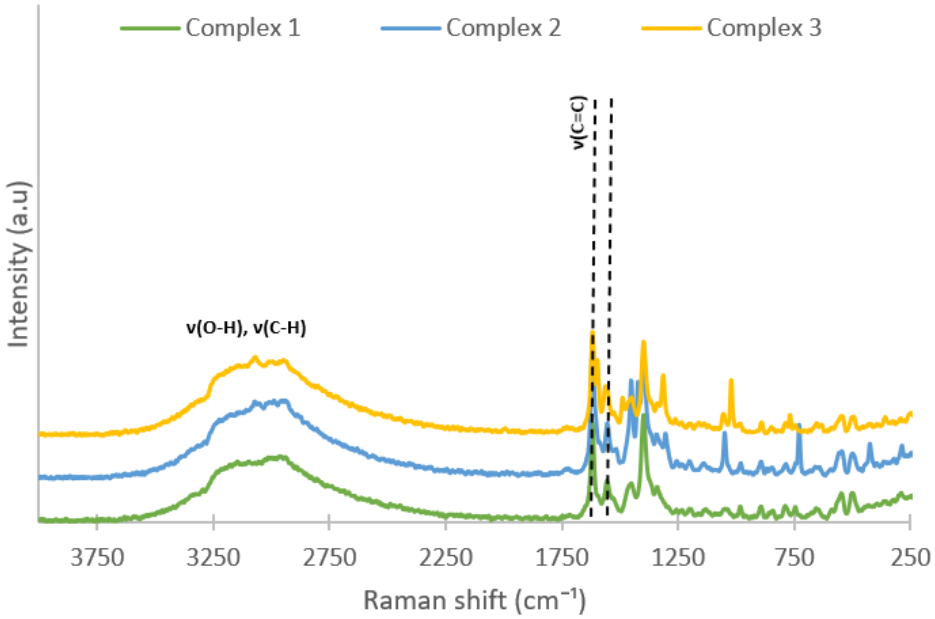

Figure 25. *Raman spectra of Complex **1**, Complex **2**, and Complex **3**.*

The Raman spectra of the complexes are very similar, as displayed in Figure 25. However, by comparing these spectra with the Raman spectrum of levofloxacin, as the example given in Figure 26, it is easy to recognize that the most notable difference lies in the region between 3500 and 2900 cm^{-1}, which is assigned to ν(O–H) stretching vibration and ν(C–H) stretching vibration of aromatic rings.[136] This difference must have occurred due to crystallinity/amorphous effects, since the presence or absence of spatial order really influences the band narrowing and the spectral behavior in hydrogen–bonding environments.[137] Thus, this indicates that the complexes have a less organized, i.e., more amorphous, structure than levofloxacin.

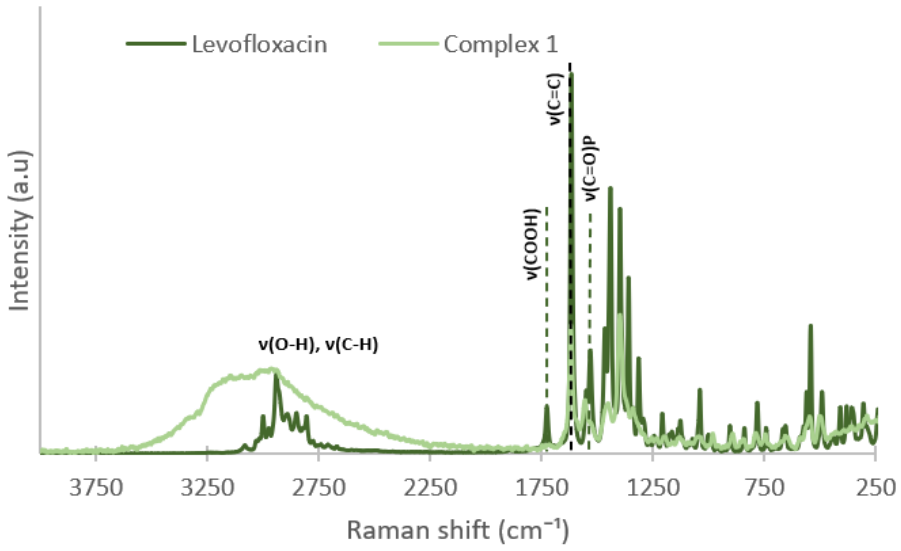

Figure 26. *Comparison between the Raman spectra of levofloxacin and Complex **1**.*

Additionally, the Raman spectrum of levofloxacin exhibits two characteristic bands, one at 1726 cm^{-1}, which is attributed to the stretching vibration of the carbonyl moiety ν(C=O) in the carboxylic group (COOH), and the other at 1532 cm^{-1}, which corresponds to the stretching vibration of the carbonyl moiety in the pyridone, $\nu(C=O)_{pyridone}$. These peaks are absent from the Raman spectra of the complexes, indicating a possible coordination with the metal ion through one oxygen atom of each functional group. Thus, these results are in agreement with the infrared spectroscopy, since they also suggest that levofloxacin acts as a bidentate ligand by coordinating to the metal ion *via* two atoms of oxygen, one from the pyridone and the other from the carboxylic group. On the other hand, both the spectrum of levofloxacin and the spectra of the complexes exhibit bands assigned to the ν(C=C) stretching vibrations of aromatic rings, at 1620 and 1554 cm^{-1}.[138]

Considering that Raman spectroscopy has excellent environmental sensitivity, some sensitive bands are wide and weak, which can be worsened by some backbone structural bands in organic molecules that usually are narrow and strong. This can explain why the bands attributed to ν(M–O) and ν(M–N), between 500 and 200 cm^{-1}, are not distinguishable in the spectra of the complexes.[136]

On the other hand, Figure 27 displays the Raman spectra of Complex **13**, Complex **14**, and Complex **15**.

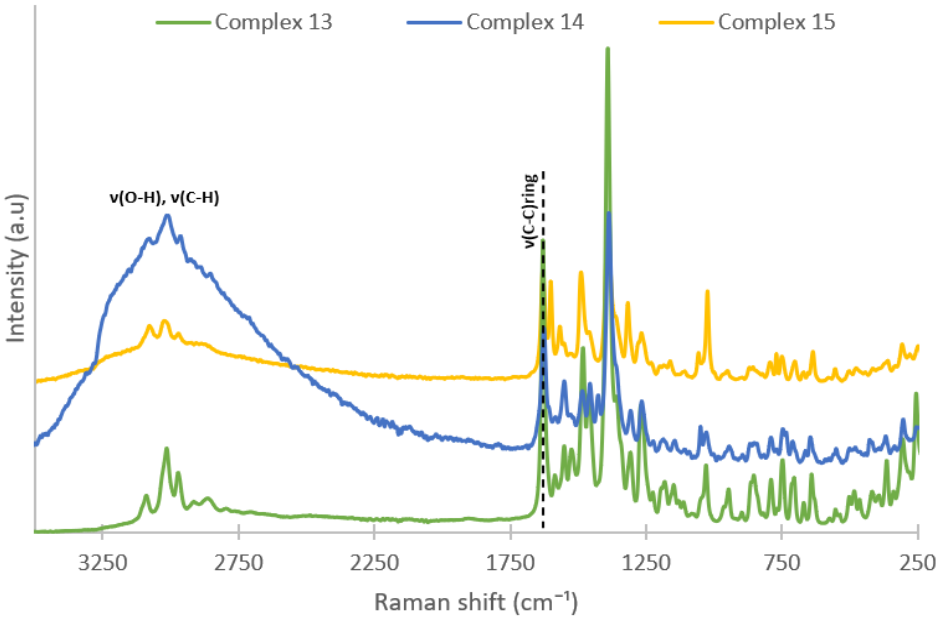

Figure 27. *Raman spectra of Complex **13**, Complex **14**, and Complex **15**.*

Once again, the Raman spectra of the complexes are quite similar. However, by comparing these spectra with the Raman spectrum of ciprofloxacin, as demonstrated in Figure 28, it is evident, once again, the difference in the region assigned to the ν(O–H) and ν(C–H) stretching vibrations of aromatic rings, between 3500 and 2900 cm^{-1}. As mentioned above, this indicates that the complexes have a more amorphous structure than ciprofloxacin, and it is also possible to infer that, in comparison with the other complexes, Complex **13** seems to have a more organized structure.[136]

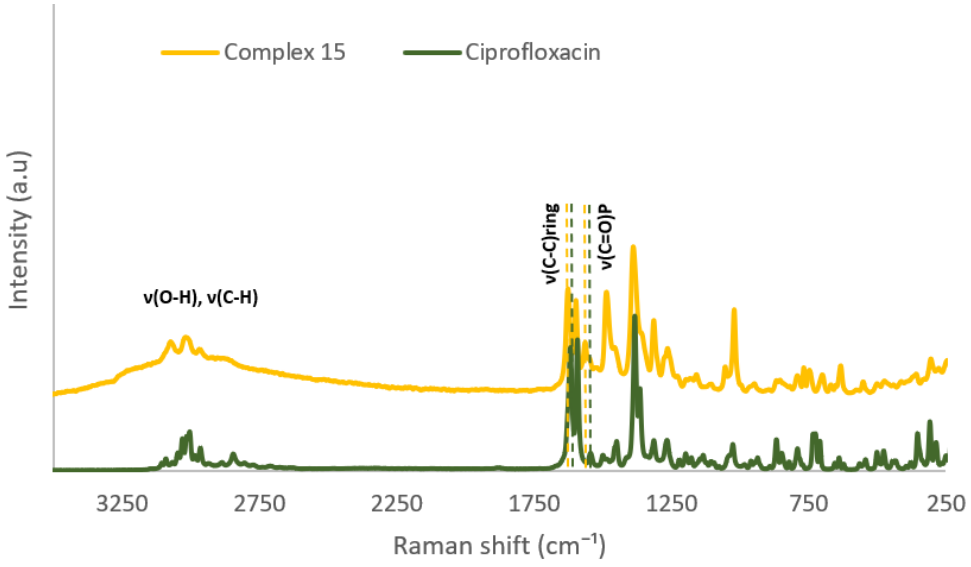

Figure 28. *Comparison between the Raman spectra of ciprofloxacin and Complex **15**.*

According to the literature, the Raman spectrum of ciprofloxacin exhibits two characteristic bands, which are attributed to the stretching vibration of the carbonyl moiety ν(C=O) in the carboxylic group and in the pyridone, near 1707 and 1540 cm^{-1}, respectively.[138] However, the first band is missing in the Raman spectrum of ciprofloxacin, which, according to Turel *et al*. (1997), is due to the deprotonation of the COOH group.[135] In the Raman spectra of the complexes, the absence of the first band and the deviation of the second to higher values (Figure 28), indicates a possible coordination with the metal ion *via* one oxygen atom of each functional group.[138] Therefore, these results are in agreement with the infrared spectroscopy, since they also suggest that ciprofloxacin coordinates through the pyridone and the carboxylic group. On the other hand, all the spectra show the band assigned to the ν(C-C) stretching vibrations of the benzene ring, around 1627 cm^{-1}, confirming the presence of ciprofloxacin in the complexes.[138]

As explained previously, the bands attributed to ν(M–O) and ν(M–N), between 500 and 200 cm^{-1}, are not identifiable in the spectra of the complexes probably due to the masking caused by the strong structural bands of organic molecules.[136]

Powder X-Ray Diffraction (PXRD)

Despite the several attempts performed, the compounds synthesized during this work were not obtained in the form of single crystals with adequate size and quality to be analyzed by single-crystal X-ray diffraction (SC XRD). Therefore, the powder X-ray patterns of the solids were acquired.

Figure 29 displays the powder diffractograms of Complex **11** and Complex **12**, the Cu(II) complexes with levofloxacin and the N-donor ligands, in comparison with the diffractogram generated from the data of SC XRD of similar complexes synthesized in a previous work. However, it is important to point out that none of the single-crystal structures were completely refined since the analysis was limited by the size and poor quality of the crystals.

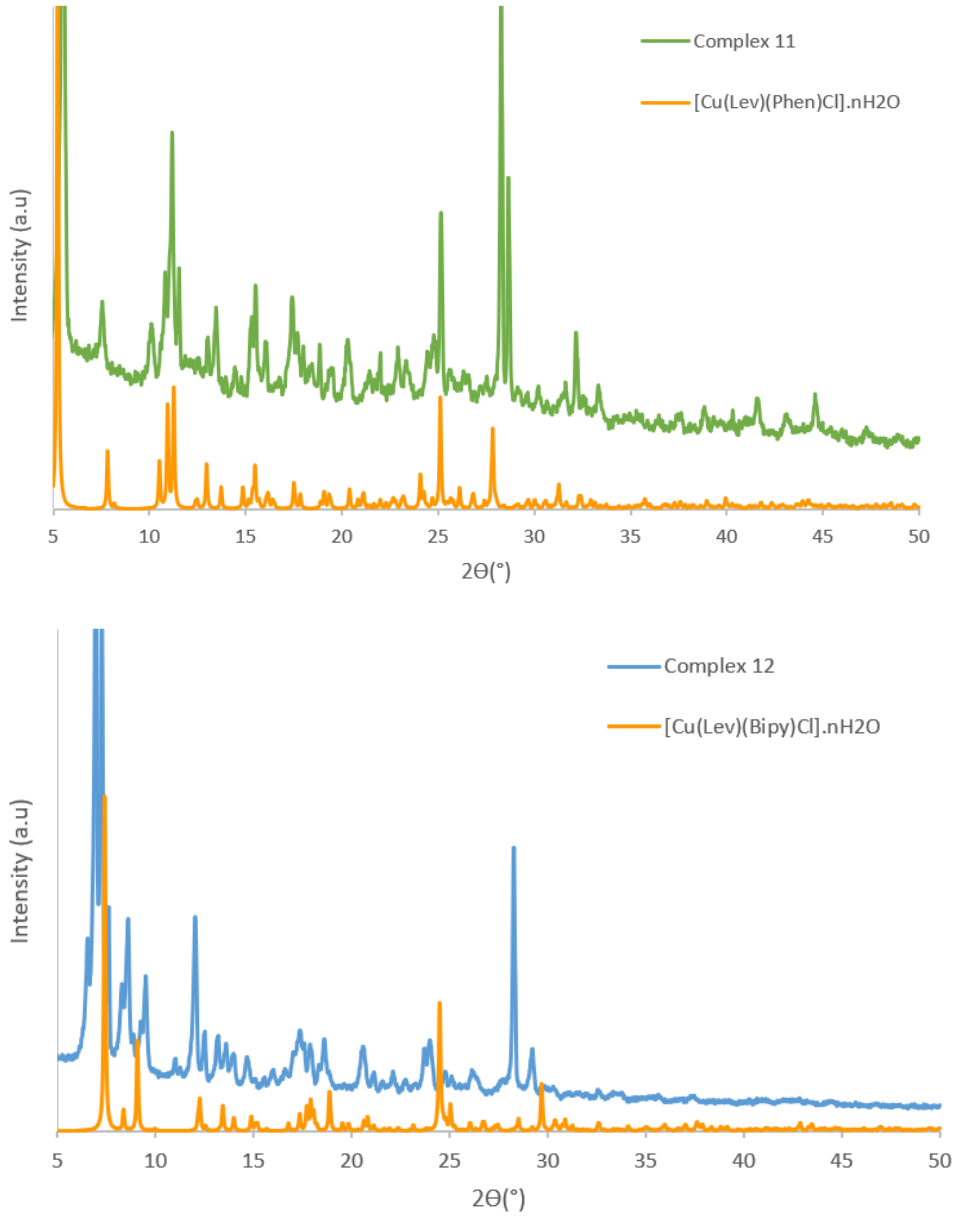

Figure 29. *Comparison between the powder diffraction data of Complex **11** and Complex **12**, and the diffractograms generated from the data of single-crystal X-ray diffraction of similar complexes synthesized in a previous work.*

Overall, it is possible to observe that powder samples present less intense and broader XRD reflections than single-crystals, since the solids obtained are less organized than typical crystals. The X-ray patterns of copper complexes displayed in Figure 29 are representative of the PXRD obtained for the other levofloxacin compounds.

On the other hand, Figure 30 displays the powder diffractograms of the ciprofloxacin compounds, namely Complex **13**, Complex **14**, and Complex **15**.

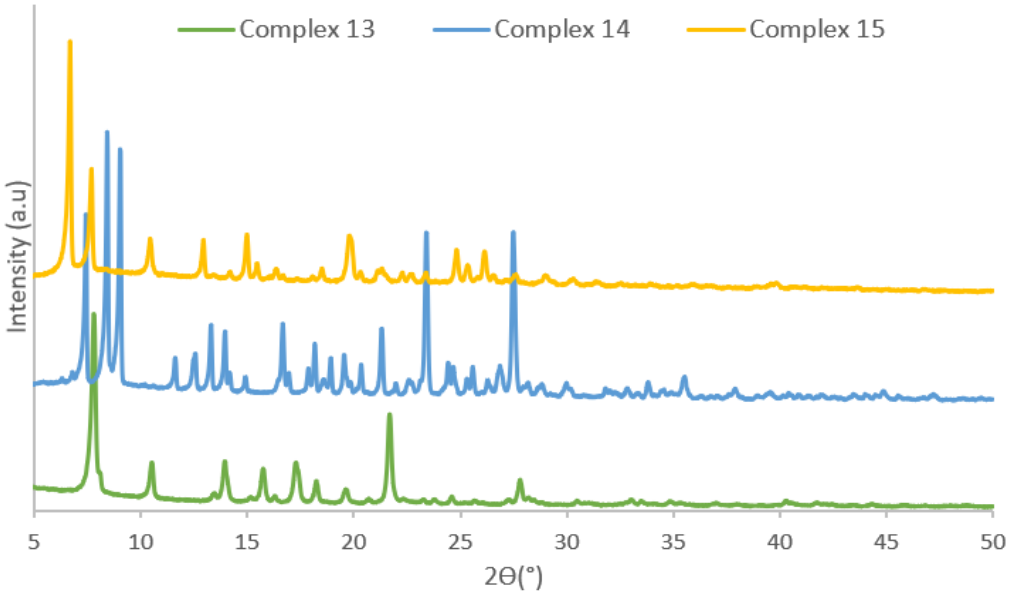

Figure 30. *Powder diffraction data of Complex **13**, Complex **14**, and Complex **15**.*

By observing Figure 30, it is possible to notice that the X-ray patterns are not similar between them, which is indicative of possible different structures. Single-crystal comparison was not performed since crystals of ciprofloxacin complexes were never obtained in our group.

Elemental Analysis (EA)

Through elemental analysis it was possible to experimentally obtain the percentage of certain elements, namely C, H, and N, in the samples. The same values can be theoretically calculated through the molar mass of the proposed chemical formulas for the complexes.

The proposed chemical formulas were considered taking into account several factors. One of them was the conclusions drawn from the analytical techniques presented above, particularly from the infrared spectroscopy, which indicated that the antibiotics coordinate in a bidentate mode. The results obtained in a previous work were also crucial, since two structures were obtained by single-crystal X-ray diffraction, in which the metal ion was coordinated to a levofloxacin molecule, a N-donor ligand molecule, both in a bidentate mode, and to a chloride ion. Moreover, all the chemical species present in each reaction mixture were also considered, as well as the bibliographic research that allowed to acknowledge the most typical structures of levofloxacin and ciprofloxacin complexes

already reported. Nevertheless, it is important to underline that, for the same complex, there is more than one possible structure.

In Table 6, the proposed chemical formulas, the theoretical values, and the experimental values are displayed.

Table 6. *AE (C, H, N) data of Complex **1** to Complex **15** and proposed chemical formulas. "Th" = Theoretical values; "Exp" = Experimental values.*

Complex	Chemical Formulas	C		H		N	
		Th(%)	Exp(%)	Th(%)	Exp(%)	Th(%)	Exp(%)
1	$[Co(Lev)_2Cl_2]\cdot 8H_2O$ $CoC_{36}H_{52}F_2N_6O_{16}Cl_2$	43.4	43.8	5.3	4.9	8.5	8.5
2	$[Co(Lev)(Phen)Cl]\cdot 8H_2O$ $CoC_{30}H_{43}FN_5O_{12}Cl$	46.2	46.5	5.6	5.1	8.9	9.1
3	$[Co(Lev)(Bipy)Cl]\cdot 6H_2O$ $CoC_{28}H_{39}FN_5O_{10}Cl$	46.8	46.9	5.5	5.1	9.7	9.5
4	$[Ni(Lev)_2Cl_2]\cdot 14H_2O$ $NiC_{36}H_{64}F_2N_6O_{20}Cl_2$	39.3	39.1	5.9	4.3	7.6	7.5
5	$[Ni(Lev)(Phen)Cl]\cdot 10H_2O$ $NiC_{30}H_{47}FN_5O_{14}Cl$	44.2	44.0	5.8	4.5	8.6	8.4
6	$[Ni(Lev)(Bipy)Cl]\cdot 9H_2O$ $NiC_{28}H_{45}FN_5O_{13}Cl$	43.5	43.0	5.9	4.5	9.1	8.0
7	$[Zn(Lev)_2Cl_2]\cdot 8H_2O$ $ZnC_{36}H_{54}F_2N_6O_{16}Cl_2$	43.2	43.1	5.5	4.2	8.4	8.4
8	$[Zn(Lev)(Phen)Cl]\cdot 8H_2O$ $ZnC_{30}H_{43}FN_5O_{12}Cl$	47.8	48.1	5.8	4.1	9.3	9.3
9	$[Zn(Lev)(Bipy)Cl]\cdot 5H_2O$ $ZnC_{28}H_{37}FN_5O_9Cl$	47.6	48.1	5.3	4.1	9.9	9.6
11	$[Cu(Lev)(Phen)Cl]\cdot 8H_2O$ $CuC_{30}H_{43}FN_5O_{12}Cl$	45.9	45.8	5.5	4.2	8.9	8.9
12	$[Cu(Lev)(Bipy)Cl]\cdot 7H_2O$ $CuC_{28}H_{41}FN_5O_{11}Cl$	45.3	45.8	5.6	4.3	9.4	9.5
13	$Zn(Cip)_2Cl_2(H_2O)_{11}$ $ZnC_{34}H_{58}F_2N_6O_{17}Cl_2$	40.9	40.7	5.9	4.6	8.4	8.3
14	$Ni(Cip)(Phen)Cl(H_2O)_9$ $NiC_{29}H_{44}FN_5O_{12}Cl$	46.9	46.5	5.8	4.8	9.1	9.4
15	$Co(Cip)(Bipy)Cl(H_2O)_7$ $CoC_{27}H_{40}FN_5O_{10}Cl$	45.8	45.8	5.7	5.0	9.9	9.6

By observing Table 6, it is possible to notice that there are significant differences between the theoretical and experimental values of some complexes, especially concerning hydrogen. However, it is important to mention that samples were obtained in the form of powders which are solids with a less organized structure in comparison with single-crystals, as supported by PXRD results.

Thermogravimetric Analysis (TGA)

In general, the thermograms of the different metal complexes follow a similar profile regardless of the metal ions and N-donor ligands used. This profile can be divided into four stages, generally attributed to the loss of water molecules, a thermally stable stage, the loss of the ligands, and the formation of a residue.

Figure 31 shows the thermograms of Complex **1**, Complex **2**, and Complex **3**.

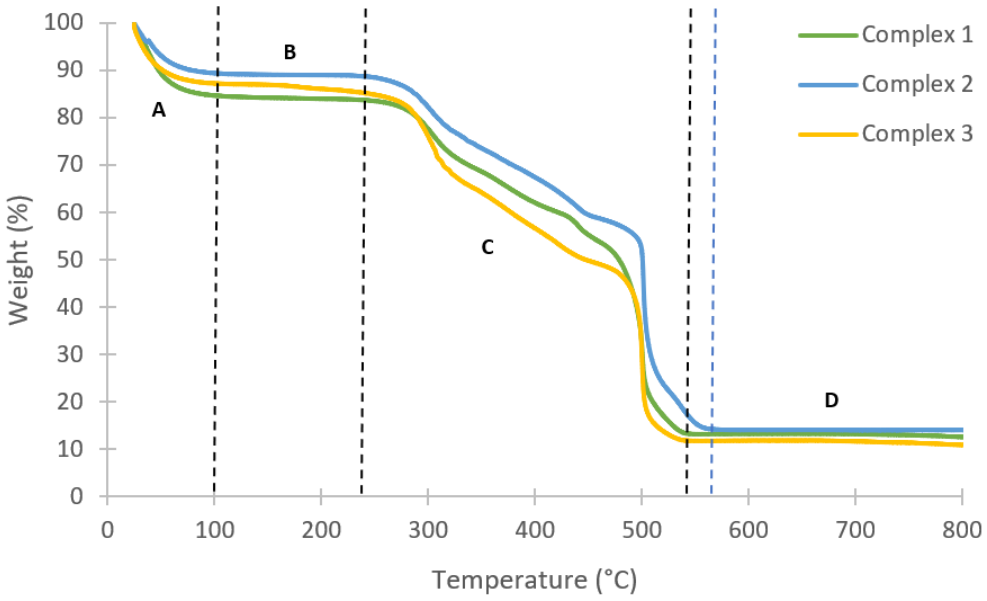

Figure 31. *TGA profiles of Complex **1**, Complex **2**, and Complex **3**.*

As is displayed, the profile of the thermogravimetric analysis is divided into four stages, A, B, C and D. In stage A, amongst 24 ºC and 100 ºC, there is an abrupt loss of mass percentage, probably attributed to the loss of water molecules. In stage B, corresponding to the range between 100 ºC and 240 ºC, there is no significant mass loss, indicating that the metal complexes are thermally stable during this temperature range. In stage C, amongst 240 ºC and 545 ºC, a marked loss of mass is once again verified, possibly associated with the loss of ligands, such as levofloxacin molecules and N-donor ligands. Finally, in stage D, in

the range between 545 ºC and 800 ºC, the mass percentage stabilizes, corresponding perhaps to the formation of a residue, cobalt(II) oxide. It should be noted that in Complex **3**, stage D starts at higher temperatures than stipulated.

Table 7 shows the theoretical mass loss percentage values, based on the molar mass of the proposed chemical formulas, and the experimental mass loss percentage values, based on the TGA results.

Table 7. *TGA data of Complex **1**, **2**, and **3**. "Th" = Theoretical values; "Exp" = Experimental values.*

	Stage A		Stage B		Stage C		Stage D	
	Th(%)	**Exp(%)**	**Th(%)**	**Exp(%)**	**Th(%)**	**Exp(%)**	**Th(%)**	**Exp(%)**
Complex 1	15	15	0	1	81	71	8	13
Complex 2	19	11	0	1	74	74	10	14
Complex 3	15	13	0	2	77	74	10	11

In a similar way, Figure 32 also displays the TGA profiles of Complex **4**, Complex **5**, and Complex **6**.

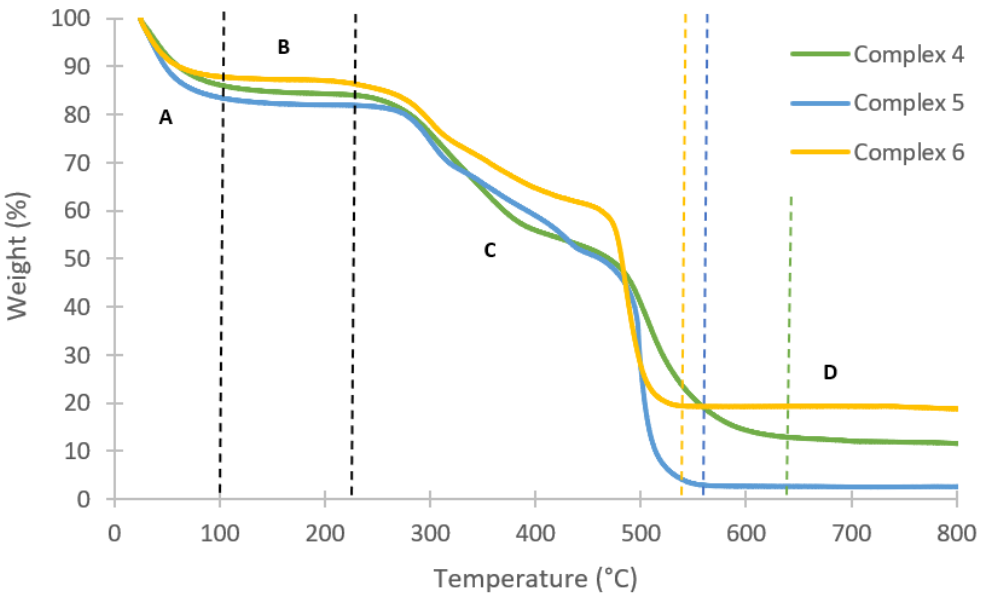

Figure 32. *TGA profiles of Complex **4**, Complex **5**, and Complex **6**.*

The TGA profiles of Complex **4**, **5**, and **6** can also be divided into four stages: A (~24-100 ºC) – loss of water molecules; B (~100-220 ºC) – thermally stable stage; C (~220-540 ºC) – loss of the ligands; D (~540-800 ºC) – formation of nickel(II) oxide. It should be

noted that in Complex **4** and **5**, stage D starts at higher temperatures than stipulated. Table 8 presents the theoretical and experimental mass loss percentage values.

Table 8. *TGA data of Complex **4**, **5**, and **6**. "Th" = Theoretical values; "Exp" = Experimental values.*

	Stage A		Stage B		Stage C		Stage D	
	Th(%)	**Exp(%)**	**Th(%)**	**Exp(%)**	**Th(%)**	**Exp(%)**	**Th(%)**	**Exp(%)**
Complex 4	23	15	0	1	72	71	7	12
Complex 5	22	17	0	1	71	79	9	3
Complex 6	21	13	0	1	71	67	10	19

Figure 33 also shows the thermogravimetric curves of Complex **7**, Complex **8**, and Complex **9**.

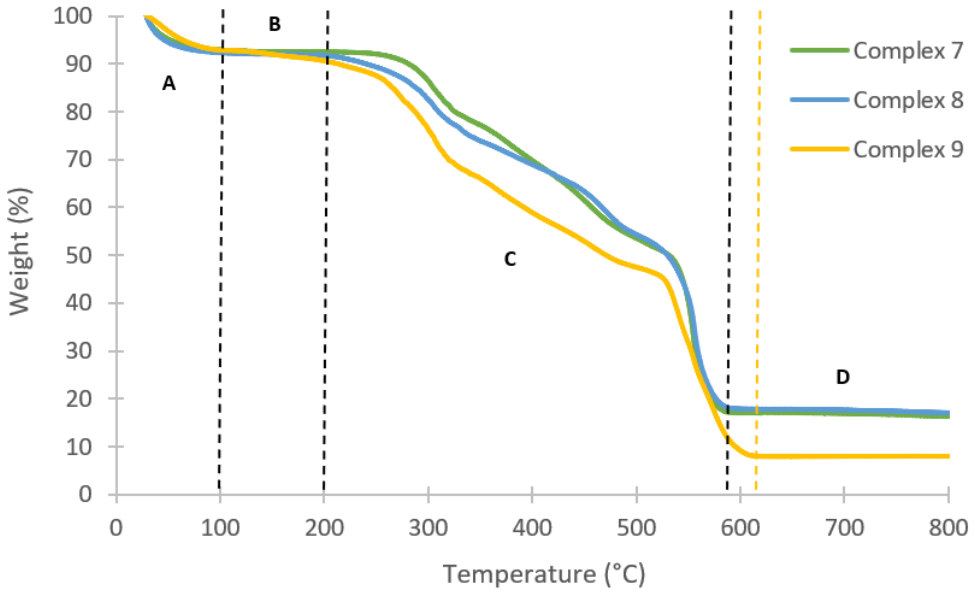

Figure 33. *TGA profiles of Complex **7**, Complex **8**, and Complex **9**.*

The thermogravimetric curves of Complex **7**, **8**, and **9** can also be divided into four stages: A (~24-90 ºC) – loss of water molecules; B (~90-200 ºC) – thermally stable stage; C (~200-580 ºC) – loss of the ligands; D (~580-800 ºC) – formation of zinc(II) oxide. It should be pointed out that in Complex **9**, stage D starts at higher temperatures than stipulated. Table 9 presents the theoretical and experimental mass loss percentage values.

Table 9. *TGA data of Complex **7**, **8**, and **9**. "Th" = Theoretical values; "Exp" = Experimental values.*

	Stage A		Stage B		Stage C		Stage D	
	Th(%)	**Exp(%)**	**Th(%)**	**Exp(%)**	**Th(%)**	**Exp(%)**	**Th(%)**	**Exp(%)**
Complex 7	14	7	0	1	79	75	8	16
Complex 8	18	8	0	1	73	74	10	17
Complex 9	13	7	0	2	78	83	11	8

Additionally, Figure 34 displays the TGA profiles of Complex **11** and Complex **12**.

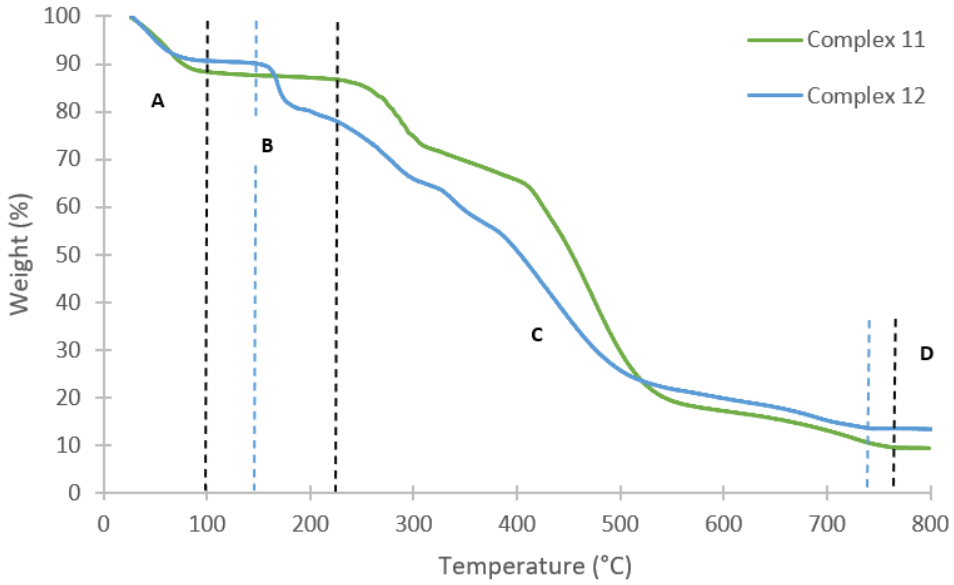

Figure 34. *TGA profiles of Complex **11** and Complex **12**.*

The TGA profiles of Complex **11** and **12** can also be divided into four stages: A (~24-100 ºC) – loss of water molecules; B (~100-210 ºC) – thermally stable stage; C (~210-760 ºC) – loss of the ligands; D (~760-800 ºC) – formation of copper(II) oxide. It should be noted that in Complex **12**, stages C and D start at lower temperatures than stipulated. Table 10 shows the theoretical and experimental mass loss percentage values.

Table 10. *TGA data of Complex **11** and **12**. "Th" = Theoretical values; "Exp" = Experimental values.*

	Stage A		Stage B		Stage C		Stage D	
	Th(%)	**Exp(%)**	**Th(%)**	**Exp(%)**	**Th(%)**	**Exp(%)**	**Th(%)**	**Exp(%)**
Complex 11	18	12	0	2	74	77	10	9
Complex 12	17	10	0	1	75	76	11	13

Finally, Figure 35 represents the TGA profiles of Complex **13**, Complex **14**, and Complex **15**.

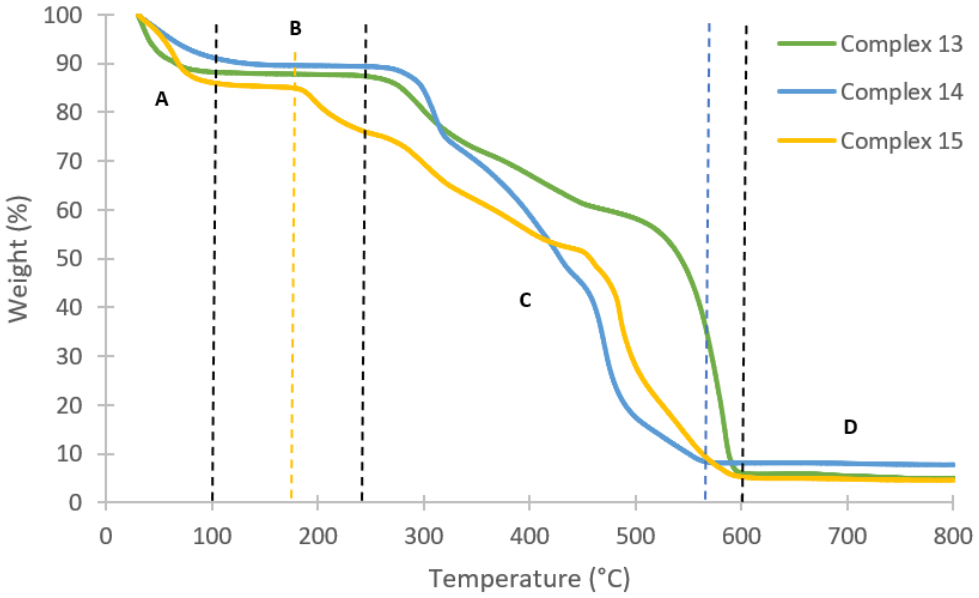

Figure 35. *TGA profiles of Complex **13**, Complex **14**, and Complex **15**.*

The thermograms of Complex **13**, **14**, and **15** can also be divided into four stages: A (~24-100 ºC) – loss of water molecules; B (~100-250 ºC) – thermally stable stage; C (~250-600 ºC) – loss of the ligands; D (~600-800 ºC) – formation of metal(II) oxide. It should be pointed out that in Complex **14**, stage D starts at lower temperatures than stipulated, as well as stage C in Complex **15**. Table 11 displays the theoretical and experimental mass loss percentage values.

Table 11. *TGA data of Complex **13**, **14**, and **15**. "Th" = Theoretical values; "Exp" = Experimental values.*

	Stage A		**Stage B**		**Stage C**		**Stage D**	
	Th(%)	**Exp(%)**	**Th(%)**	**Exp(%)**	**Th(%)**	**Exp(%)**	**Th(%)**	**Exp(%)**
Complex 13	19	12	0	1	74	82	8	5
Complex 14	21	9	0	1	71	81	10	8
Complex 15	18	13	0	2	74	80	11	5

Once again, it is possible to observe significant differences between the theoretical and experimental values of some complexes. Nevertheless, the TGA profiles are in agreement with the results reported in the literature, and with the results of the

characterization techniques discussed above, since they suggest the presence of coordination compounds.[119]

Ultraviolet-Visible Spectroscopy (UV–Vis)

As previously mentioned, the UV–Vis spectra of levofloxacin, Complex **1**, Complex **2**, and Complex **3**, displayed in Figure 36, were obtained in ethanol solutions.

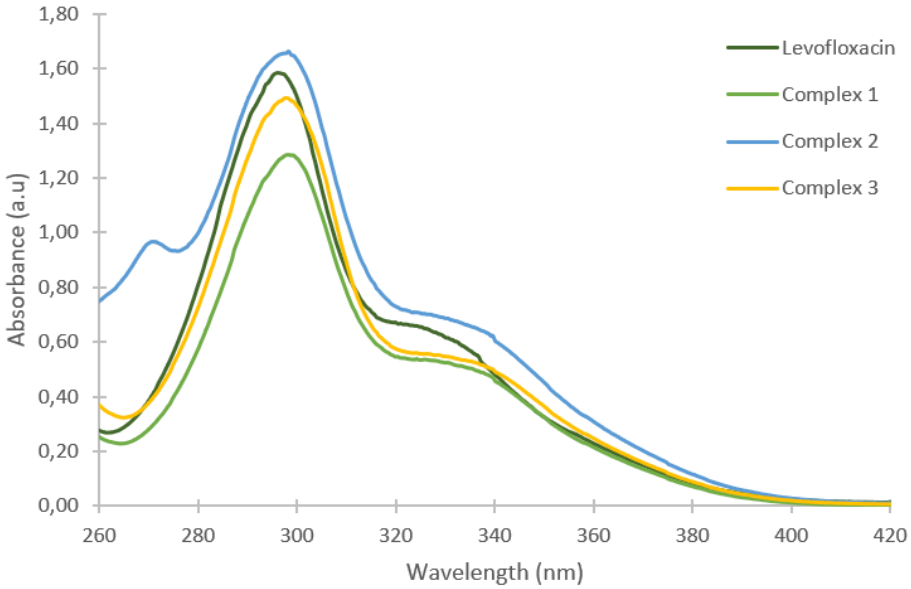

Figure 36. *UV–Vis spectra of levofloxacin, Complex **1**, Complex **2**, and Complex **3**.*

By observing Figure 36, it is noticeable that the spectrum of levofloxacin has two characteristic bands, at 298 and 329 nm, which is in agreement with what is described in the literature. Moreover, the electronic spectra of Complex **1** and Complex **3** are very similar to the spectrum of levofloxacin, but slightly shifted, indicating the formation of complexes. On the other hand, the spectrum of Complex **2** displays a third band at 273 nm, which is characteristic of the levofloxacin complexes with 1,10-phenanthroline.[122,139] The same discussion is valid for the UV–Vis spectra of Complex **11** and Complex **12**, which are displayed in Figure 37. Therefore, these results are in agreement with the analysis presented previously, since they also indicate the presence of metal complexes.

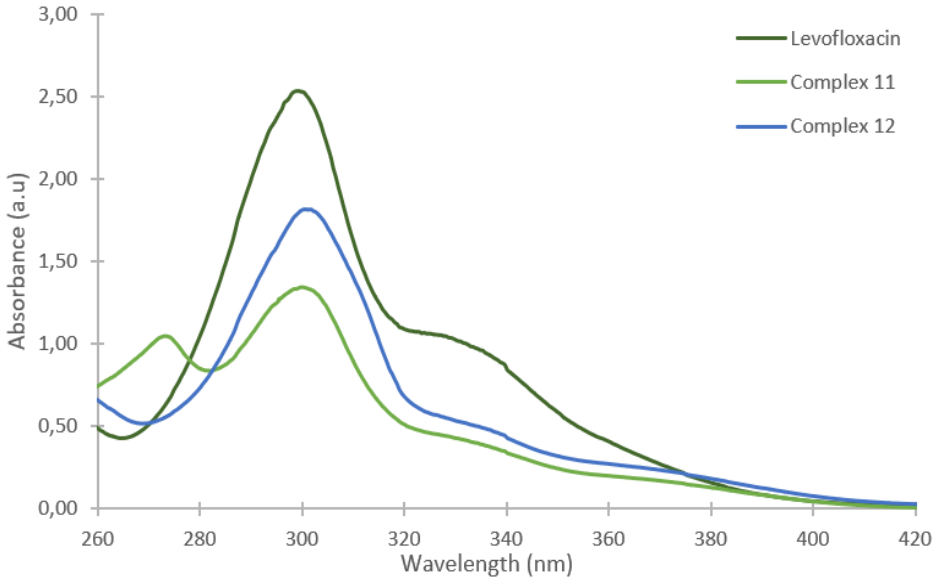

Figure 37. *UV–Vis spectra of levofloxacin, Complex **11**, and Complex **12**.*

Antibacterial studies

Antimicrobial susceptibility test

The antibacterial activity of the starting reagents and the complexes was screened against Gram-positive bacteria *Staphylococcus aureus*.

As mentioned previously, the antibacterial activity of all starting reagents except the antibiotics was tested at three concentrations, 1000 µg/mL, 100 µg/mL, and 10 µg/mL. At the maximum concentration tested, 1,10-phenanthroline showed antibacterial activity against *S. aureus*. On the other hand, the antibacterial activity of levofloxacin, ciprofloxacin, and their complexes was tested at three other concentrations, 500 µg/mL, 50 µg/mL, and 5 µg/mL. Some results can be visualized in Figure 38.

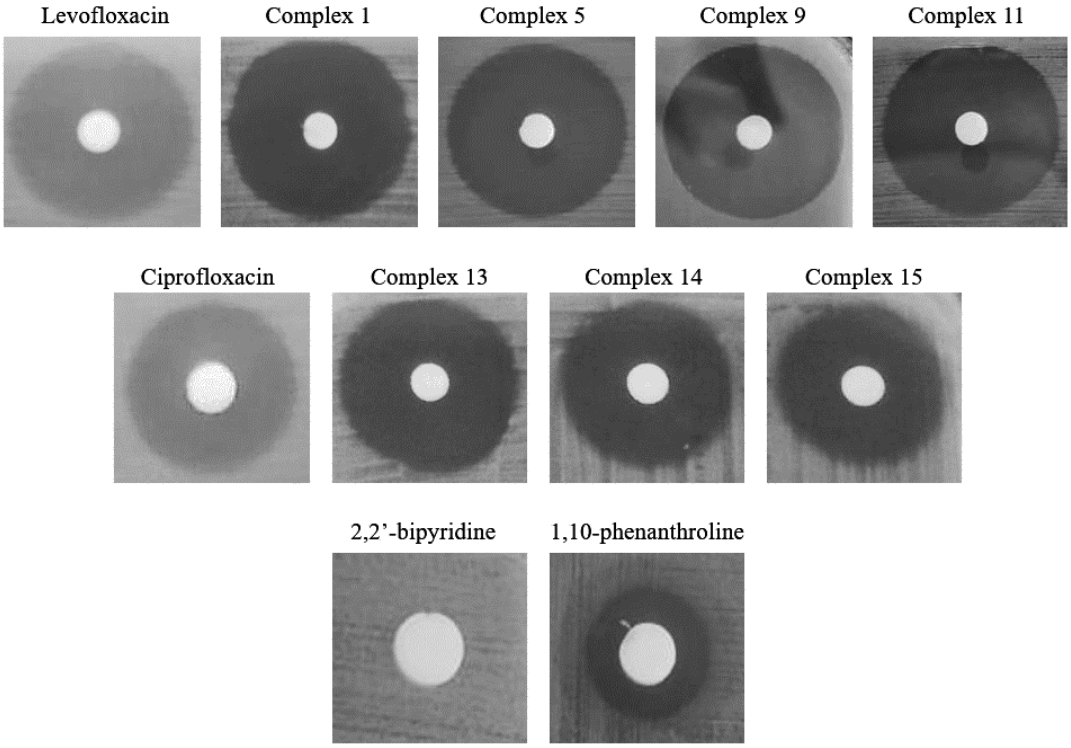

Figure 38. *Susceptibility test of S. aureus: antibacterial activity exhibited by the N-donor ligands, antibiotics, Complex **1**, Complex **5**, Complex **9**, Complex **11**, Complex **13**, Complex **14**, and Complex **15**.*

As shown in Figure 38, both antibiotics and complexes completely inhibited the growth of *S. aureus*. In order to evaluate the antibacterial effect of the complexes, each inhibition zone diameter was measured. The results of the lowest concentration, 5 μg/mL, are listed in Table 12, and the remaining results are shown in Appendix C.

Table 12. *Antibacterial activity data of levofloxacin, ciprofloxacin, and their complexes, against S. aureus.*

Sample	Disk content	Inhibition zone diameter (mm)
Levofloxacin	5 µg/mL	13
Complex 1		16
Complex 2		13
Complex 3		15
Complex 4		18
Complex 5		9
Complex 6		15
Complex 7		20
Complex 8		14
Complex 9		14
Complex 11		10
Complex 12		12
Ciprofloxacin		8
Complex 13		12
Complex 14		14
Complex 15		9

As can be seen in Table 12, all complexes exhibited antibacterial activity from the minimum concentration tested, and all of them except Complex **5**, Complex **11**, and Complex **12**, showed equal or greater antibacterial activity than the parent antibiotic.

The obtained results are in agreement with what is reported in the literature. For instance, Galani *et al*. (2014) synthesized zinc complexes with levofloxacin, 1,10-phenanthroline or 2,2'-bipyridine, which are more active than the free drug against *S. aureus*.[119] Moreover, the Co(II), Cu(II), Ni(II), and Zn(II) ciprofloxacin complexes synthesized by Chohan *et al*. (2005) also exhibited higher antibacterial activity than the parent antibiotic against *S. aureus*.[117]

On another note, it is important to mention that the antibacterial activity of all the starting reagents and complexes was also screened against Gram-negative bacteria *Pseudomonas aeruginosa*. However, these results will not be considered since there is a possibility that the bacteria could have been contaminated during the assays. Nevertheless, the obtained results are displayed in Appendix C.

Preparation of BC-metallodrug membranes

As previously mentioned, 4 mL of an aqueous solution of Complex **1** with 500 µg/mL was incorporated into BC membranes, which were later dried at 40 ºC in a ventilated oven for 12 hours. BC-metallodrug membranes were homogeneous, without aggregates, which indicates that Complex **1** was uniformly dispersed inside the three-dimensional nanofibrillar BC network.

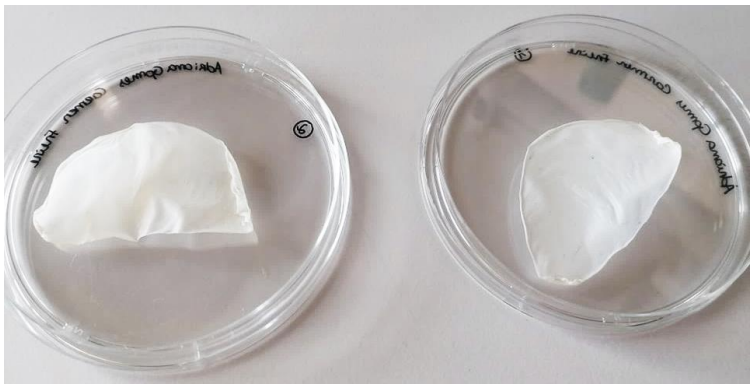

Figure 39. *BC-Complex **1** membranes.*

Characterization of BC-metallodrug membranes

Pure BC and BC-metallodrug membranes were characterized by several techniques, namely Fourier transform infrared spectroscopy - attenuated total reflection (FTIR–ATR), Fourier transform Raman spectroscopy (FT–Raman), and thermogravimetric analysis (TGA). BC is the identification given to pure BC, and BC-M is the identification given to the membranes loaded with Complex **1**.

Fourier Transform Infrared Spectroscopy – Attenuated Total Reflection (FTIR–ATR)

The infrared spectra of BC and BC-metallodrug membranes are shown in Figure 40.

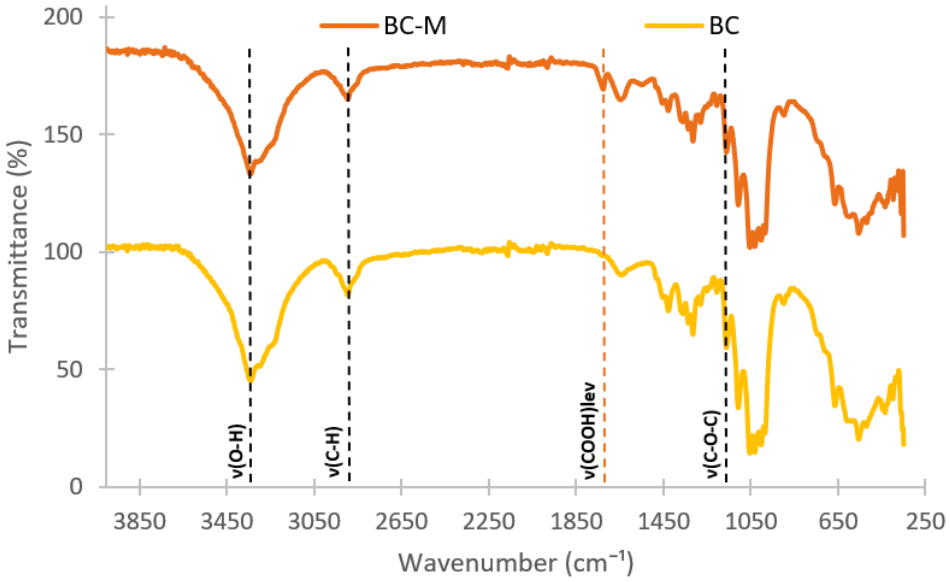

Figure 40. *Infrared spectra of BC and BC-metallodrug membranes.*

In Figure 40, it is easy to observe that the typical bands of cellulosic materials are present in both spectra. These bands occur at about 3340 cm^{-1}, 2890 cm^{-1}, and 1120 cm^{-1}, and are assigned to the vibrations of the O–H, C–H, and C–O–C groups, respectively.[24]

On the other hand, the infrared spectrum of BC-M displays a band at 1722 cm^{-1}, which is absent on the BC spectrum. This band is attributed to the stretching vibration of the carbonyl moiety ν(C=O) in the carboxylic group, COOH, of levofloxacin.[131] This way, the presence of levofloxacin in the BC-metallodrug membranes is confirmed. However, this band is missing in the infrared spectrum of Complex **1**, which could mean that, during the incorporation process, the protonation of the carboxylate group of levofloxacin occurred. In an aqueous solution, water molecules can coordinate with the metal ion, varying its coordination number. On the other hand, formation of interactions between Complex **1** and the BC network must be also considered. Nevertheless, more studies are needed in order to answer this question with certainty.

Fourier Transform Raman Spectroscopy (FT–Raman)

Figure 41 represents the Raman spectra of BC and BC-metallodrug membranes.

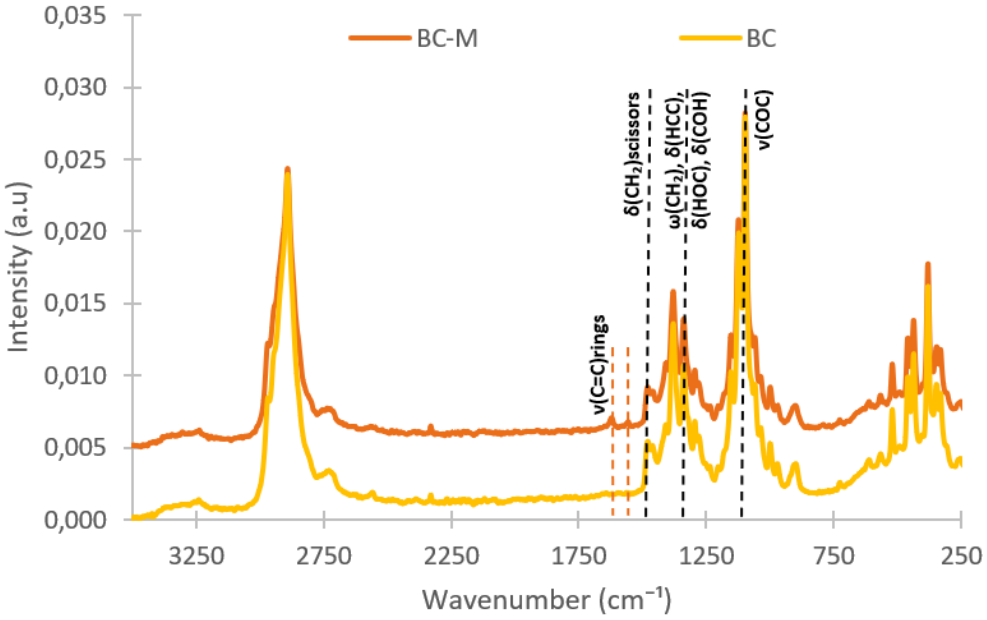

Figure 41. *Raman spectra of BC and BC-metallodrug membranes.*

The Raman spectra of pure BC and BC-metallodrug membranes, displayed in Figure 41, also exhibit the typical bands of cellulosic materials. For example, the band around 1463 cm^{-1} is assigned to the scissoring bending of H–C–H groups, the bands in the region from 1336 to 1292 cm^{-1} correspond to the bending of H–C–H, H–C–C, H–O–C, and C–O–H groups, and the bands around 1120 and 1095 cm^{-1} are attributed to the stretching of C–O–C groups.[140]

On the other hand, the Raman spectrum of BC-M displays two bands, at 1623 and 1558 cm^{-1}, that are absent from the spectrum of BC. These bands are assigned to the ν(C=C) stretching vibrations of aromatic rings, thus confirming the presence of Complex **1** in the BC-metallodrug membranes. Moreover, the Raman spectrum of BC-M does not show the band attributed to the stretching vibration of the carbonyl moiety ν(C=O) in the carboxylic group, at 1726 cm^{-1}, which indicates that the conclusions drawn for the infrared spectroscopy are not representative of the entire membrane.[138]

Thermogravimetric Analysis (TGA)

TGA was carried out in order to determine the thermal stability of BC and BC-metallodrug membranes, and to understand what changes are caused by the incorporation of the metallodrug. The TGA profiles are represented in Figure 42.

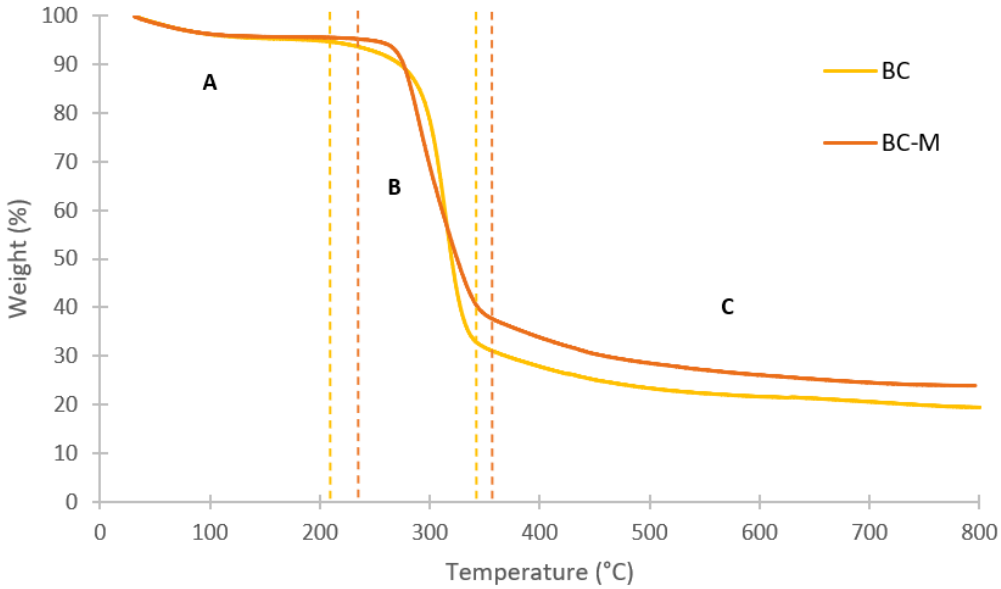

Figure 42. *TGA profiles of BC and BC-metallodrug membranes.*

The TGA profile of BC was very similar to those described in literature. In stage A, between 30 ºC and 210 ºC, the value of mass loss is 5 %, which is attributed to the evaporation of adsorbed water. In stage B, from 210 ºC to 340 ºC, a pronounced loss of mass is verified, about 61 %, due to the degradation of the polymeric backbone. In stage C, between 340 ºC and 800 ºC, the mass loss is 14 %, being the final residual percentage of 19 %.[141]

On the other hand, by observing the thermogram of BC-M, it is easy to notice that stages B and C start at higher temperatures, and that the percentage of the final residue is also higher (24 %). Therefore, this indicates that the incorporation of Complex **1** into BC increases the thermal stability of the membrane, and the reason might be the formation of interactions between Complex **1** and the BC network. These results are in agreement with the TGA data obtained by Badshah *et al*. (2018), which loaded BC matrices with famotidine and tizanidine.[141]

Dissolution assays

Linear calibration curve

In order to construct the linear calibration curve of Complex **1**, solutions with several concentrations were prepared in PBS and analyzed by ultraviolet-visible spectroscopy, in

particular to identify relevant absorbance peaks. Thus, Figure 43 exhibits the UV–Vis spectra of several concentrations of Complex **1**.

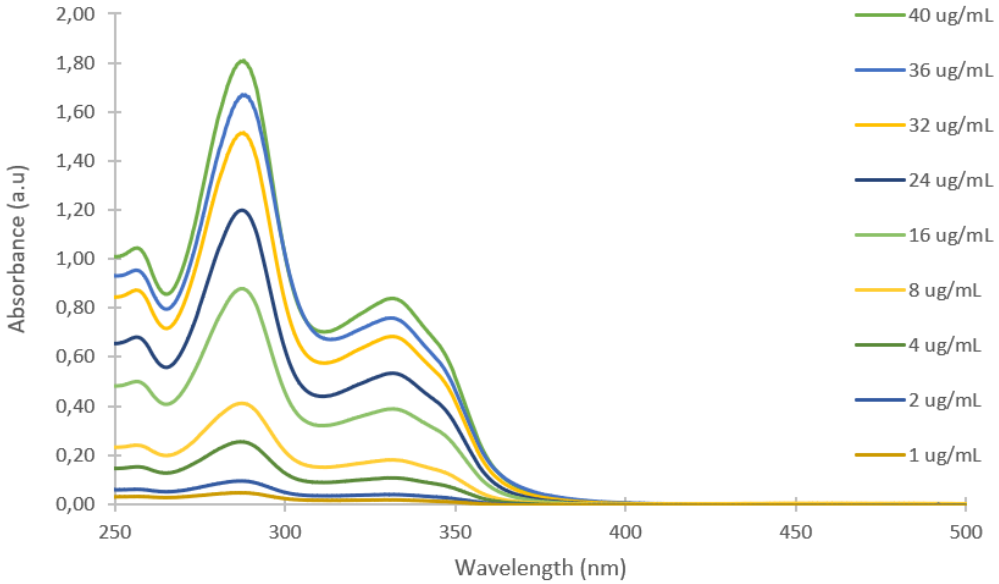

Figure 43. *UV–Vis spectra of several concentrations of Complex **1**.*

According to the UV–Vis spectra of Complex **1**, represented in Figure 43, the band at 287 nm was selected as the "fingerprint", allowing the construction of a linear calibration curve from the absorbance values at this wavelength, as displayed in Figure 44.

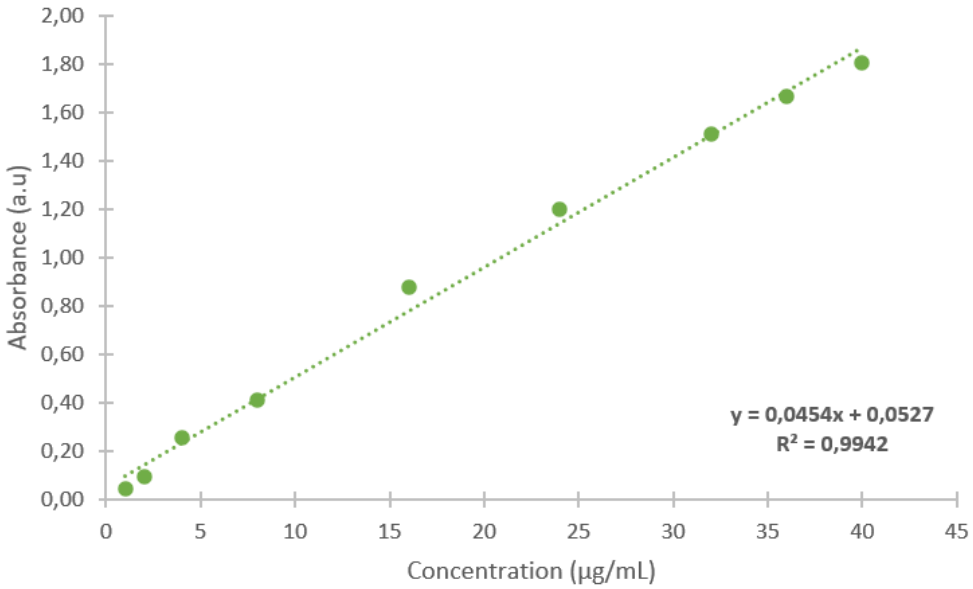

Figure 44. *Linear calibration curve of Complex **1**.*

The linear calibration curve allowed to obtain the following equation (Equation 2), which can be used to determine the concentration of Complex **1** through an absorbance value.

$$y = 0.0454\,x + 0.0527 \qquad \textbf{Equation 2.}$$
$$R^2 = 0.9942$$

In vitro metallodrug release

The release profile of Complex **1** from BC-metallodrug membranes in a phosphate-buffered saline solution is exhibited in Figure 45.

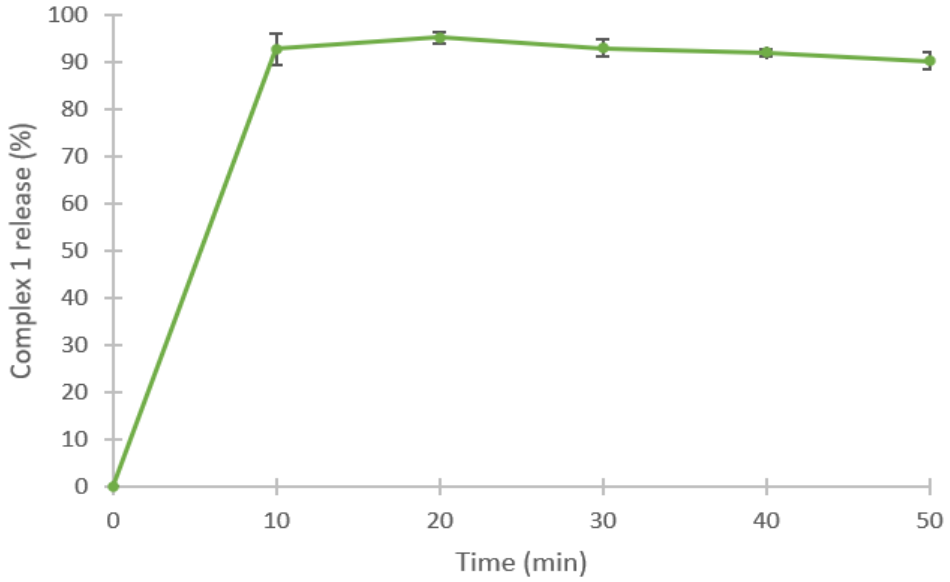

Figure 45. *Release profile of BC-metallodrug membranes.*

Almost 93 % of the total metallodrug was released in the first 10 minutes, and more than 95 % after 20 minutes. Considering that BC displays a high swelling capacity and that Complex **1** is soluble in water, it is possible to conclude that its release is mainly conducted by diffusion through the porous and three-dimensional BC network.[24,50]

These results are in agreement with the dissolution profile of diclofenac from BC membranes obtained by Silva *et al*. (2014).[24] However, Trovatti *et al*. (2011) obtained a slower release rate of lidocaine from BC membranes, indicating that the chemical nature of the drugs and their interaction with the BC nanofibrils also influence the release profile.[53]

The complete release profile of Complex **1** is displayed in Appendix D.

CHAPTER 4 – CONCLUSIONS AND FUTURE WORK

Conclusions

The main goals of this dissertation were the synthesis of metal complexes with antibacterial activity and their incorporation into bacterial cellulose membranes for wound healing applications. In order to achieve the main goals, several specific tasks were accomplished.

The first task was the synthesis of cobalt(II), copper(II), nickel(II), and zinc(II) complexes of levofloxacin and ciprofloxacin, in the presence and absence of N-donor ligands. To do so, several synthesis methods were performed, in particular one-pot synthesis, microwave-assisted synthesis, and solvothermal synthesis.

Of the several samples obtained, fourteen were selected for further characterization by several experimental analysis techniques, namely Fourier transform infrared spectroscopy (FTIR), Fourier transform Raman spectroscopy (FT-Raman), powder X-ray diffraction (PXRD), elemental analysis (EA), thermogravimetric analysis (TGA), and ultraviolet-visible spectroscopy (UV–Vis). The results indicated that N-donor ligands are coordinated, and that levofloxacin and ciprofloxacin act as bidentate ligands. Since other spectroscopic techniques that could help elucidate the structure of the complexes, such as single-crystal X-ray diffraction (SC XRD), were unavailable due to the amorphous nature of the complexes, chemical formulas were proposed according to the results drawn from the other analytical techniques, the structures of levofloxacin complexes obtained by SC XRD in a previous work, the chemical species present in each reaction mixture, and the bibliographic research performed.

Next, the antibacterial activity of the complexes against *Staphylococcus aureus* was evaluated. It was possible to conclude that all complexes exhibited antibacterial activity at the minimum concentration tested (5 µg/mL), and that most of them showed greater results than the parent antibiotic.

Subsequently, an aqueous solution of Complex **1** with 500 µg/mL was incorporated into BC membranes produced in static conditions using *Gluconacetobacter sacchari*. BC and BC-metallodrug membranes were characterized by Fourier transform infrared spectroscopy - attenuated total reflection (FTIR–ATR), Fourier transform Raman spectroscopy (FT–Raman), and thermogravimetric analysis (TGA). The results suggested that Complex **1** was incorporated into the BC membranes, and that the incorporation

increased the thermal stability of the membranes, possibly due to the formation of interactions between Complex **1** and the BC network.

In the *in vitro* release assay almost 93 % of the total metallodrug was released in the first 10 minutes, and more than 95 % after 20 minutes. The fast release profile obtained is appropriate for wound healing applications, since, in a topical administration, it is necessary an instant antimicrobial action, which is only assured if the amount of drug released from the delivery system is sufficient.

Therefore, with this work it was possible to synthesize and characterize fourteen metal complexes with antibacterial activity, and to incorporate and release one of them into bacterial cellulose membranes. Considering that, as far as we know, similar works have not been described in the literature yet, so this dissertation serves not only as a proof of concept, but also as a good starting point for the scientific community, combining the innumerous advantages of bacterial cellulose with the synergy and potential of the metallodrugs. Furthermore, it might become a future solution for a problem that affects millions of people.

Future Work

Although the main objectives proposed for this work have been successfully completed, further studies are required to better characterize, chemically and biologically, the metallodrugs, and to understand the full potential of their incorporation into bacterial cellulose membranes.

Spectroscopic techniques, such as NMR and Energy Dispersive X-Ray, could be used to further characterize the metal complexes. Moreover, their antibacterial activity against other microorganisms, for example, *Escherichia coli* and *Pseudomonas aeruginosa* (Gram negative), *Bacillus subtilis* (Gram positive), and *Aspergillus flavus* (fungus) could be evaluated, and their minimum inhibitory concentration could be determined.

On the other hand, the BC-metallodrug membranes could also be further characterized, for instance, by mechanical tensile assays, in order to determine the Young modulus, tensile strength, and the elongation at break. Furthermore, their biomedical profile and suitability could be evaluated in terms of cytotoxicity, antibacterial activity, and *in vitro* wound healing assays, in order to understand the potential for wound healing applications.

References

1. Lindholm C, Searle R. Wound management for the 21st century: combining effectiveness and efficiency. *Int Wound J*. 2016;13(suppl. S2):5-15.

2. Advanced Wound Care Market Growth, Size, Opportunities and Analysis Forecast (2020 to 2025). MarketWatch. https://www.marketwatch.com/press-release/advanced-wound-care-market-growth-size-opportunities-and-analysis-forecast-2020---2025-covid-19-impact-analysis-2020-11-18. Published 2020. Accessed December 23, 2020.

3. Sikka MP, Midha VK. The role of biopolymers and biodegradable polymeric dressings in managing chronic wounds. In: *Advanced Textiles for Wound Care*. Woodhead Publishing; 2019:463-488.

4. Ghomi ER, Khalili S, Khorasani SN, Neisiany RE. Wound dressings: Current advances and future directions. *J Appl Polym Sci*. 2019;136(47738):1-12.

5. Heinze T, Seoud OA El, Koschella A. Production and Characteristics of Cellulose from Different Sources. In: *Cellulose Derivatives: Synthesis, Structure, and Properties*. Cham, Switzerland: Springer Series on Polymer and Composite Materials; 2018:1-2.

6. Jorfi M, Foster EJ. Recent advances in nanocellulose for biomedical applications. *J Appl Polym Sci*. 2015;132(14):1-19.

7. Sahana TG, Rekha PD. Biopolymers: Applications in wound healing and skin tissue engineering. *Mol Biol Rep*. 2018;45(6):2857-2867.

8. Qi H. Structure of Cellulose: The Molecular Structure. In: *Novel Functional Materials Based on Cellulose*. Cham, Switzerland: Sringer Briefs in Applied Sciences and Technology; 2017:3-4.

9. Kargarzadeh H, Ioelovich M, Ahmad I, Thomas S, Dufresne A. Cellulose Fibers: Structure and Chemistry. In: *Handbook of Nanocellulose and Cellulose Composites*. Weinheim, Germany: Wiley-VCH; 2017:5-6.

10. Nelson DL, Cox MM. Carbohydrates and Glycobiology. In: *Lehninger. Principles of Biochemistry*. New York: W. H. Freeman and Company; 2013:243-280.

11. Qi H. Structure of Cellulose: Hydrogen Bonding. In: *Novel Functional Materials Based on Cellulose*. Cham, Switzerland: Springer Briefs in Applied Sciences and Technology; 2017:5-6.

12. Heinze T, Seoud OA El, Koschella A. Bacterial Cellulose. In: *Cellulose Derivatives: Synthesis, Structure, and Properties*. Cham, Switzerland: Springer Series on Polymer and Composite Materials; 2018:14-19.

13. Hickey RJ, Pelling AE. Cellulose biomaterials for tissue engineering. *Front Bioeng Biotechnol*. 2019;7(45):1-15.

14. Zugenmaier P. Conformation and packing of various crystalline cellulose fibers. *Prog Polym Sci*. 2001;26(9):1341-1417.

15. Moohan J, Stewart SA, Espinosa E, et al. Cellulose nanofibers and other biopolymers for biomedical applications. A review. *Appl Sci*. 2020;10(65):1-25.

16. Qi H. Nanocellulose-Based Functional Materials. In: *Novel Functional Materials Based on Cellulose*. Cham, Switzerland: Springer Briefs in Applied Sciences and Technology;

2017:69-79.

17. Sharma C, Bhardwaj NK. Bacterial nanocellulose: Present status, biomedical applications and future perspectives. *Mater Sci Eng C*. 2019;104(109963).

18. Sionkowska A, Mężykowska O, Piątek J. Bacterial nanocelullose in biomedical applications: a review. *Polym Int*. 2019;68(11):1841-1847.

19. Moniri M, Moghaddam AB, Azizi S, et al. Production and status of bacterial cellulose in biomedical engineering. *Nanomaterials*. 2017;7(9):257-283.

20. Hestrin S, Schramm M. Synthesis of cellulose by Acetobacter xylinum. Preparation of freeze-dried cells capable of polymerizing glucose to cellulose. *Biochem J*. 1954;58(2):345-352.

21. Jedrzejczak-Krzepkowska M, Kubiak K, Ludwicka K, Bielecki S. Bacterial NanoCellulose Synthesis, Recent Findings. In: *Bacterial Nanocellulose from Biotechnology to Bio-Economy*. Elsevier B.V.; 2016:19.

22. Qi H. Bacterial Nanocellulose: Introduction of BNC. In: *Novel Functional Materials Based on Cellulose*. Cham, Switzerland: Springer Briefs in Applied Sciences and Technology; 2017:79-80.

23. Daud JB, Lee K-Y. Surface Modification of Nanocellulose. In: *Handbook of Nanocellulose and Cellulose Composites*. Weinheim, Germany: Wiley-VCH; 2017:102-103.

24. Silva NHCS, Rodrigues AF, Almeida IF, et al. Bacterial cellulose membranes as transdermal delivery systems for diclofenac: In vitro dissolution and permeation studies. *Carbohydr Polym*. 2014;106(1):264-269.

25. Torres FG, Arroyo JJ, Troncoso OP. Bacterial cellulose nanocomposites: An all-nano type of material. *Mater Sci Eng C*. 2019;98:1277-1293.

26. Carvalho T, Guedes G, Sousa FL, Freire CSR, Santos HA. Latest Advances on Bacterial Cellulose-Based Materials for Wound Healing, Delivery Systems, and Tissue Engineering. *Biotechnol J*. 2019;14(12):1-19.

27. He W, Wu J, Xu J, Mosselhy DA, Zheng Y, Yang S. Bacterial Cellulose: Functional Modification and Wound Healing Applications. *Adv Wound Care*. 2020:1-54.

28. Kargarzadeh H, Ioelovich M, Ahmad I, Thomas S, Dufresne A. Main Cellulose Sources: Bacteria. In: *Handbook of Nanocellulose and Cellulose Composites*. Weinheim, Germany: Wiley-VCH; 2017:8-9.

29. Liu W, Du H, Zhang M, et al. Bacterial Cellulose-Based Composite Scaffolds for Biomedical Applications: A Review. *ACS Sustain Chem Eng*. 2020;8(20):7536-7562.

30. Park S-B, Lih E, Park K-S, Joung YK, Han DK. Biopolymer-based functional composites for medical applications. *Prog Polym Sci*. 2017;68:77-105.

31. Salimi S, Sotudeh-Gharebagh R, Zarghami R, Chan SY, Yuen KH. Production of Nanocellulose and Its Applications in Drug Delivery: A Critical Review. *ACS Sustain Chem Eng*. 2019;7(19):15800-15827.

32. Singhsa P, Narain R, Manuspiya H. Physical structure variations of bacterial cellulose produced by different Komagataeibacter xylinus strains and carbon sources in static and agitated conditions. *Cellulose*. 2018;25(3):1571-1581.

33. Orlando I, Basnett P, Nigmatullin R, Wang W, Knowles JC, Roy I. Chemical Modification of Bacterial Cellulose for the Development of an Antibacterial Wound Dressing. *Front*

Bioeng Biotechnol. 2020;8(557885):1-19.

34. Keskin Z, Sendemir Urkmez A, Hames EE. Novel keratin modified bacterial cellulose nanocomposite production and characterization for skin tissue engineering. *Mater Sci Eng C*. 2017;75:1144-1153.

35. Blanco Parte FG, Santoso SP, Chou CC, et al. Current progress on the production, modification, and applications of bacterial cellulose. *Crit Rev Biotechnol*. 2020;40(3):397-414.

36. Fijałkowski K, Żywicka A, Drozd R, et al. Increased water content in bacterial cellulose synthesized under rotating magnetic fields. *Electromagn Biol Med*. 2017;36(2):192-201.

37. Paximada P, Dimitrakopoulou EA, Tsouko E, Koutinas AA, Fasseas C, Mandala IG. Structural modification of bacterial cellulose fibrils under ultrasonic irradiation. *Carbohydr Polym*. 2016;150:5-12.

38. Santos V, Brandalise RN, Savaris M. Biomaterials: Characteristics and Properties. In: *Engineering of Biomaterials. Topics in Mining, Metallurgy and Materials Engineering*. Cham, Switzerland: Springer; 2017:5-15.

39. Picheth GF, Pirich CL, Sierakowski MR, et al. Bacterial cellulose in biomedical applications: A review. *Int J Biol Macromol*. 2017;104:97-106.

40. Ludwicka K, Jedrzejczak-Krzepkowska M, Kubiak K, Kolodziejczyk M, Pankiewicz T, Bielecki S. Medical and Cosmetic Applications of Bacterial NanoCellulose. In: *Bacterial Nanocellulose from Biotechnology to Bio-Economy*. Elsevier B.V.; 2016:145-159.

41. Portela R, Leal CR, Almeida PL, Sobral RG. Bacterial cellulose: a versatile biopolymer for wound dressing applications. *Microb Biotechnol*. 2019;12(4):586-610.

42. Qi H. Biomedical applications of BNC. In: *Novel Functional Materials Based on Cellulose*. Cham, Switzerland: Springer Briefs in Applied Sciences and Technology; 2017:80-82.

43. Fontana JD, De Souza AM, Fontana CK, et al. Acetobacter cellulose pellicle as a temporary skin substitute. *Appl Biochem Biotechnol*. 1990;24-25(1):253-264.

44. Czaja W, Krystynowicz A, Bielecki S, Brown R. Microbial cellulose - The natural power to heal wounds. *Biomaterials*. 2006;27(2):145-151.

45. Lin SP, Kung HN, Tsai YS, Tseng TN, Hsu K Di, Cheng KC. Novel dextran modified bacterial cellulose hydrogel accelerating cutaneous wound healing. *Cellulose*. 2017;24(11):4927-4937.

46. Pal S, Nisi R, Stoppa M, Licciulli A. Silver-Functionalized Bacterial Cellulose as Antibacterial Membrane for Wound-Healing Applications. *ACS Omega*. 2017;2(7):3632-3639.

47. Holzer JCJ, Tiffner K, Kainz S, et al. A novel human ex-vivo burn model and the local cooling effect of a bacterial nanocellulose-based wound dressing. *Burn J Int Soc Burn Inj*. 2020.

48. Mohamad N, Loh EYX, Fauzi MB, Ng MH, Mohd Amin MCI. In vivo evaluation of bacterial cellulose/acrylic acid wound dressing hydrogel containing keratinocytes and fibroblasts for burn wounds. *Drug Deliv Transl Res*. 2019;9(2):444-452.

49. Wahid F, Zhao XJ, Zhao XQ, et al. Fabrication of Bacterial Cellulose-Based Dressings for Promoting Infected Wound Healing. *ACS Appl Mater Interfaces*. 2021;13(28):32716-32728.

50. Silva NHCS, Mota JP, de Almeida TS, et al. Topical drug delivery systems based on bacterial

nanocellulose: Accelerated stability testing. *Int J Mol Sci*. 2020;21(4).

51. Pötzinger Y, Kralisch D, Fischer D. Bacterial nanocellulose: The future of controlled drug delivery? *Ther Deliv*. 2017;8(9):753-761.

52. Badshah M, Ullah H, Khan SA, Park JK, Khan T. Preparation, characterization and in-vitro evaluation of bacterial cellulose matrices for oral drug delivery. *Cellulose*. 2017;24(11):5041-5052.

53. Trovatti E, Silva NHCS, Duarte IF, et al. Biocellulose membranes as supports for dermal release of lidocaine. *Biomacromolecules*. 2011;12(11):4162-4168.

54. Liyaskina E, Revin V, Paramonova E, et al. Nanomaterials from bacterial cellulose for antimicrobial wound dressing. *J Phys Conf Ser*. 2017;784:1-7.

55. de Mattos IB, Holzer JCJ, Tuca AC, et al. Uptake of PHMB in a bacterial nanocellulose-based wound dressing: A feasible clinical procedure. *Burns*. 2019;45(4):898-904.

56. Ye S, Jiang L, Wu J, et al. Flexible Amoxicillin-Grafted Bacterial Cellulose Sponges for Wound Dressing: In Vitro and in Vivo Evaluation. *ACS Appl Mater Interfaces*. 2018;10(6):5862-5870.

57. Lemnaru G-M, Tru¸scă RD, Ilie C-I, et al. Antibacterial Activity of Bacterial Cellulose Loaded with Bacitracin and Amoxicillin: In Vitro Studies. *Molecules*. 2020;25(4069):1-17.

58. Antibiotic resistance. World Health Organization. https://www.who.int/news-room/fact-sheets/detail/antibiotic-resistance. Published 2020. Accessed January 12, 2021.

59. New report calls for urgent action to avert antimicrobial resistance crisis. World Health Organization. https://www.who.int/news/item/29-04-2019-new-report-calls-for-urgent-action-to-avert-antimicrobial-resistance-crisis. Published 2019. Accessed January 12, 2021.

60. Global Antibiotic Resistance Market - Market Size, Share, Growth, Trends, and Forecast (2018 to 2025). FiorMarkets. https://www.fiormarkets.com/report/global-antibiotic-resistance-market-by-disease-pathogen-drug-362194.html. Published 2019. Accessed January 12, 2021.

61. Viganor L, Howe O, McCarron P, McCann M, Devereux M. The Antibacterial Activity of Metal Complexes Containing 1,10- phenanthroline: Potential as Alternative Therapeutics in the Era of Antibiotic Resistance. *Curr Top Med Chem*. 2017;17(11):1280-1302.

62. Frei A. Metal complexes, an untapped source of antibiotic potential? *Antibiotics*. 2020;9(90):2-24.

63. Psomas G, Kessissoglou DP. Quinolones and non-steroidal anti-inflammatory drugs interacting with copper(II), nickel(II), cobalt(II) and zinc(II): Structural features, biological evaluation and perspectives. *Dalt Trans*. 2013;42(18):6252-6276.

64. Ndagi U, Ndumiso M, Soliman ME. Metal complexes in cancer therapy – an update from drug design perspective. *Drug Des Devel Ther*. 2017;1:599-616.

65. Zaki M, Arjmand F, Tabassum S. Current and future potential of metallo drugs: Revisiting DNA-binding of metal containing molecules and their diverse mechanism of action. *Inorganica Chim Acta*. 2016;444:1-22.

66. Varol M. The Importance of Metal-Based Drugs in Medicinal Inorganic Chemistry to Improve Life Quality of Patients. *J Appl Pharm*. 2016;8(1):107-109.

67. Cavaleiro AM V. Complexos de metais do bloco d: estrutura e reactividade. In: *Química*

Inorgânica Básica. Aveiro: Universidade de Aveiro Edições; 1999:255-287.

68. Crichton R. Basic Coordination Chemistry for Biologists. In: *Biological Inorganic Chemistry: A New Introduction to Molecular Structure and Function*. Elsevier B.V.; 2019:19-34.

69. Coordination Compounds. General Chemistry Principles Patterns and Applications. https://saylordotorg.github.io/text_general-chemistry-principles-patterns-and-applications-v1.0/s27-04-coordination-compounds.html. Accessed December 14, 2020.

70. Hossain MS, Mannan MA, Kudrat-E-Zahan M. Recent advances on microbial activity of metal complexes: A short review. *Int J Chem Stud*. 2020;4(1):17-24.

71. Yousuf I, Bashir M. Metallodrugs in Medicine: Present, Past, and Future Prospects. In: *Advances in Metallodrugs: Preparation and Applications in Medicinal Chemistry*. Beverly, USA: Wiley; 2020:1-40.

72. Cavaleiro AM V. Complexos de metais do bloco d: estrutura eletrónica e propriedades. In: *Química Inorgânica Básica*. Universidade de Aveiro Edições; 1999:291-344.

73. Fikadu T, Abera Mitiku A, Ligands H, Fekadu Egza T, Seifu Lemma T, Chinna Eeranna B. A Review on Pharmacological Activity of Some Selected Transition Metal Complexes With Heterocyclic Ligands. *World J Pharm Res*. 2020;9(12):100-127.

74. Crans DC, Kostenkova K. Open questions on the biological roles of first-row transition metals. *Commun Chem*. 2020;3(104):1-4.

75. Malik MA, Dar OA, Hashmi AA. Recent Advances in Cobalt Derived Complexes as Potential Therapeutic Agents. In: *Advances in Metallodrugs: Preparation and Applications in Medicinal Chemistry*. Beverly, USA: Wiley; 2020:137-156.

76. Crichton R. Nickel and Cobalt: Evolutionary Relics. In: *Biological Inorganic Chemistry: A New Introduction to Molecular Structure and Function*. Elsevier B.V.; 2019:435-457.

77. Al-fartusie FS, Mohssan SN. Essential Trace Elements and Their Vital Roles in Human Body. *Indian J Adv Chem Sci*. 2017;5(3):127-136.

78. Dwyer FP, Gyarfas EC, Rogers WP, Koch JH. Biological Activity of Complex Ions. *Nature*. 1952;170(4318):190-191.

79. Kumar M, Kumar G, Kant A, Masram DT. Copper-Based Anticancer Complexes. In: *Advances in Metallodrugs: Preparation and Applications in Medicinal Chemistry*. Beverly, USA: Wiley; 2020:82-89.

80. Crichton R. Copper - Coping with Dioxygen. In: *Biological Inorganic Chemistry: A New Introduction to Molecular Structure and Function*. Elsevier B.V.; 2019:405-433.

81. Conry RR, Karlin KD. Copper: Inorganic & Coordination Chemistry. *Encycl Inorg Bioinorg Chem*. December 2011:1-19.

82. Kumar M, Kumar G, Kant A, T. MD. Zinc Anticancer Complexes. In: *Advances in Metallodrugs: Preparation and Applications in Medicinal Chemistry*. Beverly, USA: Wiley; 2020:89-103.

83. Crichton R. Zinc - Lewis Acid and Gene Regulator. In: *Biological Inorganic Chemistry: A New Introduction to Molecular Structure and Function*. Elsevier B.V.; 2019:339-362.

84. Maret W. New perspectives of zinc coordination environments in proteins. *J Inorg Biochem*. 2012;111:110-116. https://linkinghub.elsevier.com/retrieve/pii/S0162013411003576.

85. Kumar M, Mogha NK, Kumar G, Hussain F, Masram DT. Biological evaluation of copper(II) complex with nalidixic acid and 2,2′-bipyridine (bpy). *Inorganica Chim Acta*. 2019;490:144-154.

86. Bencini A, Lippolis V. 1,10-Phenanthroline: A versatile building block for the construction of ligands for various purposes. *Coord Chem Rev*. 2010;254(17-18):2096-2180.

87. Sammes PG, Yahioglu G. 1,10-Phenanthroline: A Versatile Ligand. *Chem Soc Rev*. 1994;23(5):327-334.

88. PubChem Compound Summary for CID 1318, 1,10-Phenanthroline. National Center for Biotechnology Information. https://pubchem.ncbi.nlm.nih.gov/compound/1_10-Phenanthroline. Accessed December 16, 2020.

89. Constable EC, Housecroft CE. The early years of 2,2'-bipyridine — A ligand in its own lifetime. *Molecules*. 2019;24(21):3951.

90. Fletcher NC. Chiral 2,2′-bipyridines: Ligands for asymmetric induction. *J Chem Soc Perkin Trans 1*. 2002;(16):1831-1842.

91. PubChem Compound Summary for CID 1474, 2,2'-Bipyridine. National Center for Biotechnology Information. https://pubchem.ncbi.nlm.nih.gov/compound/2_2_-Bipyridine. Accessed December 15, 2020.

92. Mayer P, Yumata NC, Gerber TIA, Abrahams A. Coordination of the bidentate ligands 2,2'-dipyridylamine, 1-phenyl-1,3 butadione and N'-(propan-2-ylidene)benzohydrazide to rhenium(III). *South African J Chem*. 2010;63:180-185.

93. Wang S, Bruneau C, Renaud JL, Gaillard S, Fischmeister C. 2,2′-Dipyridylamines: More than just sister members of the bipyridine family. Applications and achievements in homogeneous catalysis and photoluminescent materials. *Dalt Trans*. 2019;48(31):11599-11622.

94. Brogden DW, Berry JF. Coordination Chemistry of 2,2'-Dipyridylamine: The Gift That Keeps on Giving. *Comments Inorg Chem*. 2016;36(1):17-37.

95. PubChem Compound Summary for CID 14547, 2,2'-Dipyridylamine. National Center for Biotechnology Information. https://pubchem.ncbi.nlm.nih.gov/compound/2_2_-Dipyridylamine. Accessed December 16, 2020.

96. Biradha K, Sarkar M, Rajput L. Crystal engineering of coordination polymers using 4,4′-bipyridine as a bond between transition metal atoms. *Chem Commun*. 2006;(40):4169-4179.

97. Woodward JD, Backov R V., Abboud KA, Talham DR. Monomers, chains, ladders, and two-dimensional sheets: Structural diversity in six new compounds of Zn(II) with 4,4′-bipyridine. *Polyhedron*. 2006;25(13):2605-2615.

98. Aoyagi M, Biradha K, Fujita M. Formation of Two, One, and Zero-Dimensional Coordination Assemblies from Cd(II) Ion and 4,4'-Bipyridine. *Chem Soc Japan*. 2000;73:1369-1373.

99. PubChem Compound Summary for CID 11107, 4,4'-Bipyridine. National Center for Biotechnology Information. https://pubchem.ncbi.nlm.nih.gov/compound/4_4_-Bipyridine. Accessed December 16, 2020.

100. Waksman SA. What is an Antibiotic or an Antibiotic Substance? *Mycologia*. 1947;39(5):565-569.

101. Mohr KI. History of Antibiotics Research. In: *How to Overcome the Antibiotic Crisis. Current Topics in Microbiology and Immunology*. Springer; 2016:237-272.

102. Walsh C, Wencewicz T. Antibiotics: Initial Concepts and Considerations. In: *Antibiotics: Challenges, Mechanisms, Opportunities*. Washington, DC: ASM Press; 2016:5-15.

103. Etebu E, Arikekpar I. Antibiotics: Classification and mechanisms of action with emphasis on molecular perspectives. *Int J Appl Microbiol Biotechnol Res*. 2016;4:90-101.

104. Walsh C, Wencewicz T. Antibiotics That Target DNA and RNA Information Transfer. In: *Antibiotics: Challenges, Mechanisms, Opportunities*. Washington, DC: ASM Press; 2016:148-163.

105. Pham TDM, Ziora ZM, Blaskovich MAT. Quinolone antibiotics. *Med Chem Comm*. 2019;10:1719-1739.

106. Gallagher J, MacDougall C. Fluoroquinolones. In: *Antibiotics Simplified*. Burlington, MA: Jones & Bartlett Learning; 2018:258.

107. Naeem A, Badshah SL, Muska M, Ahmad N, Khan K. The current case of quinolones: Synthetic approaches and antibacterial activity. *Molecules*. 2016;21(4):268-287.

108. Rusu A, Hancu G, Tóth G, et al. New silver complexes with levofloxacin: Synthesis, characterization and microbiological studies. *J Mol Struct*. 2016;1123:384-393.

109. Alwan SM, Abdulhadi SL, Abbas A. Synthesis of Levofloxacin Derivatives with some Amines and their Complexes with Copper(II) Salts and Evaluation of their Biological Activity. *Int J Drug Deliv Technol*. 2020;10(3):408-413.

110. Rusu A, Hancu G, Cristina Munteanu A, Uivarosi V. Development perspectives of silver complexes with antibacterial quinolones: Successful or not? *J Organomet Chem*. 2017;839:19-30.

111. PubChem Compound Summary for CID 149096, Levofloxacin. National Center for Biotechnology Information. https://pubchem.ncbi.nlm.nih.gov/compound/Levofloxacin. Accessed January 9, 2021.

112. Hurst M, Lamb HM, Scott LJ, Adis DPF. Levofloxacin: An Updated Review of Its Use in the Treatment of Bacterial Infections. *Drugs*. 2002;62(14):2127-2167.

113. Noel GJ. A Review of Levofloxacin for the Treatment of Bacterial Infections. *Clin Med Ther*. 2009;1:433-458.

114. Davis R, Markham A, Balfour JA. Ciprofloxacin: An Updated Review of its Pharmacology, Therapeutic Efficacy and Tolerability. *Drugs*. 1996;51(6):1019-1074.

115. Sharma PC, Jain A, Jain S, Pahwa R, Yar MS. Ciprofloxacin: Review on developments in synthetic, analytical, and medicinal aspects. *J Enzyme Inhib Med Chem*. 2010;25(4):577-589.

116. PubChem Compound Summary for CID 4011971, Cipro. National Center for Biotechnology Information. https://pubchem.ncbi.nlm.nih.gov/compound/Cipro. Accessed January 11, 2021.

117. Chohan ZH, Supuran CT, Scozzafava A. Metal binding and antibacterial activity of ciprofloxacin complexes. *J Enzyme Inhib Med Chem*. 2005;20(3):303-307.

118. Hayashi Y. Pot economy and one-pot synthesis. *Chem Sci*. 2016;7(2):866-880.

119. Galani A, Efthimiadou EK, Theodosiou T, Kordas G, Karaliota A. Novel levofloxacin zinc(II) complexes with N-donor heterocyclic ligands, as potential fluorescent probes for cell imaging: Synthesis, structural characterization and in vitro cytotoxicity. *Inorganica Chim Acta*. 2014;423:52-59.

120. Akram SMM, Tak AA, Mustafa PG, Parray JA. DNA binding and biological activity of mixed ligand complexes of Cu(II), Ni(II) and Co(II) with quinolones and N donor ligand. *Mediterr J Chem*. 2015;4(5):227-238.

121. Al-Saif FA, Alibrahim KA, Alfurhood JA, Refat MS. Synthesis, spectroscopic, thermal, biological, morphological and molecular docking studies of the different quinolone drugs and their cobalt(II) complexes. *J Mol Liq*. 2018;249:438-453.

122. Sousa I, Claro V, Pereira JL, et al. Synthesis, characterization and antibacterial studies of a copper(II) levofloxacin ternary complex. *J Inorg Biochem*. 2012;110:64-71.

123. Lai J, Niu W, Luque R, Xu G. Solvothermal synthesis of metal nanocrystals and their applications. *Nano Today*. 2015;10(2):240-267.

124. Dojer B, Pevec A, Jagličić Z, Drofenik M, Kristl M. Nickel(II) pyridinecarboxamide complexes: Solvothermal synthesis, crystal structures and magnetic properties. *Inorganica Chim Acta*. 2016;446:124-131.

125. Mendes RF, Rocha J, Almeida Paz FA. Microwave synthesis of metal-organic frameworks. In: Mozafari M, ed. *Metal-Organic Frameworks for Biomedical Applications*. Elsevier; 2020:159-176.

126. Ikotun AA, Omolekan TO. Microwave-assisted Synthesis, Characterization, Antimicrobial and Antioxidant Activities of 1-Benzyl-3-[(4-Methylphenyl)Imino]-Indolin-2-One and Its Co(II) Complex. *Chem Sci Int J*. 2019;28(1):1-12.

127. Mubarak A, Abu Ali H, Metani M. Two novel Cu (II) levofloxacin complexes with different bioactive nitrogen-based ligands; single-crystal X-ray and various biological activities determinations. *Appl Organomet Chem*. September 2021.

128. Kumar M, Kumar G, Dadure KM, Masram DT. Copper(II) complexes based on levofloxacin and 2N-donor ligands: Synthesis, crystal structures and: In vitro biological evaluation. *New J Chem*. 2019;43(38):15462-15481.

129. Horozić E, Cipurković A, Ademović Z, et al. Synthesis, spectral characterization and antimicrobial activity of some M(II) complexes with Ciprofloxacin. *J Eng Process Manag*. 2018;10(2):16-22.

130. Almeida IF, Pereira T, Silva NHCS, et al. Bacterial cellulose membranes as drug delivery systems: An in vivo skin compatibility study. *Eur J Pharm Biopharm*. 2014;86(3):332-336.

131. Alghamdi MT, Alsibaai AA, Shahawi MS, Refat MS. Synthesis and spectroscopic studies of levofloxacin uni-dentate complexes of Ru(II), Pt(IV) and Ir(III): Third generation of quinolone antibiotic drug complexes. *J Mol Liq*. 2016;224:571-579.

132. Obaleye J, Lawal M, Jadeja RN, et al. Crystal structure, spectroscopic, DFT calculations and antimicrobial study of the Cu(II) complex bearing second-generation quinolone ofloxacin and 2,2'-bipyridine. *Inorganica Chim Acta*. 2021;519(120264):1-12.

133. Kakoulidou C, Kalogiannis S, Angaridis P, Psomas G. Synthesis, characterization and biological activity of Zn coordination compounds with the quinolone gatifloxacin. *Polyhedron*. 2019;166:98-108.

134. Psomas G. Mononuclear metal complexes with ciprofloxacin: Synthesis, characterization and DNA-binding properties. *J Inorg Biochem*. 2008;102(9):1798-1811.

135. Turel I, Bukovec P, Quirós M. Crystal structure of ciprofloxacin hexahydrate and its characterization. *Int J Pharm*. 1997;152:59-65.

136. Smith E, Dent G. Introduction, Basic Theory and Principles. In: *Modern Raman Spectroscopy - A Practical Approach*. Wiley; 2019:1-20.

137. Larkin P. General Outline and Strategies for IR and Raman Spectral Interpretation. In: *Infrared and Raman Spectroscopy: Principles and Spectral Interpretation*. Elsevier; 2011:117-133.

138. Sinha RK, Biswas P. Structural elucidation of Levofloxacin and Ciprofloxacin using density functional theory and Raman spectroscopy with inexpensive lab-built setup. *J Mol Struct*. 2020;1222(128946):1-8.

139. Galani A, Efthimiadou EK, Mitrikas G, et al. Synthesis, crystal structure and characterization of three novel copper complexes of Levofloxacin. Study of their DNA binding properties and biological activities. *Inorganica Chim Acta*. 2014;423:207-218.

140. Schenzel K, Fischer S. NIR FT Raman spectroscopy - A rapid analytical tool for detecting the transformation of cellulose polymorphs. *Cellulose*. 2001;8(1):49-57.

141. Badshah M, Ullah H, Khan AR, Khan S, Park JK, Khan T. Surface modification and evaluation of bacterial cellulose for drug delivery. *Int J Biol Macromol*. 2018;113:526-533.

Appendix

Appendix A

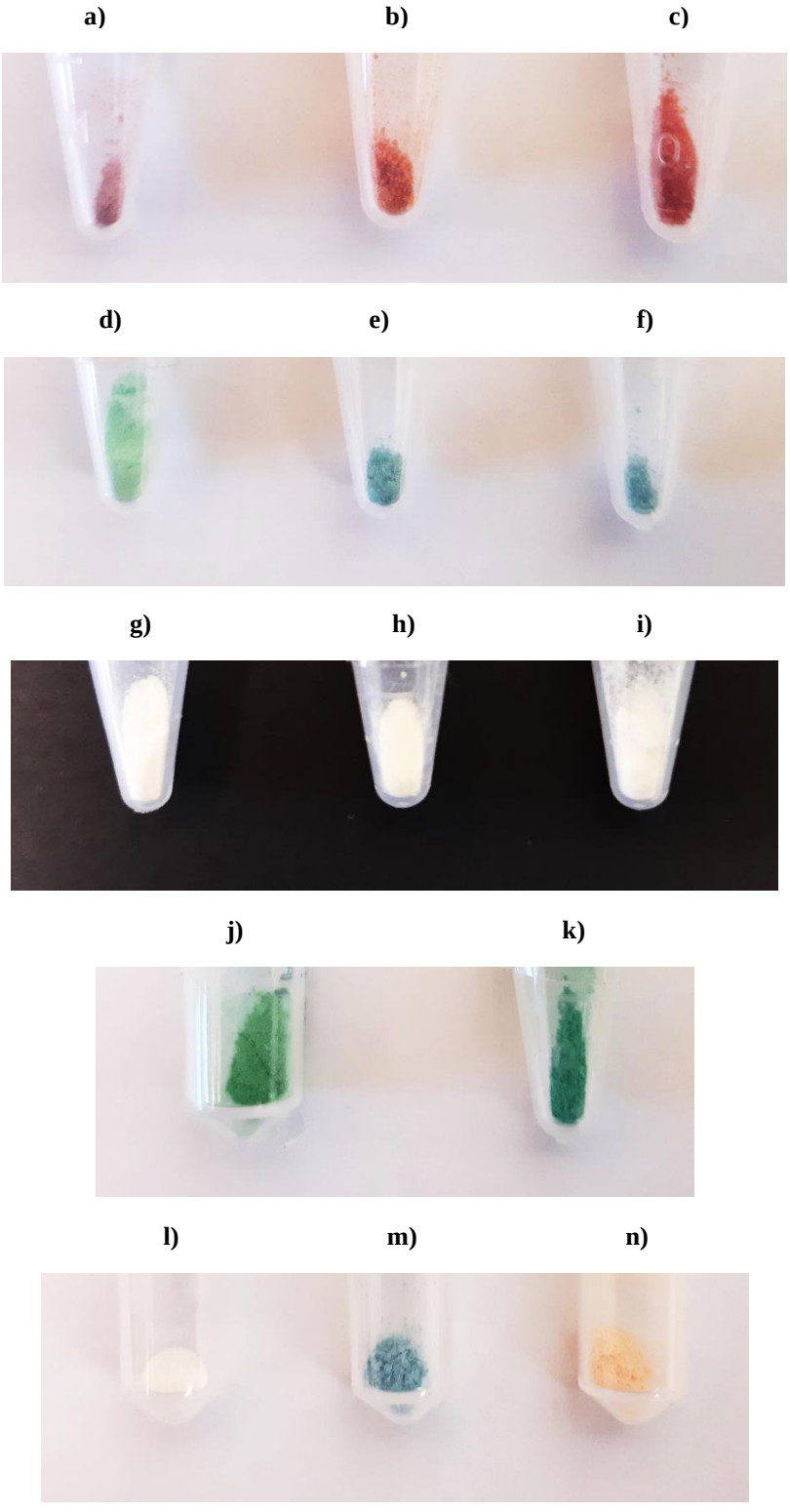

Appendix A1. *Obtained products: a) Complex **1**; b) Complex **2**; c) Complex **3**; d) Complex **4**; e) Complex **5**; f) Complex **6**; g) Complex **7**; h) Complex **8**; i) Complex **9**; j) Complex **11**; k) Complex **12**; l) Complex **13**; m) Complex **14**; n) Complex **15**.*

Appendix B

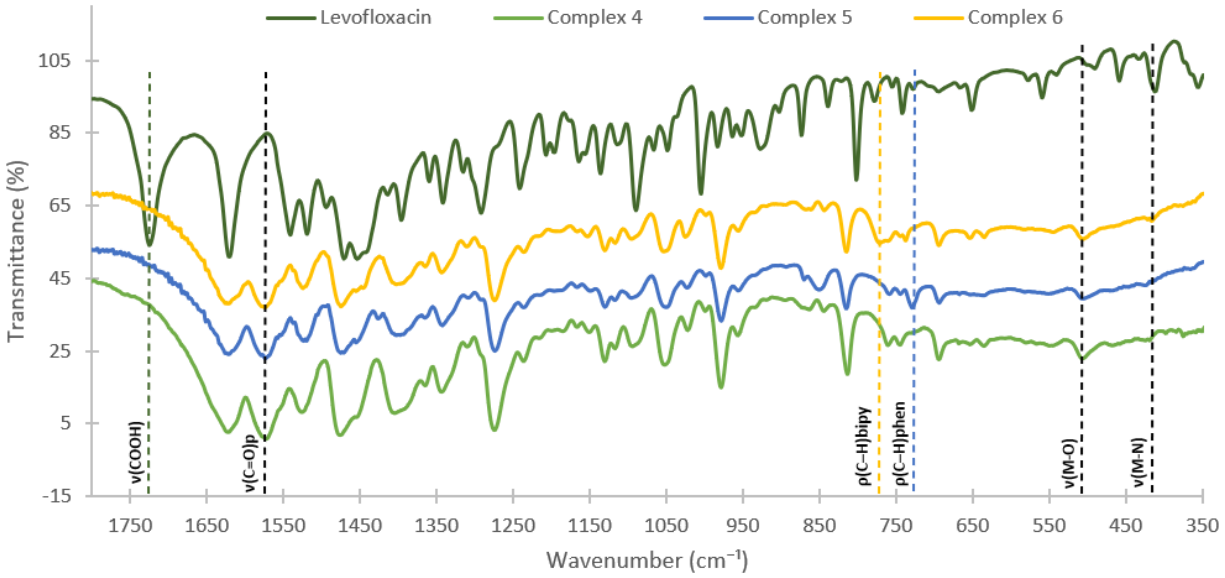

Appendix B1. *Infrared spectra of Complex **4**, Complex **5**, and Complex **6**.*

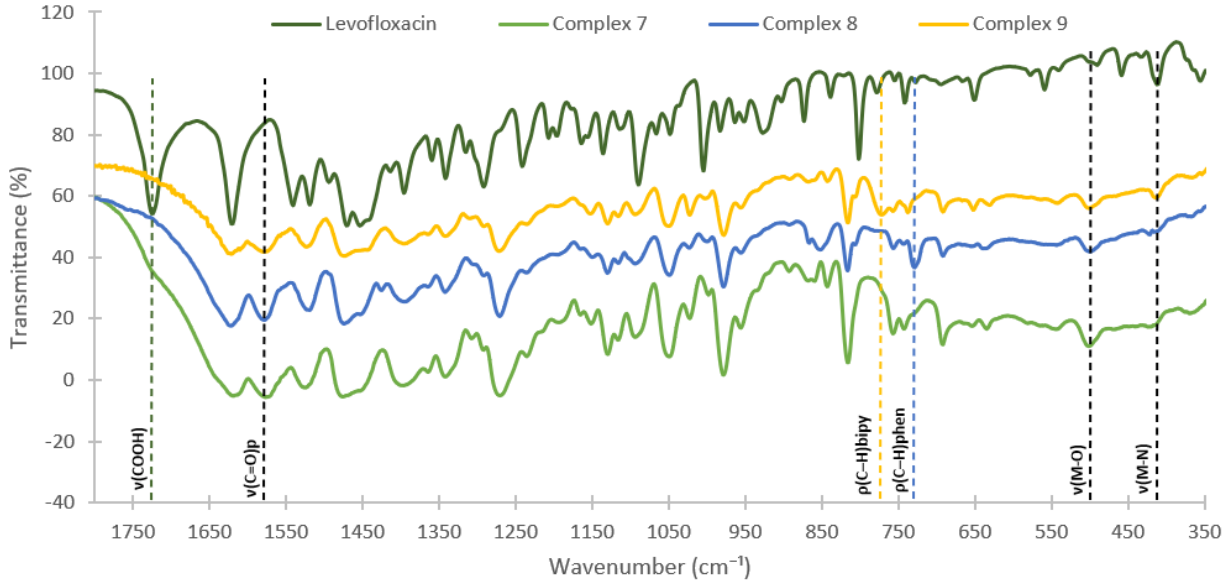

Appendix B2. *Infrared spectra of Complex **7**, Complex **8**, and Complex **9**.*

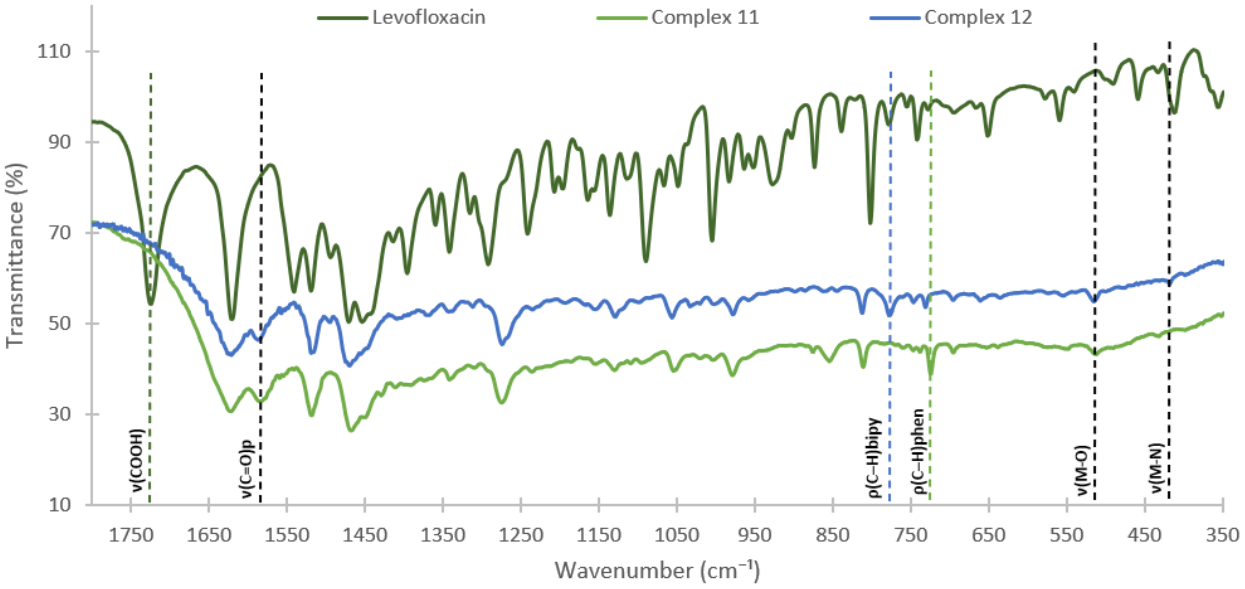

Appendix B3. *Infrared spectra of Complex **11** and Complex **12**.*

Appendix C

Appendix C1. *Antibacterial activity data of levofloxacin, ciprofloxacin, and their complexes at 50 and 500 µg/mL, against S. aureus.*

S. aureus	**Disk content**	
	50 µg/mL	500 µg/mL
Sample	**Inhibition zone diameter (mm)**	
Levofloxacin	22	29
Complex 1	27	34
Complex 2	25	32
Complex 3	24	33
Complex 4	21	30
Complex 5	21	32
Complex 6	28	31
Complex 7	25	34
Complex 8	25	39
Complex 9	20	33
Complex 11	21	33
Complex 12	23	32
Ciprofloxacin	15	22
Complex 13	20	31
Complex 14	19	28
Complex 15	18	27

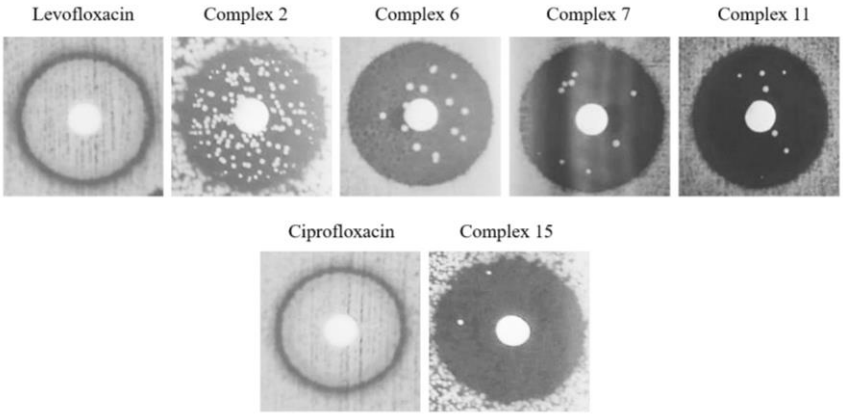

Appendix C2. *Susceptibility test of P. aeruginosa: antibacterial activity exhibited by levofloxacin, Complex **2**, Complex **6**, Complex **7**, Complex **11**, ciprofloxacin, and Complex **15**. The growth of bacteria was inhibited, but afterwards some colonies were able to grow back due to contamination.*

Appendix C3. *Antibacterial activity data of levofloxacin, ciprofloxacin, and their complexes, against P. aeruginosa.*

		Inhibition zone diameter (mm)
Sample	**Disk content**	***P. aeruginosa***
Levofloxacin	5 µg/mL	21
Complex 1		21
Complex 2		18
Complex 3		21
Complex 4		19
Complex 5		20
Complex 6		12
Complex 7		24
Complex 8		19
Complex 9		17
Complex 11		19
Complex 12		19
Ciprofloxacin		16
Complex 13		26
Complex 14		26
Complex 15		22

Appendix D

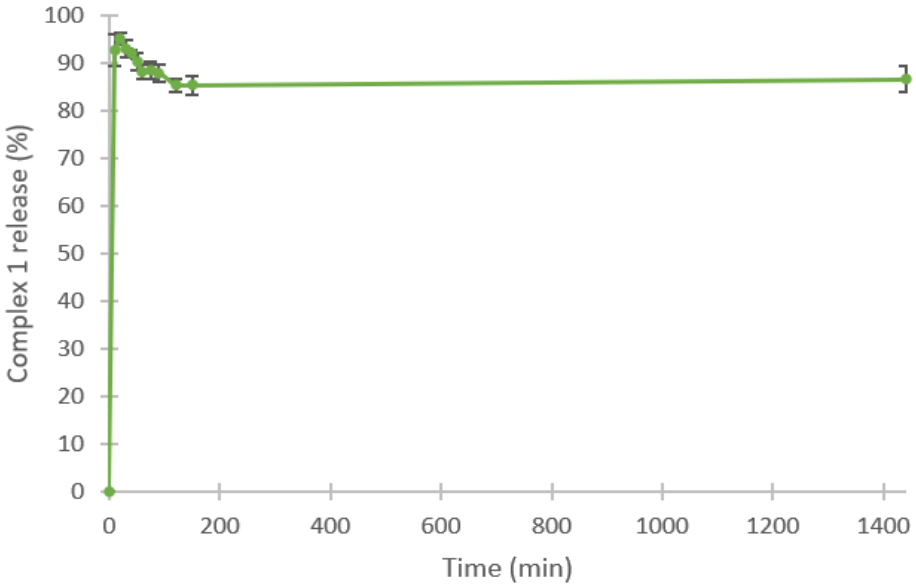

Appendix D1. *Complete release profile of BC-metallodrug membranes.*